April 2019

Synthesis and Characterization of Molybdenum Disulfide/ Conducting Polymer Nanocomposite Materials for Supercapacitor Applications

Turki S. Alamro
University of South Florida, alamro@mail.usf.edu

Synthesis and Characterization of Molybdenum Disulfide/Conducting Polymer Nanocomposite Materials for Supercapacitor Applications

by

Turki S. Alamro

A dissertation submitted in partial fulfillment
of the requirements for the degree of
Doctor of Philosophy
Department of Mechanical Engineering
College of Engineering
University of South Florida

Co-Major Professor: Ashok Kumar, Ph.D.
Co-Major Professor: Manoj K. Ram, Ph.D.
Arash Takshi, Ph.D.
Rajiv Dubey, Ph.D.
Ajit Mujumdar, Ph.D.
Jiangfeng Zhou, Ph.D.

Date of Approval:
September 24, 2018

Keywords: electrochemical capacitors, electrode deposition, poly(3,4-ethylenedioxythiophene), polyaniline emeraldine, polymerization techniques

DEDICATION

To my beloved daughter Taraf whose presence is a blessing in my life. Since last November, my world has become so empty without your voice. My love for you can never be quantified, and if I could change only one thing, I would just turn the clock back, so you can say: "DADDY" again.

To my father Sulaiman Alamro and mother Mariam Alorini who taught me how to combine knowledge and wisdom to pursue my goals and fulfil my dreams.

ACKNOWLEDGMENTS

I would like to express my sincere thanks to my co-major advisor Dr. Manoj Ram who has helped me throughout my graduate studies to accomplish this dissertation work; a wise gentleman I very well admire. I am thankful to my co-major advisor Dr. Ashok Kumar for affording me the opportunity to work in his research team. I owe Dr. Arash Takshi immense gratitude for the constant help he offered; he has been always there, and his advice has significantly enriched me academically and personally throughout my presence in the PhD program. I would like to thank the members of my dissertation committee: Dr. Rajiv Dubey, Dr. Ajit Mujumdar and Dr. Jiangfeng Zhou who have generously dedicated their time and expertise to improve my work. I owe a heartfelt thanks to Dr. Rajiv Dubey and Dr. Rasim Guldiken who always supported and helped me through challenges that I have encountered along the way. I would also like to thank the Nanotechnology Research and Education Center (NREC) at USF for their kind support to provide the facilities for conducting experiments and measurements.

My genuine gratefulness and warmest regard go to the doctors, nurses and staff at St. Joseph's Children's Hospital, Dr. Arash Takshi and his wife, Dr. Manoj Ram and his wife, Dr. Rajiv Dubey, Dr. Rasim Guldiken, Dr. Adeeb Bulkhi, Dr. Michael McCrory and his wife, Belqasem Aljafari, all of my friends and the people at the USF for their kindness and devotion, when my daughter Taraf was ill. Their endless support in those stressful times will always be remembered, and without them all I would not be graduating.

My utmost regard and sincere appreciation also go to my wife, my siblings (Noura, Hissah, Abdullah, Fatmah, Mohammed, Asma, Ebtisam, Amro, Amnah and Sultan), my nieces, my

nephews, my in-laws, Hanna Haddad and his family for their invaluable guidance throughout the journey of my education; I will forever be grateful to you all and this page cannot tell it all.

TABLE OF CONTENTS

LIST OF TABLES

LIST OF FIGURES

ABSTRACT

The needs for energy storage devices have kindled researchers desire to explore and synthesize nanocomposite materials. Storing energy efficiently, effectively and sustainably are the science and engineering communities' highest priorities to develop electrochemical energy storage devices. Supercapacitors have become power solution not only because supercapacitors can bridge the gap between the traditional capacitors and rechargeable batteries but also because of many other advantages which include extraordinary electrochemical properties, wide working-temperature range, cost effective, safe operation and long/stable cycle life. They have higher current pules than batteries due to the mechanism of charging and discharging. Batteries charging and discharging via chemical reactions, whereas supercapacitors utilize electrochemical double layer capacitors, in which nanoscopic charge separation is employed for energy storage at the electrode/electrolyte interface of the device.

One of the key factors that determine the performance and properties of electrochemical capacitors is the electrode material. The performance of supercapacitor relies on features such as specific surface area, electronic conductivity as well as mechanical and chemical stability of the electrode materials. Using conventional electrode materials, it is challenging to address all critical features include: toxicity, low specific capacitance and energy density, poor cycle stability, high cost and self-discharge. One of most intensive approaches of overcoming these obstacles is by introducing and developing nanocomposite materials for supercapacitors.

In this investigation, a MoS_2/PEDOT nanocomposite material was chemically synthesized at various ratios of MoS_2 to ethylenedioxythiophene (EDOT) to understand the charge mechanism

in a symmetric supercapacitor. Whereas, previous attempts have been made to homogeneously cover MoS_2 nanosheets with a PANI coating layer to obtain nanocomposite electrodes. However, emeraldine salt (ES) form of PANI is an insoluble polymer which may impede advantageous deposition techniques. Taking advantage of the processability of emeraldine base (EB) form of PANI, this approach can create an orderly distribution and homogeneous layer of PANI/N-Methyl-2-pyrrolidone (NMP) over MoS_2 allowing the nanocomposite to coat over conducting substrates. The targeted nanocomposite material was finally de-doped to convert the PANI to ES, the conducting form, and enhanced the supercapacitor performance. Finally, after understanding the interesting combined effects of the material's chemistry and capacitive properties in both two and three electrodes based electrochemical cells configuration and sponge based substrates was proposed for solid-state supercapacitor. The electrochemical deposition technique was applied, along with in-situ self-assembled polymerization of PPy and PANI, to fabricate the device. The morphological and crystal structures of the nanomaterials and nanocomposites of all projects were investigated by scanning electron microscopy (SEM), transmission electron microscopy (TEM), particle size analyzer (PSA), Raman spectroscopy, Fourier transform infrared (FTIR) spectroscopy, and X-ray-diffraction (XRD) techniques. In addition, the electrochemical properties of them were investigated to reveal their intriguing electrochemical and physicochemical properties using four-point probe, cyclic voltammetry (CV), constant current charging–discharging (CCCD), electrochemical impedance spectroscopy (EIS) in aqueous electrolytes. MoS_2/PANI/PPy nanocomposite materials were considered for ideal supercapacitors which rendered highest specific capacitance around 631 F g^{-1}. Owing to its superior electrochemical performance with the merits supercapacitors were produced for storing energy. This approach has

revealed the possibility of using the natural or synthesized porous substrate to obtain a high surface area based supercapacitor.

CHAPTER 1: INTRODUCTION

Since the late 20th century, supercapacitor technology has been one of the emerging research areas, due to the rapid growing demand in environmentally compatible energy storage devices [1-4]. This demand for the energy storage systems becomes more critical, especially when the whole society face an energy crisis [5]. Several types of energy storage devices include: fuel cells, conventional capacitors, supercapacitors and batteries. These devices can fulfill the needs of usage in the consumable and industrial electronic devices, as well as the transportation industry [6]. Supercapacitors are well known for their high capacitances and low internal resistances, which enable them to be charged rapidly and deliver the stored charges in very short times (i.e. high power densities). In contrast, batteries need more time to deliver the charges. The mechanism of charge storage in electric double-layer capacitors (EDLCs) is based on a physical charge storage at the electrode-electrolyte interface, that allows cycle lifetime to be higher than one million charging-discharging cycles, whereas the reversible chemical reactions in batteries is limited to only several thousand cycles [7]. Overall, the unique features in supercapacitors, such as high cycle life, age and wide working temperature, have made them suitable energy storage devices for many applications, particularly for devices being used in difficult to reach areas [2].

As shown in Figure 1.1, among various types of energy storage devices, supercapacitors cover a broader range of power density-energy density characteristics than batteries and capacitors [8] . This wide range of characteristics is due to a large number of material choices that can be used as the electrode and electrolyte of supercapacitors [4]. Also, it should be mentioned that with

constant development of new materials, especially composites, the range is expanding toward higher energy and power density values.

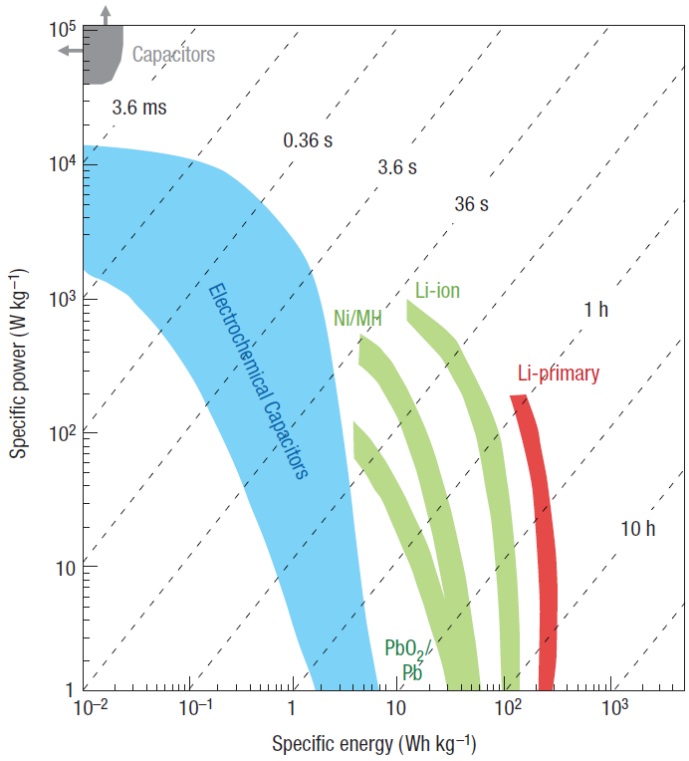

Figure 1.1 The specific power vs. specific energy for various types of energy storage device [8]. By Simon et al. © (2008) Springer Nature.

For practical applications, it is vital to have supercapacitors with high power and energy density, large cycle life time, and low cost. The key to fabricate devices with high performance is to employ nanocomposites and nanostructures in the electrodes. In general, significant features of different materials can be combined in a composite material to improve two or more aspects of the device. For instance, conducting polymers (CPs) have presented excellent capacitance densities due to the feasibility of storing charges via both double-layer and pseudocapacitive charge storage mechanisms, but their relative high resistivity hinders fabrication of large devices with a low internal resistance [9-12]. Also, the stability of CPs based electrodes is a concern for making devices with high cycle lifetime [10, 13]. To address the shortcomings of CPs, extensive researches have been done to develop composite of CPs with various nanomaterials. The applied

nanomaterials include different forms of carbon (i.e. carbon nanotubes (CNTs) [14-17] and graphene (G) [18-20]), metal oxide nanoparticles (i.e. Ruthenium(IV) oxide (RuO_2) [21, 22] and Manganese (IV) oxide (MnO_2) [23-25], and transition metal dichalcogenides (i.e. MoS_2 [25-28]). Designing a nanocomposite material for supercapacitor applications requires material characterization. Also, studying the interface between the composite and electrolyte is essential to optimize performance of supercapacitor devices.

The properly designed synthesis of the supercapacitor nanostructured electrode materials can be optimized not only for the power density but also the energy density, cycle number and lifetime. Besides, the nanostructure effect is prominent and unique to obtain high specific capacitance based on nanocomposite materials. This dissertation has enriched and nourished the relation between nanocomposite electrodes and supercapacitors for obtaining high specific capacitance, power density, energy density and cyclability. Emphasis has been given to discuss comprehensibility the implementation and effectiveness feasibility of various conducting polymers (polyethylenedioxythiophene (PEDOT), polyaniline (PANI), polypyrrole (PPy) and two dimensional transition metal dichalcogenides (molybdenum disulfide '(MoS_2)'-) nanomaterial based on nanocomposite electrodes for supercapacitor applications. Additionally, the fabrication, characterizations and testing of the sponge based supercapacitors fabricated from MoS_2/PANI/ PPy electrodes have been studied.

1.1 Objectives of the Dissertation

The development of sustainable energy technologies is also could be a history of finding new materials and composites with nanostructures which could enhance the capability of the supercapacitors or other energy storage systems. Transition metal dichalcogenides (TMDs) are a promising new class of materials that's being heavily investigated for remarkable properties. They

have d-electrons in the outermost electron shell, which tend to share them, that plays an important role in determining their properties. Transition metal atoms (M) form covalent chemical bonds with chalcogens (X). For the compounds, I am interested in here, each metal (M) bonds with two chalcogens (X), giving the generic chemical formula: MX_2. When covalent chemical bonds form TMDs, the transition metal readily transfers its electron to chalcogen atom, which essentially fills the chalcogen atoms valence shells with electrons. This fact is responsible for the highly planar structure of TMDs, in which single molecular units of MX_2 can make up two-dimensional layers. Strong molecular interlayer covalent bonds (coordination bonds) and weak molecular interlayer van der Waals bonds between the layers, give rise to their layered structure. Within the past decade, TMDs have become an intriguing and prominent material for both producing and storing energy due to the above properties and its ability to store charges in both EDLCs and pseudocapacitors [29, 30]. Whereas, CPs are one of the most interesting materials currently in the development today [31]. With its fascinating characteristics of outstanding electrical and thermal properties and highly specialized geometry, CPs are revolutionizing countless fields, with new applications continuously being discovered [32].

The objectives of this dissertation are:

- To explore new nanocomposite materials used for supercapacitor electrodes which could enhance the capability and performance of the supercapacitors.
- To overcome the obstacles of aggregation and solubility of 2D-TMDs and CPs by using surfactants and mutable oxidation states, which are significant factors of determining electrochemical properties.
- To apply various synthesis processes and characterization techniques to investigate the development of the next-generation electrodes including: chemical oxidative

polymerization, in-situ self-assembled polymerization and electrochemical deposition techniques. The physical and electrochemical properties were measured using equipment such as SEM, TEM, XRD, Raman spectroscopy, FTIR spectroscopy, PSA, CV, CCCD and EIS.

- To design a solid-state supercapacitor as a real device by an assembly of the multilayer films approach into a sponge substrate.

1.2 Organization of the Dissertation

The structure of this dissertation can be briefly outlined as follows.

Chapter 1 provides a brief overview to the energy storage devices and nanocomposite materials of supercapacitor electrodes, followed by information about objectives and organization of the dissertation.

Chapter 2 presents the basic principles and configuration of supercapacitors, as well as investigation of research activities and achievements on supercapacitor electrode materials. The last part of chapter 2 is devoted to the parts of supercapacitors, which determine their performance.

Chapter 3 focusses on the metrology and techniques used to evaluate the morphology, crystallinity, electrical and electrochemical properties of the electrode materials and the performance of supercapacitors.

Chapter 4 presents an innovative nanocomposite electrode which was chemically synthesized using MoS_2-polyethylenedioxythiophene (PEDOT) to understand the charge mechanism in a symmetric supercapacitor. The MoS_2-PEDOT nanocomposite was produced at various ratios of MoS_2 to ethylenedioxythiophene (EDOT) in an aqueous medium of polyanions polystyrene sulfonate (PSS) and cetyltrimethylammonium bromide (CTAB) at controlled conditions.

Chapter 5 describes the chemical oxidative polymerization, reduction/oxidation synthesis techniques, characterization and supercapacitor properties of processed polyaniline (PANI)-MoS_2 based nanocomposite materials. Further, the effect of doping and undoping of PANI to exploit the surface chemistry by uniformly covering MoS_2 nanosheets with PANI coating layers to enhance the supercapacitor performance.

Chapter 6 applies the results of the previous chapters to fabricate a sponge type supercapacitor by in-situ self-assembled polymerization of the monomers pyrrole and aniline on a sponge, followed by electrochemical polymerization of MoS_2-CPs nanocomposite to obtain the supercapacitor electrode. Further, different polyvinyl alcohol (PVA) gel is synthesized to obtain highly conducting electrolyte to fabricate the solid-state supercapacitor. The sponge type supercapacitor construction consists of two porous sponge electrodes, gel electrolyte, and membrane of paper that is sandwiched between the two sponge electrodes.

Chapter 7 concludes the study with the major findings of the biggest determiners of a supercapacitor's performance. This chapter also proposes future work recommendations for the development of the materials chosen as part of the design, as well as the fabrication process of the supercapacitor.

CHAPTER 2: LITERATURE REVIEW

2.1 Introduction

Due to the worlds demand for energy storage systems, there has been excitement in developing supercapacitors for electrical energy storage applications [6, 33]. The present research trend shows that this kind of mechanism is relatively new and possesses incredible potential for applications in not only supercapacitors, but also other applications such as aerospace, marine and mechatronics engineering [2].

The fabrication and design of supercapacitor devices and their associated working principles were presented in this chapter. Meanwhile, research activities and achievements on supercapacitor electrode materials are introduced as well as other supercapacitor cell components [1, 3, 34]. Designing an optimum supercapacitor strongly depends on the selection of electrode materials. Some important properties need to be met, such as long and stable cycle life, high conductivity, and a highly porous structure to increase the capacitance [35, 36].

2.2 Principles and Configuration of Supercapacitors

Electric charges in supercapacitors are stored either via formation of double-layer charges at the electrode-electrolyte interfaces or through the change in the oxidation state of the electrodes (i.e. pseudocapacitive storage) [37]. Devices that rely only on double-layer charge storage are called electric double-layer capacitors (EDLCs).

Supercapacitors that are made from electrode materials with more than one stable redox state are called pseudocapacitors. The following sections discuss the energy storage configurations of the supercapacitors.

2.2.1 Electric Double Layer Capacitance

The mechanism of charge storage in EDLC is based on ions adsorption, known as purely electrostatic operation, at the interference between the solid electrode and liquid electrolyte without any charge transfer across the interface (i.e. non-faradic reaction). An electrical double layer charge is created when an electrode makes an electrochemical interface with an electrolyte (Figure 2.1(a)). In a supercapacitor device, when the device is charged, positive and negative electronic charges accumulate on the surface of the positive and negative electrodes, respectively. The charges on the electrodes surfaces attract opposite ions to form the double-layer charges at the interface of the electrode-electrolyte. This process relies on the physical movement of ions from the bulk of the electrolyte to the electrode-electrolyte interfaces; and it is different than the charge storage in batteries where chemical reactions are involved [38].

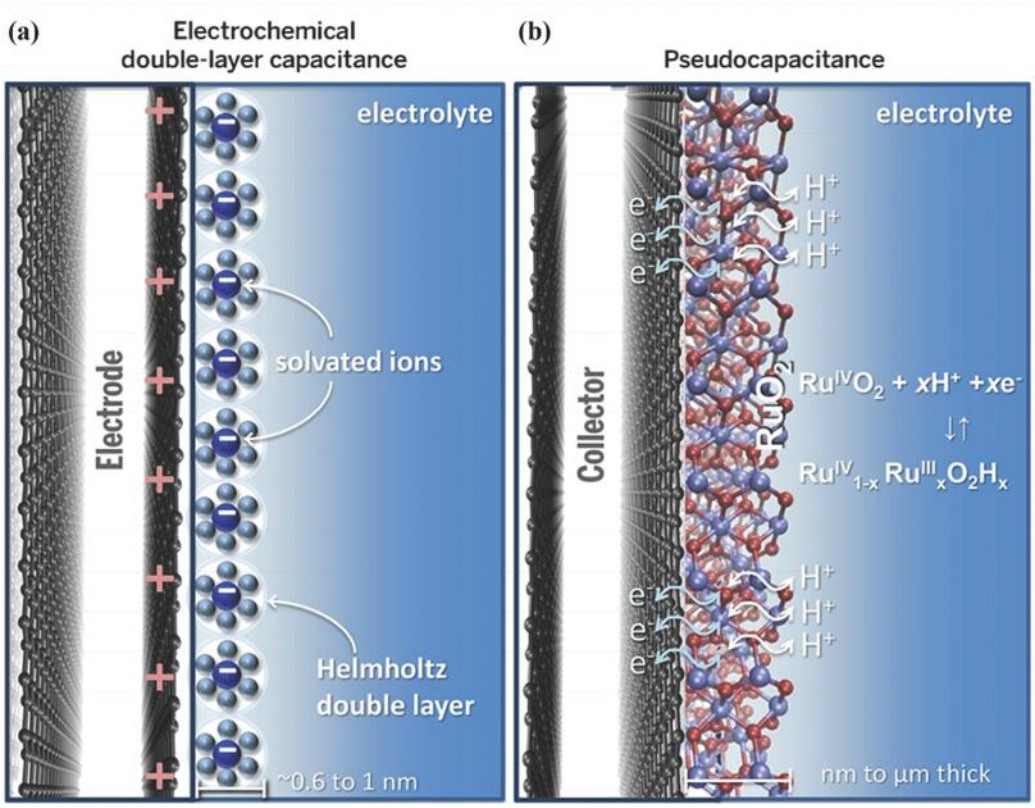

Figure 2.1 Schematic diagram illustrating the mechanism of charge storage in (a) EDLC and (b) pseudocapacitance [39]. By Bonaccorso et al. © (2015) The American Association for the Advancement of Science.

Due to the physical rearrangement of charges in EDLCs, the process of charging and discharging can be very fast; therefore, EDLCs have been utilized in systems that require peak power demand [40]. However, great attention has given to solve the problem of relatively low energy density by optimizing the existing materials and exploring new materials. For fabricating EDLC electrodes, it is required to use materials with stable redox states. Table 2.1 illustrates the recent electrochemical studies that have been used in EDLC electrode materials.

Table 2.1 Summary of the electrochemical performance based on various EDLC electrode materials.

Materials	Electrolyte	Current Density or Scan Rate	Potential Range (V)	Specific Capacitance ($F\ g^{-1}$)	Ref.
Activated carbon fabrics	6 M KOH	0.1 A g^{-1}	-1 to 0	205**	[41]
Activated carbon cloths	1 M H_2SO_4	1 mV·s^{-1}	0 to 0.8	227**	[42]
Activated carbon microspheres	6 M KOH	1 A g^{-1}	-1 to 0	275**	[43]
Activated carbons	1 M H_2SO_4	0.5 A g^{-1}	-0.2 to 0.8	401.6	[44]
Bowl-like monodispersed porous carbon nanoparticles	6.0 M KOH	0.5 A g^{-1}	-1.1 to -0.2	281**	[45]
Microporous carbons	EMI-TFSI	5 mV·s^{-1}	0 to 3	180*	[46]
Reduced graphene oxide	BMIM BF_4 EMIM TFSI	5.7 A g-1 0.7 A g-1	0 to 3.5	166* 200*	[47]
SW-CNTs	PVA/LiCl	1.32 A cm^{-3}	0 to 1	15.34* ($F\ cm^{-3}$)	[48]
Short SW-CNTs	1M Na_2SO_4	0.2 A g^{-1}	0 to 1	127*	[49]
MW-CNTs	6 M KOH	1 A g^{-1}	0 to 0.5	132*	[50]
MW-CNTs	1 M H_2SO_4	2 mV·s^{-1}	-0.2 to 1.1	278.5**	[51]
Porous graphene	6 M KOH	1 mV·s^{-1}	-1 to 0	261**	[52]
mesoporous perforated graphene	1M Na_2SO_4	2.28 A g^{-1}	0 to 1	458*	[53]
CNTs	1 M H_2SO_4	1 mV s^{-1}	0 to 0.8	43**	[54]
Ultra-microporous carbon nanoparticle	6 M KOH	2 A g^{-1}	-1 to 0	225**	[55]
Graphene	6 M KOH	2 mV·s^{-1}	-1 to 0	349**	[56]

Table 2.1 (Continued)

Materials	Electrolyte	Current Density or Scan Rate	Potential Range (V)	Specific Capacitance ($F\ g^{-1}$)	Ref.
Holey graphene oxide	1 M H_2SO_4	2 $mV \cdot s^{-1}$	0 to 1	301**	[57]
Graphene nanosheets	AMIM-DCA	5 $mV \cdot s^{-1}$	0 to 4	228**	[58]
Graphite	1 M Et_4NBF_4/PC	1 mA	0 to 3	12*	[59]

** Three-electrode cell system, * Two-electrode cell system
(KOH): Potassium hydroxide, (H_2SO_4): Sulfuric acid, PVA: Polyvinyl alcohol, LiCl: Lithium chloride, (EMIM TFSI): T ethyl-methyl- imidazolium bis(trifluormethylsulfonyl)imide, (BMIM BF_4): D 1-butyl-3-methyl-imidazolium tetrafluoroborate, Na_2SO_4: Sodium sulfate, (AMIM-DCA): 1-allyl-3-methylimidazolium dicyanmide, Et4NBF4: Tetraethylammonium-tetrafluoroborate/ propylene carbonate, and (PC): Propylene carbonate.

2.2.2 Pseudocapacitance

Unlike EDLCs, the mechanism of charge storage in pseudocapacitors is based on chemical reactions (i.e. Faradic reaction) at the electrode-electrolyte interfaces. The charge-storage mechanism involves the transfer of charges though the double layer. It is often accompanied by fast and reversible electron charge transfer between electrode and electrolyte, which originates from de-solvated and absorbed ion. In a pseudocapacitive charge storage device, the transferred charge to the electrode changes the oxidation state of the electrode material (Figure 2.1(b)). This provides additional capacitance to the double-layer effect and results in higher specific capacitances in pseudocapacitors than EDLCs.

To design a supercapacitor with high cycle lifetime, it is required to use a material with high stability at different oxidation states and reversible redox reactions. Although many metal oxide and transition metal dichalcogenides have shown promising characteristics for pseudocapcitor applications, electrodes fabricated with those materials are generally too expensive. Therefore, there is an interest to develop electrodes with conducting polymers, which are much cheaper, and have proven to be reliable materials for energy storage applications [32,

60]. Among various forms of CPs, poly(3,4-ethylenedioxythiophene) (PEDOT), polyaniline (PANI), and polypyrrole (PPy) have been studied extensively for applications in pseudocapacitors. Table 2.2 summarizes the electrochemical performance of these materials.

Table 2.2 Summary of the electrochemical performance based on various pseudocapacitance electrode materials.

Materials	Electrolyte	Current Density or Scan Rate	Potential Range (V)	Specific Capacitance ($F\ g^{-1}$)	Ref.
Ruthenium sulfide nanoparticles	0.5 M H_2SO_4	0.5 mA cm^{-1}	0 to 0.8	17* 85**	[61]
Manganese selenide nanoparticles	1 M Li_2SO_4	0.1 mA cm^{-1}	0 to 0.8	23.44* 96.76**	[62]
Iron oxide nanoparticles	1 M Na_2SO_3	0.5 A g^{-1}	−1 to 0.1	195.8**	[63]
RuO_2 Nanoparticles	1 M/L H_2SO_4	1 mV s^{-1}	0 to 0.8	648**	[54]
Porous manganese dioxide	0.5 M K_2SO_4	0.5 mA cm^{-1}	0 to 0.8	261**	[64]
MoS_2 ultrathin nanoflakes	0.5 M Na_2SO_4	5 mV s^{-1}	−0.1 to −0.8	576**	[65]
MoS_2 nanosheets	1 M Na_2SO_4	1 A g^{-1}	−0.8 to 0.2	129.2**	[66]
2D graphene analog MoS_2	1 M H_2SO_4	1 A g^{-1}	− 0.4 to 0.6	98**	[67]
Hollow MoS_2 nanospheres	1 M KCl	0.59A g^{-1}	−0.9 to −0.3	142**	[68]
3D flower like MoS_2	1 M KCl	1 A g^{-1}	−0.9 to −0.2	168**	[69]
MoS_2	1 M Na_2SO_4	1 A g^{-1}	−1 to 0	120**	[70]
PANI	1 M H_2SO_4	0.4 A g^{-1}	0 to 0.6	210*	[71]
PANI	1 M H_2SO_4	0.8 A g^{-1}	−0.2 to 1	131**	[72]
PANI	3 M NaOH	1 A g^{-1}	−0.4 to 0.6	316**	[73]
PPy nanopore array	1 M H_2SO_4	0.5 A g^{-1}	−1 to 0.5	114.2*	[74]
PPy nanobricks	0.5 M H_2SO_4	5 mV s^{-1}	− 0.4 to 0.6	476**	[75]
PPy	1 M H_2SO_4	1 A g^{-1}	−0.4 to 0.8	155*	[76]
PPy nanowire	0.5 M Na_2SO_4	1 A g^{-1}	−0.8 to −0.2	145**	[77]
PEDOT by ultrasonic irradiation	1 M H_2SO_4	5 mV s^{-1}	0 to 1	100*	[78]

Table 2.2 (Continued)

Materials	Electrolyte	Current Density or Scan Rate	Potential Range (V)	Specific Capacitance ($F\ g^{-1}$)	Ref.
PEDOT nanocapsules	1 M H_2SO_4	5 mV s^{-1}	0 to 1	170**	[79]
PEDOT nanotubes	1 M $LiClO_4$	100 mV s^{-1}	0 and 1.2	140**	[80]

** Three-electrode cell system, * Two-electrode cell system
Li_2SO_4: Lithium sulfate, Na_2SO_3: Sodium sulfite, KCl: Potassium chloride, NaOH: Sodium hydroxide, and $LiClO_4$: Lithium perchlorate.

2.2.3 Hybrid Capacitor

A hybrid capacitor is a combination of two types of electrodes (example: a DL carbon material and a pseudocapacitive material), which can be either be in an asymmetrical or a symmetrical configuration. One of them stores charge faradaically (redox reaction) and the other one stores charge electrostatically. Hybrid capacitors have a great advantage over other capacitors because they can operate with high temperatures and manufacturers use them for the equipment in oil and gas exploration. The other benefits come from the fact that they have high energy density and power, as opposed to electrolytic capacitors. The working voltage also can be increased as well as specific capacitance especially when pseudocapacitive materials are used as the cathode [81-83].

Naturally, a solid-state film of a conducting polymer has a porous structure which is suitable for supercapacitor applications. To enhance the porosity, the structure of the film can be engineered [84]. However, other factors such as the conductivity and stability of the film are important for practical applications. To address those, an emerging approach is to develop a composite of a conducting polymer and a nanostructure. Various types of capacitors have been investigated with electrodes made from these composite materials. The nanocomposites can yield to hybrid supercapacitor which can store charges via a redox reaction in addition to the double

layer form. Summary of the electrochemical performance based on various nanocomposite materials is shown in table 2.3.

Table 2.3 Summary of the electrochemical performance based on various nanocomposite electrode materials.

Materials	Electrolyte	Current Density or Scan Rate	Potential Range (V)	Specific Capacitance ($F\ g^{-1}$)	Ref.
PANI nanoparticles grew on 3D reduced graphene oxid framework	1 M H_2SO_4	0.5 A g^{-1}	0 to 0.8	438.8*	[85]
Cerium oxide nanoparticles/ MW-CNTs	6 M KOH	1 A g^{-1}	0 to 0.5	455.6*	[50]
Iron oxide nanoparticles/ MW-CNTs	3 M KOH	1 A g^{-1}	-1.3 to -0.3	787**	[86]
PANI/MW-CNTs	1 M H_2SO_4	2 $mV \cdot s^{-1}$	−0.2 to 1.1	540.29**	[51]
Polypyrrole/nanoporous gold	$HClO_4$/PVA	0.6 A g^{-1}	0 to 0.85	270*	[87]
RuO_2 nanoparticles/CNTs	1 M H_2SO_4	1 mV s^{-1}	0 to 0.8	953**	[54]
RuO_2 Nanoparticles graphene oxide	1 M H_2SO_4	2 $mV \cdot s^{-1}$	0 to 1	199* ($F\ cm^{-3}$)	[57]
RuO_2/PPy composite	0.5 M H_2SO_4	50 $mV \cdot s^{-1}$	−0.6 to 0.6	657**	[88]
Graphite/PEDOT/MnO_2 Composites	0.5 M Na_2SO_4	0.5 A g^{-1}	−0.2 to 0.8	195.7**	[89]
MWNTs/TiO_2/PANI	1 M H_2SO_4	0.4 A g^{-1}	0 to 0.6	270*	[71]
PPy/PANI coaxial nanoarray	1 M H_2SO_4	0.5 A g^{-1}	−1 to 0.5	209.5*	[74]
Reduced graphene oxide/carbon nanoparticles/PANI composite	1 M H_2SO_4	1 A g^{-1}	−0.2 to 0.8	787.3**	[90]
3D Manganese oxide/PANI/graphene hybrid material	1 M H_2SO_4	1 A g^{-1}	−0.2 to 0.9	321.7**	[91]
3D ternary nanocomposites of MoS_2/PANI/reduced graphene oxide aerogel	1 M Na_2SO_4	1 A g^{-1}	−0.8 to −0.2	618**	[92]
Layered MoS_2/graphene composites	1 M Na_2SO_4	1 A g^{-1}	−1 to 0	243**	[70]
MoS_2/PANI nanocomposite	1 M H_2SO_4	0.8 A g^{-1}	−0.2 to 1	390**	[72]

Table 2.3 (Continued)

Materials	Electrolyte	Current Density or Scan Rate	Potential Range (V)	Specific Capacitance ($F\ g^{-1}$)	Ref
Carbon Nanoparticles/PANI	1 M Na_2SO_4	1 A g^{-1}	0 to 0.8	147**	[93]
Silver nanoparticle/PANI/short MWNTs nanocomposites	3 M NaOH	1 A g^{-1}	−0.4 to 0.6	615**	[73]
Graphene/polypyrrole nanoparticle hybrid aerogels	1 M KOH	0.5 A g^{-1}	-0.9 to -0.1	418**	[94]
Reduced graphene oxide–PPy–MnO_2 composites	1 M NaCl	1 A g^{-1}	−1 to 0	356**	[95]
3D tubular MoS_2/PPy nanowire composites	0.5 M Na_2SO_4	1 A g^{-1}	-0.8 to -0.2	462**	[77]
PEDOT/nickel ferrite nanocomposite	1 M $LiClO_4$	1 mA cm^{-2}	0 to 1	251**	[96]
MoS_2/PEDOT nanocomposite	1 M H_2SO_4	0.8 A g^{-1}	−0.2 to 0.8	405**	[97]
MoS_2/ tungsten trioxide nanorod	1 M H_2SO_4	0.5 A g^{-1}	0 to 0.6	522**	[98]
MoS_2/nickel ferrite nanoparticle	1 M KOH	1 A g^{-1}	0 to 0.45	506**	[99]
Polyindole/ carbon black/MoS_2	1 M H_2SO_4	1 A g^{-1}	0 to 0.8	442**	[100]
porous tubular C/MoS_2 nanocomposites	3 M KOH	1 A g^{-1}	0 to 0.5	210**	[101]

** Three-electrode cell system, * Two-electrode cell system
$HClO_4$: Perchloric acid.

2.3 Design of Supercapacitors

A cross-section of two-electrode supercapacitor cell is seen in Figure 2.2. The cell contains two identical electrodes held apart by a separator and electrolyte and both are connected to current collectors. In order to enhance the supercapacitor properties, we needed to determine the functionality and material characteristics of each component which are also discussed in this section.

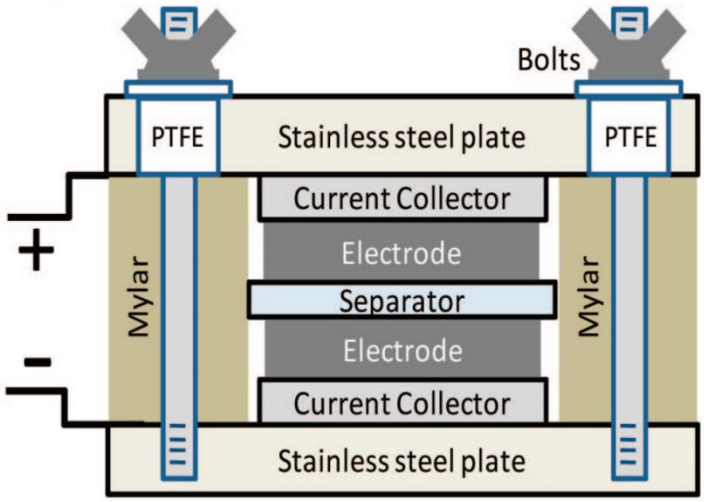

Figure 2.2 A cross-sectional view of two-electrode supercapacitor cell [102]. By Stoller et al. © (2008) American Chemical Society.

2.3.1 Supercapacitor Based on Electrode Materials

Several prominent electrode materials such as conducting polymers (polyaniline, polythiophene, polyethylenedioxythiophene, polypyrrole, etc.), transition metal dichalcogenide (molybdenum disulfide MoS_2), metal oxide (manganese oxide, ruthenium oxide), and carbon based materials (activated carbon, carbon nanofibers, carbon nanotubes, graphene, etc.) have been used for achieving the high-performance of electrochemical energy storage devices [103]. However, recent advancement has shown the use of nanomaterials and their composites to achieve superior electrochemical properties (capacitance, power and energy) to facilitate nanocomposite electrode materials for supercapacitor applications [83]. Here we have reviewed promising materials that have been studied for fabricating electrode materials for supercapacitors.

2.3.1.1 Carbon-Based Materials

Carbon is one of the main components of electrodes for EDLCs. This is mainly due to the high chemical resistance of carbon in almost any electrolyte, as well as abundance of the material [104]. Among different forms of carbon materials, the most commonly used are activated carbons, carbon nanofibers, carbon nanotubes, and graphene. To achieve high capacitances, it is desired to

use highly porous carbon structures [105]. However, the size of pores is required to be large enough for facile diffusion of ions. On the other hand, too much of porosity results in poor conductivity, which negatively affects the power density of EDLCs.

2.3.1.1.1 Activated Carbon

Activated carbon (AC) consists mostly of pure carbon and is known as one of the most adsorbent materials. AC has been used widely as an electrode material for supercapacitors due to its good electrical properties and low cost. The main aspect of activated carbons is their porous characteristic, which results in immense surface area, but only small specific capacitance. Other factors influencing the specific capacitance are electrical conductivity, accessibility of the electrolyte, as well as pore size distribution. AC also is used widely as adsorbent and is well known for its low chemical reactivity with adsorbed materials [106].

In terms of renewable nature and economic scalability, many studies have been done to fabricate activated carbon electrode materials by recycling waste products. For instance, Zhi et.al prepared waste tire-derived activated carbon (WTAC) as a precursor via the pyrolysis and chemical activation processes (Figure 2.3(a)). These effective synthetic methods revealed a specific capacitance of about 70 F g^{-1} at 10 A g^{-1} with 97% reserved capacitance over 1000 cycles, which indicated that the AC supercapacitor can be run in practice (Figure 2.3(b)) [107]. Furthermore, natural precursors (e.g., corn grain, potato starch, coconut shell, banana fiber, wood, etc.) have been used to produce activated carbon [108]. The schematic in Figure 2.3(c) illustrates how porous activated carbon materials can be produced from microalgae and glucose to fabricate supercapacitor electrodes [109]. The low-cost hydrothermal carbonization, along with chemical activation processes, have been applied to synthesis N-doped porous carbon materials with sponge-

like particles, as shown in the SEM image in Figure 2.3(c). In this structure, a specific capacitance as high as 200 F g^{-1} was found with an excellent long-term cycling stability.

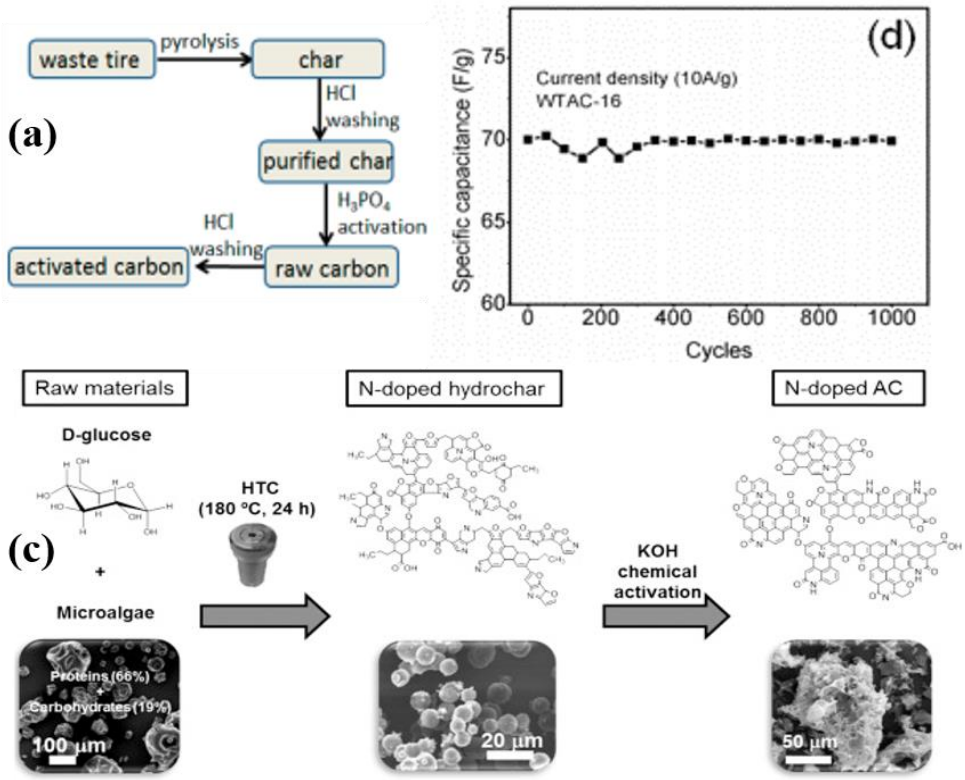

Figure 2.3 (a) Flow chart showing the preparation of activated carbon with waste tire, (b) the specific capacitances vs cycle numbers and (c) schematic reveals how porous carbon materials were produced from the microalgae [107, 109]. By Zhi et al. © (2014) American Chemical Society and Sevilla et al. © (2014) Elsevier.

2.3.1.1.2 Carbon Nanotubes

Carbon Nanotubes (CNTs) are well known as materials that are highly applicable in supercapacitor materials [110]. Some of the best aspects of CNT's are superb electronic conductivity and mechanical strength, as well as being relatively inexpensive.

CNTs can be synthesized in either single-walled nanotube (SWNT) or multi-walled nanotube (MWNT) forms. Both have been extensively used in fabricating energy storage devices. The structure of each type depends on the number of graphene layers being rolled to make nanotubes. SWNT is a single graphene layer being rolled, whereas MWNT is a coax structure of

multiple rolled layers. Supercapacitor performance and properties for both CNT types have drawn remarkable attention especially in designing and fabricating flexible devices [48, 111, 112].

Kaempgen et. al., have made flexible SWNTs-based supercapacitors using both aqueous gel and organic liquid electrolytes (Figure 2.4(b)) [111]. TEM was used to investigate the surface morphology and confirm MWCNTs exfoliation, as shown in figure 2.5. The structural changes of the MWCNTs after the oxidation yielded a higher specific capacitance due to the increase of effective surface area and water solubility in exfoliated MWCNTs. The resulting electrochemical properties of exfoliated MWCNTs revealed very high specific capacitance and columbic efficiency, with a long-term stability compered to MWCNTs, as shown in Figure 2.5.

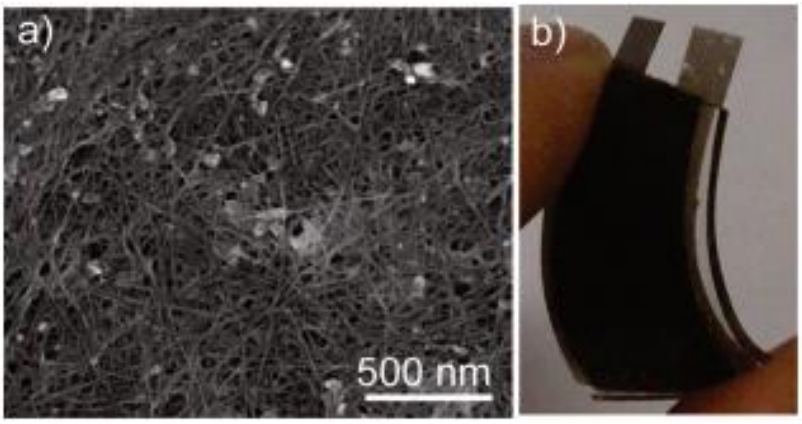

Figure 2.4 (a) SEM of SWCNT networks and (b) the flexible SWNTs supercapacitors [108]. By Kaempgen et al. © (2009) American Chemical Society.

Wang et. al., deposited exfoliated MWCNTs (Ex-CNT), graphene and MWCNT on carbon cloth to fabricate supercapacitor electrodes [113]. In order to investigate the surface morphology and confirm MWCNTs exfoliation TEM test was applied as shown in figure 2.5. The structural changes of the MWCNTs after the oxidation which yielded to a higher specific capacitance due to the increase of effective surface area and water solubility in exfoliated MWCNTs. The resulting electrochemical properties of exfoliated MWCNTs revealed very high specific capacitance and columbic efficiency with a long-term stability compered to MWCNTs as shown in Figure 2.5.

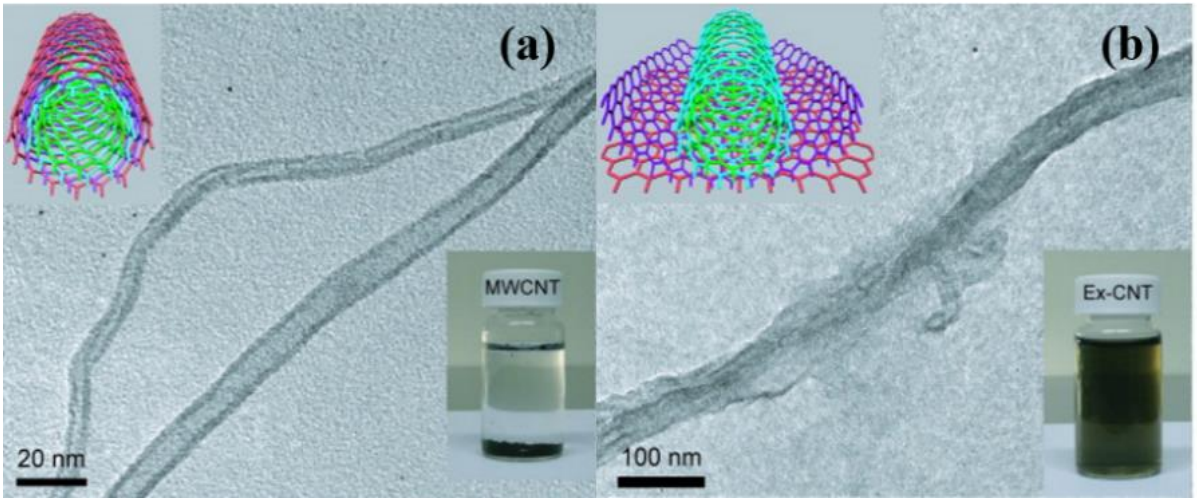

Figure 2.5 TEM of (a) MWCNTs and (b) Ex-CNTs. Insets: pictures of MWCNTs and Ex-CNTs dispersed in aqueous solution, and the schematic diagrams of MWCNT and Ex-CNT [110]. By Wang et al. © (2011) Elsevier.

2.3.1.1.3 Graphene

Graphene is an emerging material for supercapacitor applications [114]. Graphene is a single layer of pure carbon bonded together in a hexagonal honeycomb lattice. Its large surface area per mass and high electronic conductivity are the promising features for energy storage applications [115]. The results of some studies stated that graphene is an eco-friendly material [116-118]. However, graphene has been also considered as a health hazard material based on other studies[119, 120]. Additionally, it is feasible to fabricate graphene based electrodes for flexible and chemically stable devices [121, 122]. They can also withstand a lot of charging cycles. Table 2.4 gives a comparison between the properties of graphene and other carbon materials [123].

Table 2.4 A comparison between the properties of graphene and other carbon materials [120]. By Wu et al. © (2012) Elsevier.

Carbon allotropes	Graphite	Diamond	Carbon nanotube	Graphene
Hybridization	sp^2	sp^3	Mainly sp^2	sp^2
Crystal system	Hexagonal	Octahedral	Icosahedral	Hexagonal
Dimensions	3	3	1	2
Experimental specific surface area (m^2 g^1)	~10–20	20–160	~1300	~1500
Density (g cm^3)	2.09–2.23	3.5–3.53	>1	>1

Table 2.4 (Continued)

Carbon allotropes	Graphite	Diamond	Carbon nanotube	Graphene
Optical properties	Uniaxial	Isotropic	Structure dependent properties	97.7% of optical transmittance
Thermal conductivity ($W\ m^{-1}\ K^{-1}$)	1500–2000 (a-direction), 5-10 (c-direction)	900–2320	3500	4840–5300
Hardness	High	Ultrahigh	High	Highest (single layer)
Tenacity	Flexible non-elastic	–	Flexible elastic	Flexible elastic
Electronic properties	Electrical conductor	Insulator, semiconductor	Metallic and semiconducting	Semimetal, zero-gap semiconductor
Electrical conductivity ($S\ cm^{-1}$)	Anisotropic, $2–3 \times 10^4$ (a-direction) 6 (c-direction)	–	Structure-dependent	2000

A challenge in using only graphene is the tendency of graphene sheets to restack back to graphite. This is due to the hydrophobic nature of graphene. A study [124] on graphene material reported the fabrication of coin shaped graphene based supercapacitor device, with the structure shown in Figure 2.6. The supercapacitor was made by mixing 2D graphene material with a 10% polytetrafluoroethylene (PTFE) solution then separated by a thin polypropylene film and sandwiched between Ni foam current collector electrodes. The atomic force microscopy (AFM) image (Figure 2.6(a)) indicates the thickness of a single layer carbon sheets to be ~1.2 nm, and the small dots in the AFM and SEM images (Figure 2.6(b & c)) suggest a low degree of agglomeration and wrinkle compared with other studies of graphene. The enhancement of electrode and electrolyte interface led to better electrochemical performance in the supercapacitor.

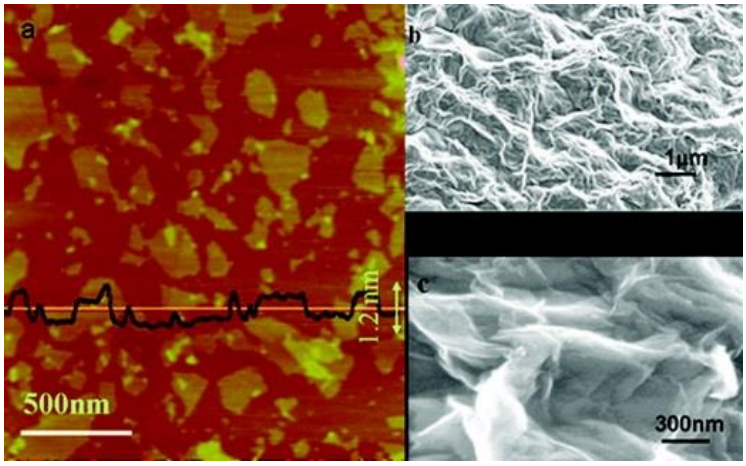

Figure 2.6 (a) AFM and (b & c) SEM images of graphene [121]. By Wang et al. © (2009) American Chemical Society.

2.3.1.2 Transition Metal Oxide

Transition metal oxides (TMOs) (example: MnO_2, RuO_2, SnO_2, WO_3, Fe_2O_3, ZnO etc.) have been used for fabrication of supercapacitors [125-129]. TMO's valuable trait is its high conductivity, availability, synthesis process, and recyclability. Besides, it has also long operation time and shows larger specific capacitance. RuO_2 is the most prominent materials used in supercapacitor applications due to high specific capacitance, power and energy densities.

2.3.1.2.1 Ruthenium Oxide

Ruthenium oxide (RuO_2) in its hydrous form is considered to be superior to other materials such as conducting polymers and carbon due to its higher specific capacitance. Among outstanding features of RuO_2, its stable multiple redox states and metal-like conductivity are the main reasons of interest to their applications for supercapacitors [130].

Zheng et al., synthesized 2D RuO_2 using a sol-gel technique and fabricated electrodes by mixing RuO_2 powder with 5 wt % Teflon binder [131]. The electrodes were annealed at 150° C and then tested in aqueous 0.5M H_2S0_4 electrolyte at 2 mV s^{-1} scan rate. They showed specific capacitance as high as 720 F g^{-1}. Their experiments also presented ~90% stability of the electrode after 4000 cycles of charging-discharging test.

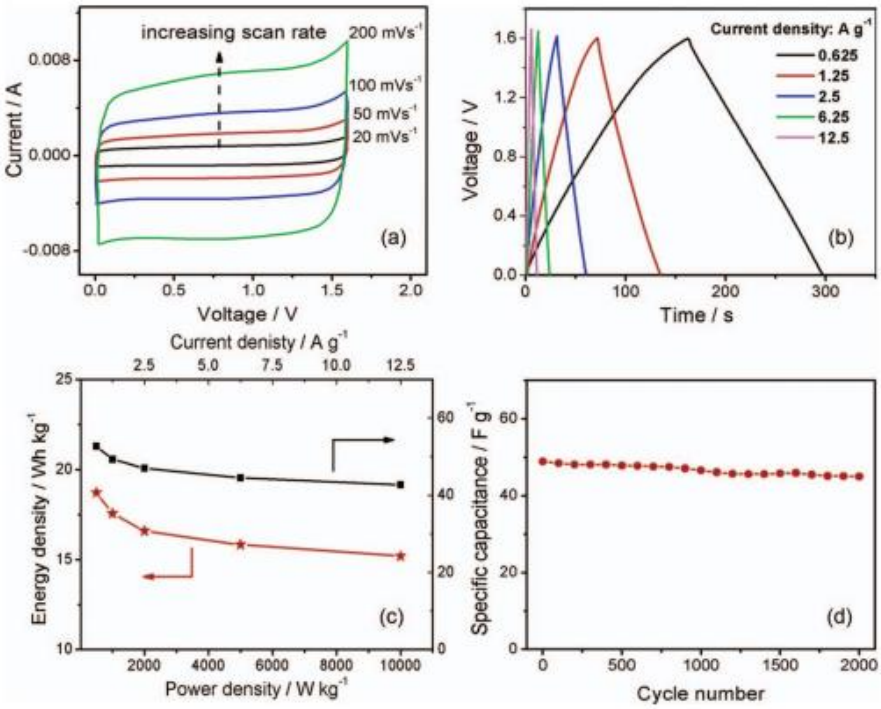

Figure 2.7 Electrochemical characterization of the symmetric RuO_2/RuO_2 supercapacitor [129]. By Xia et al. © (2012) The Electrochemical Society.

In another study by Xia el al., a nanocrystalline hydrous RuO_2 was used to fabricate a symmetric RuO_2/RuO_2 supercapacitor with a wide voltage widow (1.6 V) [132]. Figure 2.7 (a & b) shows the cyclic voltammetry and galvanostatic charging–discharging at constant current at different rates and current densities of a symmetric RuO_2/RuO_2 supercapacitor. Both three-electrode cell and two-electrode cell were used in aqueous Na_2SO_4 electrolyte. They showed specific capacitance as high as 236.1 F g^{-1} and 52.66 F g^{-1} and with good electrochemical stability around 92% of the initial capacitance as shown in Figure 2.7 (b).

However, despite the promising results from RuO_2, the major downside is the high cost of the material. A solution for reducing the cost is to employ the material in a composite.

2.3.1.3 Transition Metal Dichalcogenides

Transition metal dichalcogenides are known as layered two-dimensional materials. Examples of most commonly used transition metal dichalcogenides for the electrodes are MoS_2,

molybdenum diselenide ‘$MoSe_2$’, tungsten disulfide ‘WS_2’, and titanium disulfide ‘TiS_2’. Among them, MoS_2 has attracted recent attention as one of the best electrode materials because of a combination of physicochemical and electrochemical properties, such as redox active structures with wide range of oxidation states (+2 to +6) as well as high specific surface area [133, 134]. MoS_2 can be produced with various methods such as ultrasonic treatment in specially chosen solvents, mechanical peeling and chemical vapor deposition [26, 135-137]

2.3.1.3.1 Molybdenum Disulfide

Molybdenum Disulfide (MoS_2) is considered as an excellent candidate material for electrochemical energy storage. One of the most valuable characteristics of MoS_2 is its high catalytic activity, which can also be used in hydrogen generation and sodium/lithium batteries [138-140].

Recently, enormous research interest has been attracted toward MoS_2 as a suitable electrode material for supercapacitor and batteries applications[141]. Flower-like morphology of the MoS_2 is the most studied morphology [141]. In one method developed by Wang et al., the hydrothermal method was applied for the MoS_2 nanostructure synthesis [69]. The morphology of the flower-like MoS_2 is shown in the low/high magnification SEM images (Figure 2.8 (a & b)). Uniform 3D MoS_2 nanostructures with 300–500 nm diameters were composed of intercrossed curved nanoflakes. Electrodes made of such structures presented specific capacitance of 168 F g^{-1} in 1 M KCl aqueous solution electrolyte. Also, a long-term stability of ~92.6% after 3000 cycles was obtained at a current density of 1 A g^{-1}.

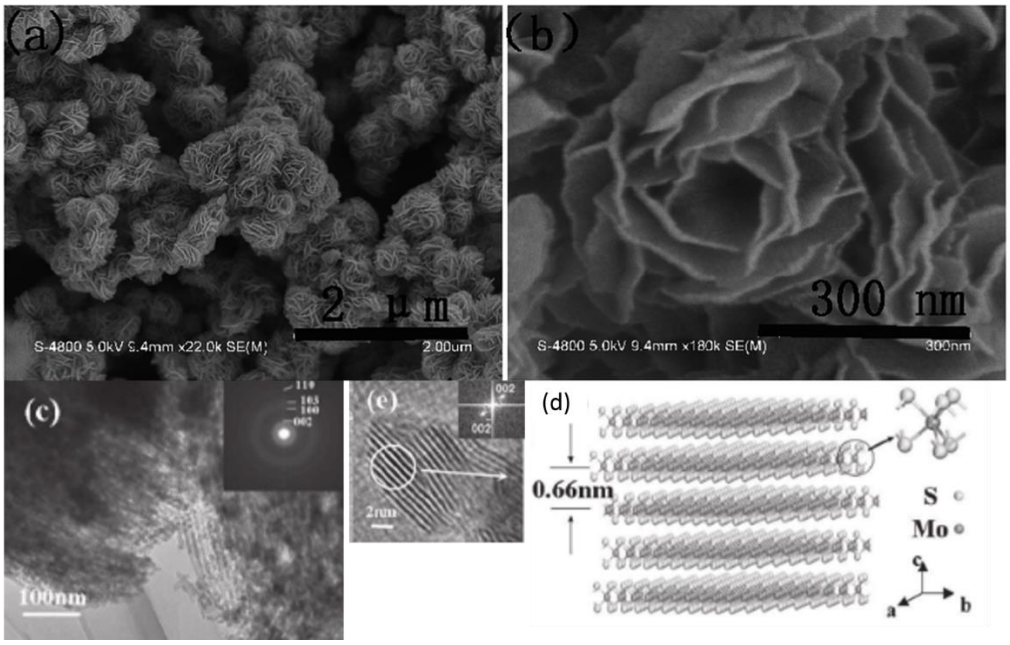

Figure 2.8 (a & b) Low/high magnification SEM images of the flower-like MoS_2 and (c, d & e) HTEM and atomic construction of MoS_2 solid-state phase [70, 139]. By Wang et al. © (2014) Royal Society of Chemistry and Liu et al. © (2012) John Wiley and Sons.

Another important factor of MoS_2 is the d-spacing, which controls ion diffusion in MoS_2. An expanded d-spacing of 0.66 nm has been demonstrated in a study by Liu and co-worker [142]. Figure 2.8 (c) shows TEM images of highly porous MoS_2 as well as its layered lattice structure. A rod-like MoS_2 with a lattice spacing of 0.66 nm, corresponding to (002) crystal plane, is shown in Figure 2.8 (d). The fabricated structure had a specific charge density of 608 mA h g^{-1} at 10 A g^{-1} in a non-aqueous electrolyte. However, the low bulk conductivity of MoS_2 thin films is a major weakness of the material [143, 144]. The problem can be addressed by using nano-sized MoS_2 or in nanocomposite materials (will be discussed in details in this dissertation).

2.3.1.4 Conducting Polymers

Like TMOs, conducting Polymers (CPs) are able to store charges via pseudocapacitive effect. CPs are organic materials that have attracted researchers' interest due to their conductivity, low cost, simple synthesis methods and electrochemical properties. The conduction mechanism in CPs relies on the conjugated structure at the backbone of the polymer chains. Some of the valuable

characteristics of CPs are high charge density, reversible faradaic redox nature and fairly low cost in comparison to metal oxides and transition metal dichalcogenides [10]. Among many different CPs, a few polymers that have been studied extensively for various applications are: polyaniline (PANI), polyethylenedioxythiophene (PEDOT) and polypyrrole (PPy). The chemical structure of these polymers is shown in Figure 2.9.

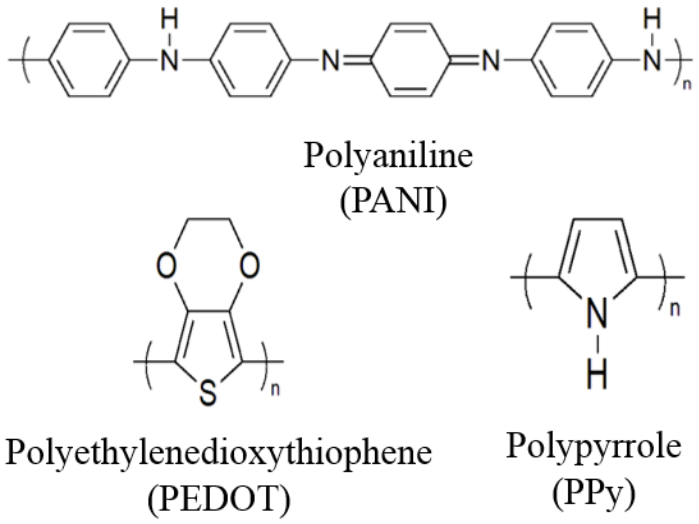

Figure 2.9 Chemical structures of polyaniline, polyethylenedioxythiophene and polypyrrole.

In situ self-assembly, photochemical polymerization electrochemical polymerization, and chemical vapor deposition are examples of CPs' synthesis techniques [145, 146]. Also, various forms of CPs such as nanorods, bulk powder, nanowalls and nanosheets can be fabricated [12]. Due to these fascinating characteristics, CPs have been utilized as a new, but competitive material for fabrication of electrodes for supercapacitance. One drawback of CPs it that they can suffer from cycling degradation due to the mechanical stress on them during charge-discharge cycles [147].

2.3.1.4.1 Polyethylenedioxythiophene

Polyethylenedioxythiophene (PEDOT) is an excellent conjugated polymer that has been extensively studied due to its outstanding chemical and electrochemical stability compared to other

CPs. Some of the advantages of PEDOT include superior conductivity, even in the undoped state, and larger electrochemical window among all CPs, as well as a low band gap of ~1.5 eV [148]. These remarkable features inspired researchers to investigate PEDOT based supercapacitors [78, 149-151]. The structure and morphology of CPs is an important factor that can influence the properties and performance of these materials in solid-state forms. The nanostructured CPs (example: nanorods, nanotubes, nanowalls, nanofibers, etc.) can enhance their electrochemical stability [152]. For instance, Laforgue [153] have obtained PEDOT nanofibers (diameters ~350 nm) using electrospinning and vapor-phase polymerization methods to fabricate textile flexible supercapacitors. The resulting supercapacitor displayed very high flexibility and conductivity, with long-term stability but low supercapacitor performance compared to the previous materials.

In another work, Liu et al. demonstrated that engineering the structure and morphology of PEDOT can dramatically improve both the electrochemical performance and stability of the material [80]. In their method, PEDOT nanotubes were synthesized electrochemically in a porous alumina template. Following the template structure, the PEDOT electrode had a high level of porosity with convenient paths for fast diffusion of ions. Consequently, high power and energy densities of 25 kW kg^{-1} and 5.6 W h kg^{-1} were reached with a potential window of 1.2 V.

2.3.1.4.2 Polyaniline

Polyaniline (PANI) is known as one of the most promising conducting polymers for positive electrode in energy storage devices [151, 154, 155]. Some of the most promising features of PANI are its low cost, excellent conductivity, doping-dedoping characteristics, as well as variable oxidation states. PANI can achieve the maximum doping level of 0.5 of p-typed PANI with a capacitance up to 240 F g^{-1} in an acidic electrolytes [10]. PANI can undergo electrical and

chemical synthesis with use of materials such as flexible substrates, nickel, carbon and stainless steel [156].

The wide range in the specific capacitance of PANI based supercapacitors is due to several important factors such as polymer morphology, synthesis method, mass loading and type of binders. This makes PANI the have the most variable specific capacitance compared to other CPs. For instance, Fusalba et al prepared a PANI based supercapacitor using an electrochemical method with carbon paper electrodes, and measured the specific capacitance to be 150 F g^{-1} in a nonaqueous electrolyte [155]. In another work, PANI doped with HCl and $LiPF_6$ was synthesized chemically by Ryu et al [157].

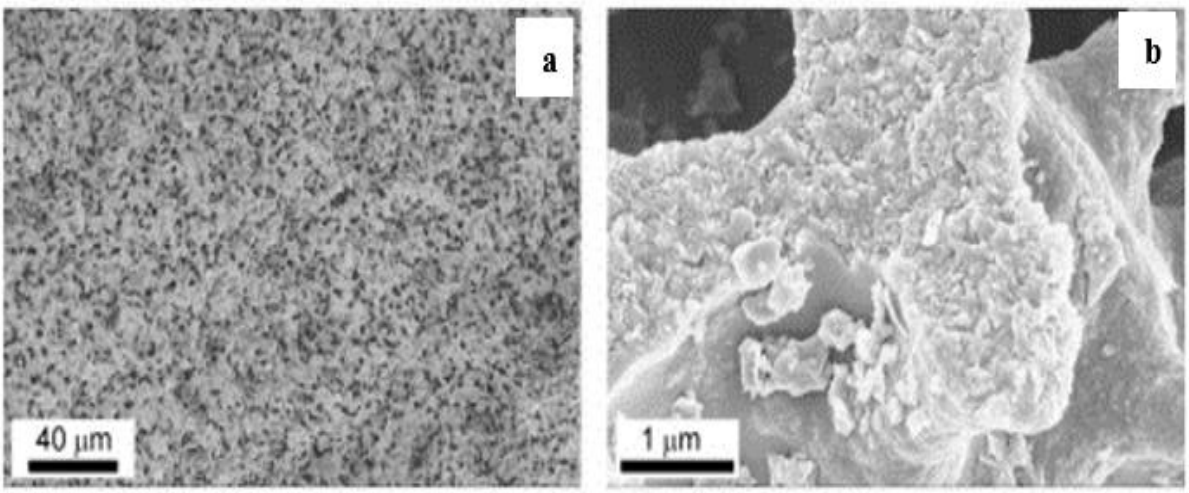

Figure 2.10 Scanning electron microscopy (SEM) images of (a & b) PANI+HPCM [155]. By Fan et al. © (2007) John Wiley and Sons.

The stability and electrochemical performance of PANI can be enhanced by using parent templates as a porous support. The SEM image in Figure 2.10 shows that the PANI particles (average sizes of around 50 nm) were deposited on a hierarchically porous carbon monolith (HPCM) that was used as a support, and to make it more stable with high capacitance [158]. The cycling performance was investigated at different discharging currents, and only showed a 7% loss

compared to the original specific capacitance. Additionally, no binder was needed for the electrode fabrication, which can reduce the fabrication cost.

2.3.1.4.3 Polypyrrole

Polypyrrole (PPy) is yet another p-type CP that has been used extensively for supercapacitor applications [159-163]. It is also considered as one of the promising for Faradaic pseudocapacitor applications. PPy is also known for its fast charge and discharge mechanism, high energy density and conductivity, low cost, as well as good thermal stability.

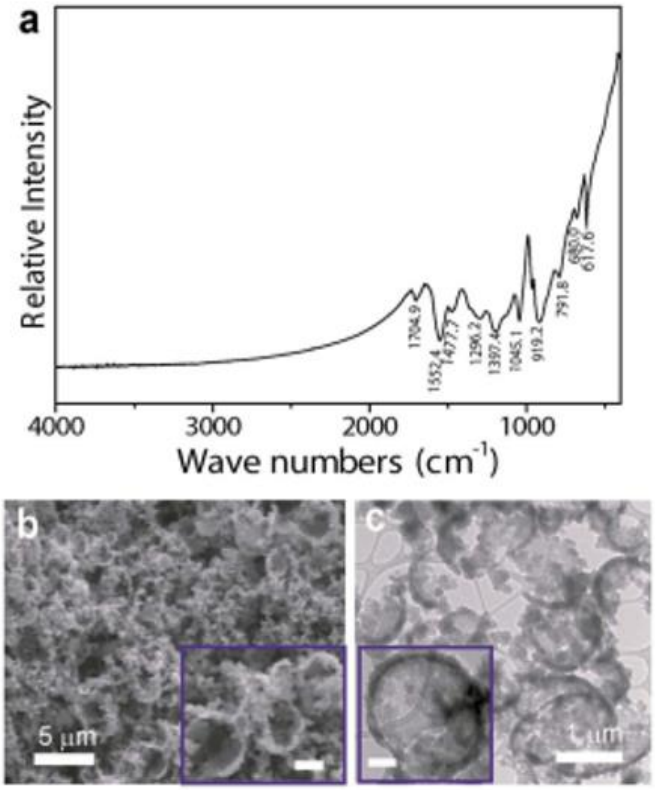

Figure 2.11 (a) The FTIR spectrum of the as-synthesized conductive polypyrrole (PPy) hydrogel, (b) SEM image showing the microstructure of a piece of dehydrated hydrogel and (c) TEM image showing the top view [161]. By Wang et al. © (2014) Royal Society of Chemistry.

Recently, PPy hydrogels have been used in the production of flexible electrodes by Shi et al [164]. Nanostructured PPy was obtained via interfacial polymerization technique. The absorption peak of FTIR spectra shown in Figure 2.11(a) confirmed the formation of PPy. The 3D

porous structure of PPy with hollow spheres is shown in SEM and TEM images shown in Figure 2.11 (b and c), respectively. The specific capacitance of the flexible symmetric PPy hydrogel supercapacitors was ~380 F g^{-1} using PVA–H_2SO_4 as the electrolyte.

Flexible PPy coated papers have been fabricated via chemical oxidative polymerization as shown in Figure 2.12(a). This method can be used for making highly conductive paper-based electrodes at a very low cost [163]. The tape test was applied to investigate the mechanical adhesion of PPy film as shown in Figure 2.12(b). The PPy film showed strong mechanical property of the PPy film (Figure 2.12(c)). The measured electrical conductivity of the PPy coated paper was (15.0 S cm^{-1}) which was higher than the pure PPy film (1.14 S cm^{-1}) [165]. The flexible PPy/paper supercapacitor exhibited high energy density and power density, with values of 1 mW h cm^{-3} and 0.27 W cm^{-3}, respectively.

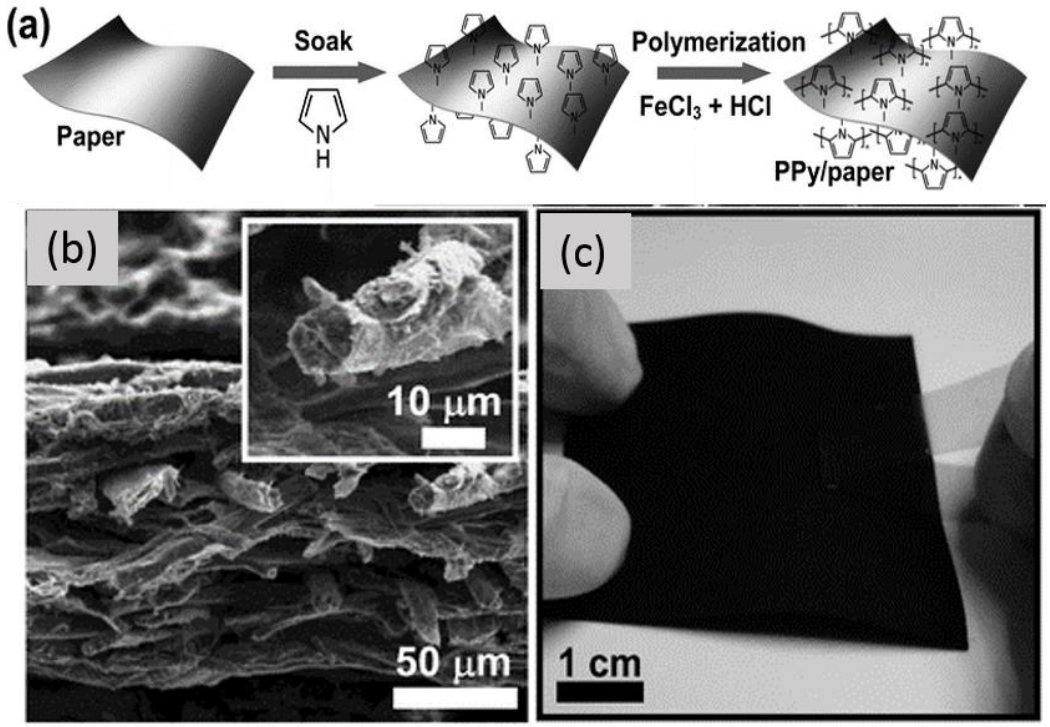

Figure 2.12 (a) The fabrication method of PPy coated papers, (b) a cross-section SEM image of PPy coated papers and (c) the tape test on the PPy film [160]. By Yuan et al. © (2012) Royal Society of Chemistry.

However, the main drawback of using CPs in general is poor cycling and stability due to volume change and chemical/mechanical degradation during repeated doping and de-doping processes [147]. One of the ways to mitigate this problem is by fabricating nanocomposite materials, which are discussed in the next section.

2.3.1.5 Nanocomposite Materials

Nanocomposite materials have been used widely for fabricating electrodes of commercial supercapacitors [166]. However, non-composite materials have some limitations. For instance, conductive polymers (CPs) can have higher specific capacitances than carbon-based materials, but generally they have lower cycle stability. The stability issues in CP based electrodes can be addressed by formation of a nanocomposite with graphene [102, 167]. RuO_2 also possesses high specific capacitance [168], but electrodes made of only RuO_2 are extremely expensive. A composite of a CP and RuO_2 offers a promising combination of superior capacitance performance with cycle stability [169]. Hence, in recent years, extensive research has been conducted to study and develop composite materials for commercial applications in supercapacitors.

2.3.1.5.1 Conducting Polymers/Metal Oxide

Due to the unique features of CP and TMO composites, these new materials are considered next generation materials. Their ability to provide higher pseudocapacitance through bulk redox reactions and the enhanced conductivity of the material are very promising properties [169, 170]. Another benefit is that their price is much lower than a pure TMO-based electrode.

In 2008, Zang et al proved that RuO_2 can enrich the capacitance of a CP [170]. The capacitance of well-aligned cone-shaped nanostructured polypyrrole showed an increase of three times after coated with a thin layer of RuO_2. Another study showed the same effect, where the specific capacitance was increased by loading hydrous RuO_2 particles in a PEDOT-PSS film

(Figure 2.13 (a & b)) [171]. The combination of both materials can enhance features of each component and create an excellent material. In addition, CPs can reduce the aggregation of some TMOs via steric and electrostatic stabilization mechanisms, which enhance the distributing properties of TMOs on the CP matrix, as well as mechanical adhesion of the CP and TMOs in the composite and to the current collector [171].

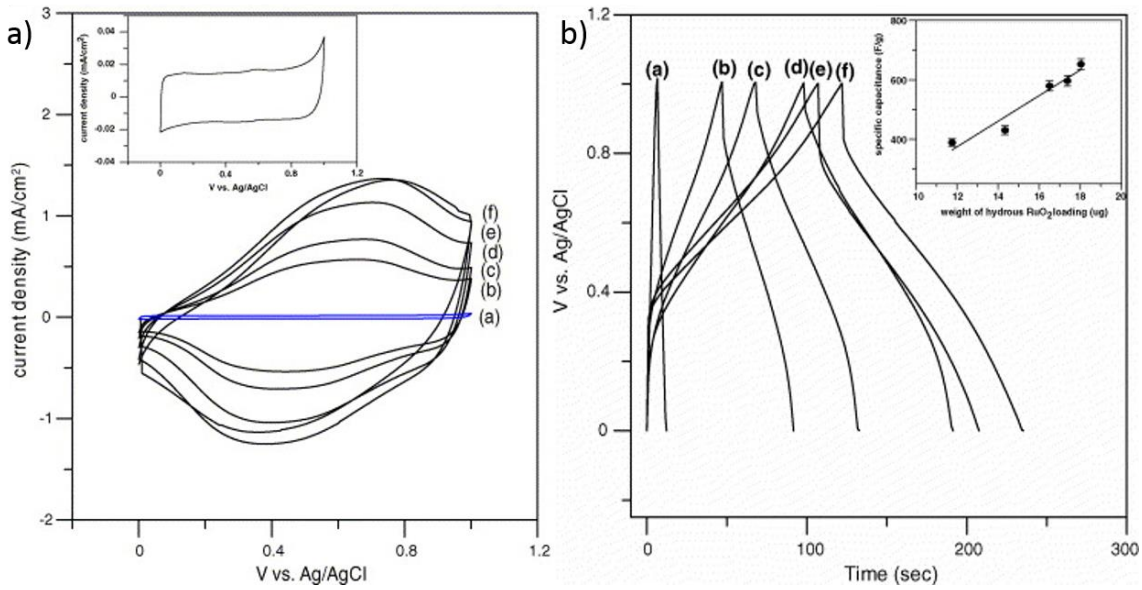

Figure 2.13 (a) CVs of (i) PEDOT-PSS (inset) and (ii-Vi) PEDOT-PSS-$RuO_2 \cdot xH_2O$ composite with different cycles at a scan rate of 50 mV s^{-1} and (b) galvanostatic charge–discharge of: (i) PEDOT-PSS and (ii-iV) PEDOT-PSS-$RuO_2 \cdot xH_2O$ with different cycles. The inset is the variation of the capacitance with cycle numbers for the PEDOT-PSS-$RuO_2 \cdot xH_2O$ composite [168]. By Huang et al. © (2006) Elsevier.

On the other hand, TMOs can enhance the electrochemical properties and cyclability of pure CPs. A study conducted by Song and coworker, showed chemical polymerization and electrochemical deposition techniques to prepare PANI/Nafion/RuO_2 composite electrodes [169]. Figures 2.14 (a & b) shows their composite improved not only the specific capacitance, but also cyclability of the material in comparison with pure PANI. The specific capacitances of PANI/Nafion/RuO_2 and pure PANI found to be 475 F g^{-1} (scan rate of 100 mV s^{-1}) with stability of about 80 % and 62% up to 10000 cycles, respectively.

To tackle the poor conductivity issues of the metal oxide, Hou and coworkers have used CNTs and PEDOT with MnO_2 to fabricate (MnO_2/CNTs/PEDOT) nanocomposite electrode for supercapacitor applications [23]. Carbon nanotubes have been prepared via chemical vapor deposition technique before using ultrasound-mediated techniques to synthesize a MnO_2/CNT composite. PEDOT-PSS was used as a binder to enhance the electrical conductivity and electrochemical performance of the electrodes. The electrode exhibited a specific capacitance of 427 F g^{-1} (at 5 mA cm^{-2}, 1 M KCl) and retained ~99% capacitance after 10000 cycles.

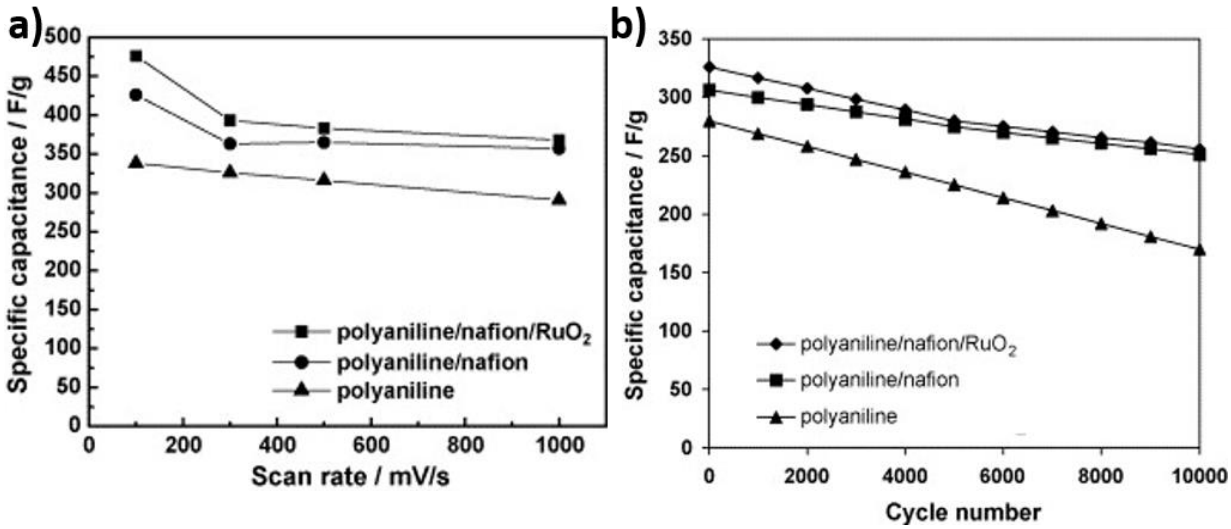

Figure 2.14 (a) The specific capacitance of three types of electrode as a function of scan rate and (b) the specific capacitance of types of electrode recorded as function of cycle number both recorded in 1.0 M H_2SO_4 solution in voltage range of −0.2 to 0.8 V [166]. By Song et al. © (2007) Elsevier.

Another TMO, titanium oxide (TiO_2), was used with PANI as a composite supercapacitor electrode material by Mujawar and coworkers [172]. A composite was made between PANI and titanium oxide nanotubes via the electrochemical polymerization method. PANI nanotubes grew in the titanium nanotube template. Aniline was first polymerized along with the titanium nanotube template, before the pore PANI was coated to the top of the titanium nanotube template, then planar sheets and circular nanotubes of PANI were added to the outside of the template. In order to investigate the electrochemical performance and cycling stability of the TiO_2/PANI

supercapacitor, cyclic voltammetry (CV) and a galvanostatic charge–discharge technique were used in 0.5 H_2SO_4 electrolyte at scan rates of 10 to 50 mV s^{-1} and a current density of 3 A g^{-1}, respectively. They achieved a specific capacitance of 740 F g^{-1} and the capacitance dropped by only 13 % after 1100 cycles.

2.3.1.5.2 Conducting Polymers/Graphene

Graphene has a very unique characteristic, which is a one atom-thick, 2D structure. However, a nanocomposite of graphene and CP also possess features such as high thermal and electronic conductivity, high specific surface area, fantastic mechanical strength and inherent flexibility that have attracted attention for studying CP+graphene composites [173]. The composite has also been studied for applications in flexible electrostatic electrodes [174, 175] and electrochemical devices where transportation of ions is required [176, 177].

Sahoo et al., used CP/graphene materials to develop flexible and uniform graphene/PPy nanofiber composites [178]. The nanocomposite was synthesized using the process depicted in Figure 2.15 (a). The electrochemical studies reveled energy density of 165.7 Wh/kg and capacitance value of 466 F g^{-1}, with the capacitance having decayed 15% after 600 cycles. Our group employed the chemical oxidative polymerization technique using ammonium peroxydisulfate [$(NH_4)_2S_2O_8$)] to synthesis graphene/PANI [179], graphene/PEDOT [180], graphene/PPy [181] and graphene/polythiophene [182] nanocomposite materials. These studies have revealed that the specific capacitances exceeding 400 F g^{-1}, 374 F g^{-1}, 270 F g^{-1} and 154 F g^{-1} using aqueous electrolytes, respectively.

In situ oxidative polymerization method was used to fabricate PANI and graphene for supercapacitor electrodes [183]. The approach demonstrated enhanced specific capacitance compared to pure PANI. In that study, Yan et al. reported nanoparticles of PANI grown on

graphene nanosheets for supercapacitors. Graphene nanosheets were first prepared via chemical reduction of exfoliated graphite oxide with hydrazine hydrate. Then the composite of graphene and PANI was obtained by polymerization of PANI. Figure 2.15 (b) illustrates the significant increase in the specific capacitance of the composite to 978 F g^{-1} while the specific capacitance of pure graphene and pure PANI was 169 F g^{-1} and 46 F g^{-1}, respectively.

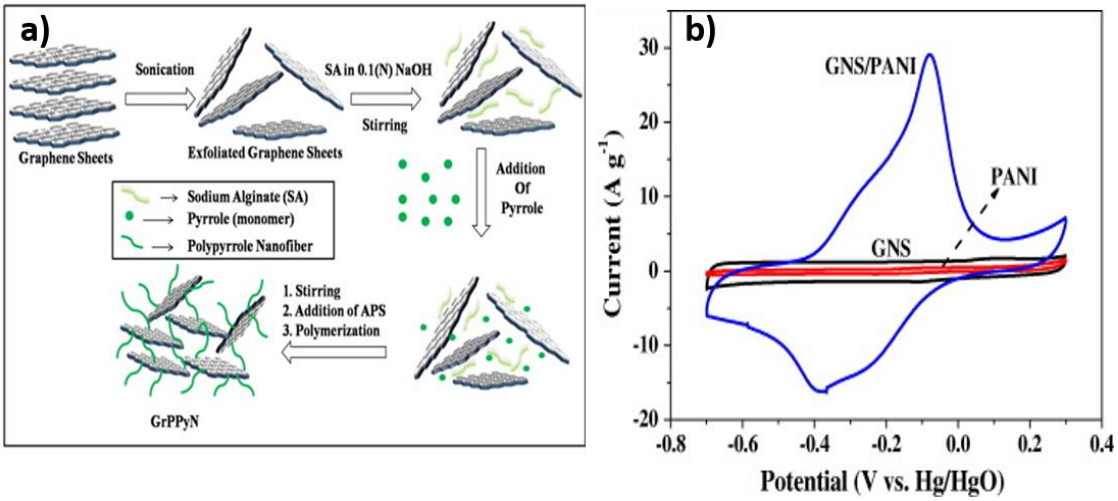

Figure 2.15 (a) Schematic diagram for the synthesis of graphene/PPy nanocomposite and (b) CV of graphene, PANI and graphene /PANI composite [175, 180]. By Sahoo et al. © (2013) Elsevier and Yan et al. © (2010) Elsevier.

Another [174] report on the performance of graphene/PANI composite showed about 10 times increase in the conductivity (5.5×10^2 S m^{-1}) than that of pure PANI (50 S m^{-1}). The structural comparison of graphene/polyaniline, pure graphene and pure PANI are shown in Figure 2.16. Cross-sectional SEM images (Figure 2.16 (c and d)) revealed the layer structure of graphene/PANI with PANI nanofibers sandwiched between the layers of graphene. Furthermore, increases in electrochemical performance and stability of the graphene/PANI supercapacitor are shown in Figure 2.16 (a & b), which was attributed to the low internal resistance “IR drop” compared with pure PANI.

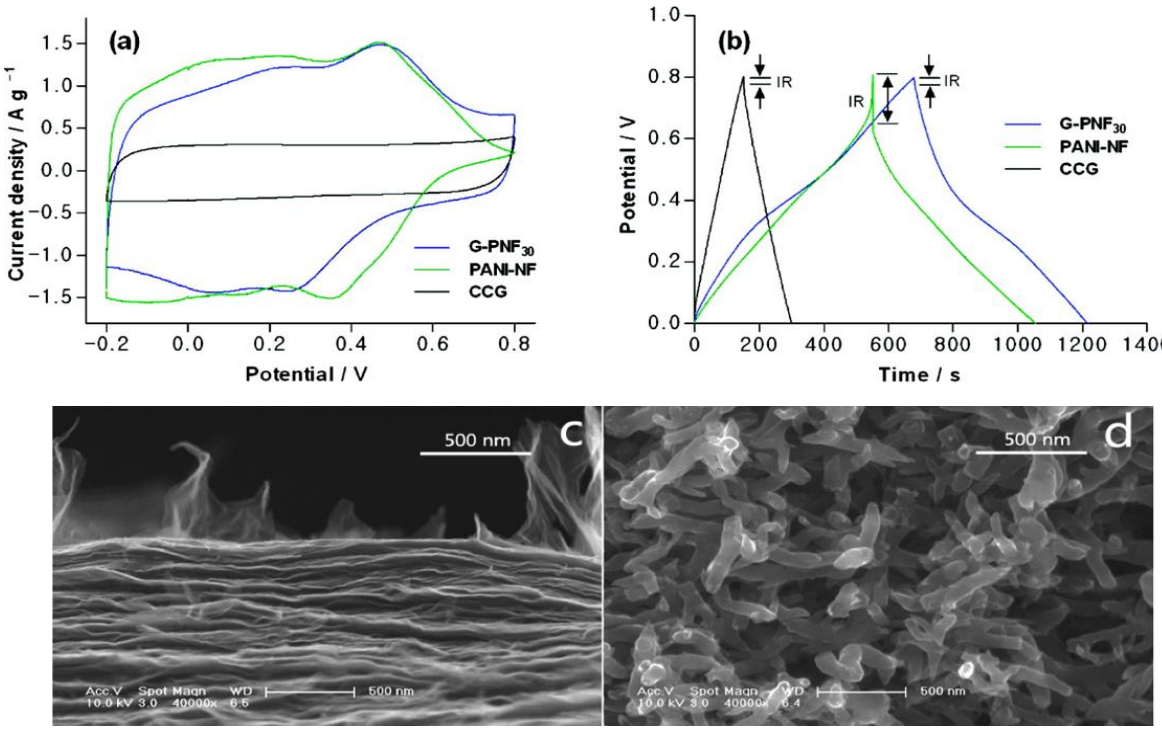

Figure 2.16 (a) Cyclic voltammograms of (b) galvanostatic charge/discharge curves (c,d) SEM images of graphene/polyaniline nanofibers [171]. By Wu et al. © (2010) American Chemical Society.

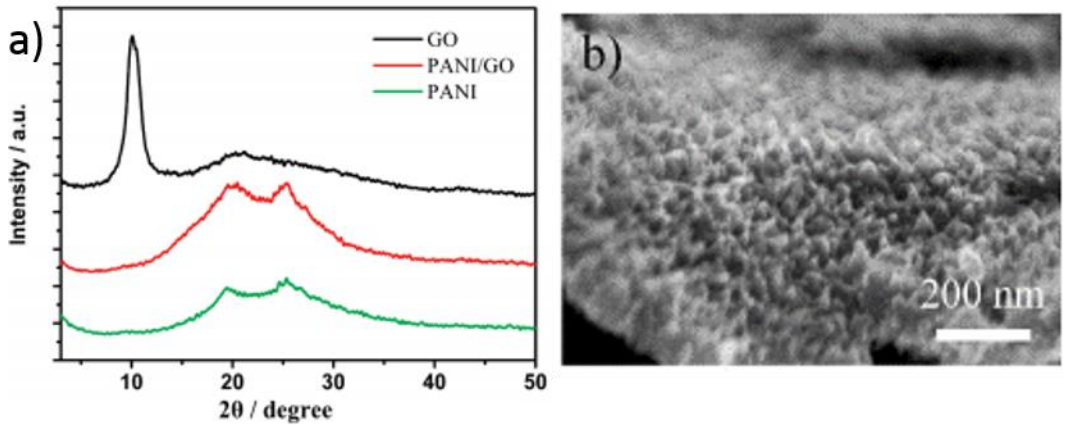

Figure 2.17 (a) XRD spectra of pristine GO, random connected PANI nanowires, and PANI−GO nanocomposite and (b) SEM images of PANI−GO nanocomposites [182]. By Xu et al. © (2010) American Chemical Society.

The use of graphene/CP composites as an active electrode material for supercapacitors was extensively investigated due to the extraordinary electrochemically accessible area and lack of the graphene aggregation [184]. PANI nanowires arrays, for example [185], were obtained on the graphene nanosheets via dilute polymerization including initial nucleation, followed by

homogeneous nucleation of aniline in graphene aqueous solution. The possible interaction between PANI nanowires arrays and graphene nanosheets was measured by XRD and SEM (Figure 2.17 (a & b)). The XRD patterns of pure PANI and graphene/PANI composite shows 2θ peaks at 20.12° and 25.26° which reveal the successful polymerization of PANI. The high intensity peak of 10.04° is attributed to (002) graphene diffraction planes while absence of the peak of graphene at is confirmed that PANI effectively decreases the graphene nanosheets aggregation. Morphological investigation confirmed that PANI nanowire arrays were successfully synthesized on the graphene nanosheets. A high specific capacitance of 555 F g^{-1} was obtained for graphene/PANI composite while the pure PANI showed only 225 F g^{-1} at 0.2 A g^{-1}.

2.3.1.5.3 Conducting Polymers/Molybdenum Disulfide

The unique combination of transition metal dichalcogenides and CPs has been explored for applications in supercapacitor electrodes [26, 141]. Addition of nanostructures of dichalcogenide materials to a CP can increase the specific capacitance and also reinforce the polymer, preventing the swelling and/or shrinking of the CP during charging/discharging cycles [67]. In the nanocomposite electrode materials, the goal is to utilize the outstanding features that each single material has to offer. Some of the advantages of using MoS_2 (a promising alternative to graphene)/CPs nanocomposites are enhanced electrical conductivity, improved electrochemical redox properties, increased voltage window, provides simplistic synthesis process and reduced volume expansion and agglomeration of MoS_2 [72]. Although metal oxides and CPs have already revealed superior results, the challenge for mass production of those composites are the fabrication costs, and toxic and environmental problems (very small doses of RuO_2 can potentially be harmful). Transition metal dichalcogenides and CPs nanocomposites have been considered eco-friendly materials [26, 186, 187]. MoS_2/CPs have been synthesized through several methods.

Chemical oxidative polymerization and in-situ polymerization are the most commonly used synthesis techniques [26].

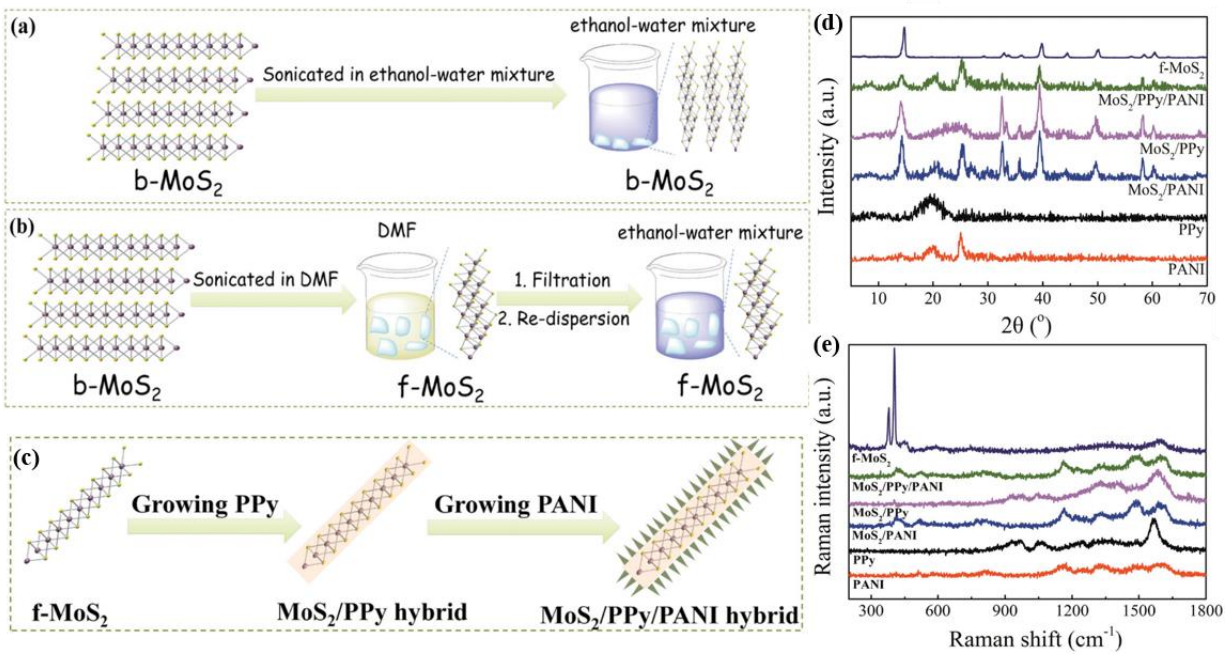

Figure 2.18 (a-c) The preparation process of a "pizza-like" MoS_2/PPy/PANI ternary nanostructure, (d) XRD patterns and (e) Raman spectra of pure and nanocomposite materials [185]. By Wang et al. © (2016) John Wiley and Sons.

Wang and coworkers demonstrated the synthesis of a "pizza-like" MoS_2/PPy/PANI ternary nanostructure using a solvent-exchange method for MoS_2, followed by in situ polymerization of pyrrole, and in situ growth and attachment of PANI (Figure 2.18 (a-c)) [188]. In order to attain the successful synthesis processes and give some information about the hybridization of MoS_2/CPs, X-ray diffraction (XRD) and Raman spectra of the related materials are shown in Figure 2.18 (d & e). The XRD pattern and Raman spectra of MoS_2/PPy/PANI validate that the MoS_2/CPs are successfully attached. Among all of them, the MoS_2/PPy/PANI nanocomposite presents the best electrochemical performance with great cycling stability for supercapacitors.

A study by Ma et al. has incorporated PPy into flowerlike MoS_2 with intertwined sheet-like subunits to form supercapacitor electrodes [189]. This study proposed two methods to synthesize the nanocomposite electrode materials to further improve both capacitance and cycling

performances. First, a hydrothermal method was applied to prepare MoS_2 with graphene-like structure then in situ oxidation polymerization to prepare MoS_2/PPy composite in order to provide a path for ions movements (Figure 2.19 (a)). Significantly, the cycling performance has increased from around 69% (pure PPy) to 90% (PPy/MoS_2 nanocomposite) after 500 cycles as well as the specific capacitance of 235 F g^{-1} (MoS_2), 285 F g^{-1} (pure PPy) and 554 F g^{-1} (PPy/MoS_2 nanocomposite) as shown in Figure 2.19 (b and c).

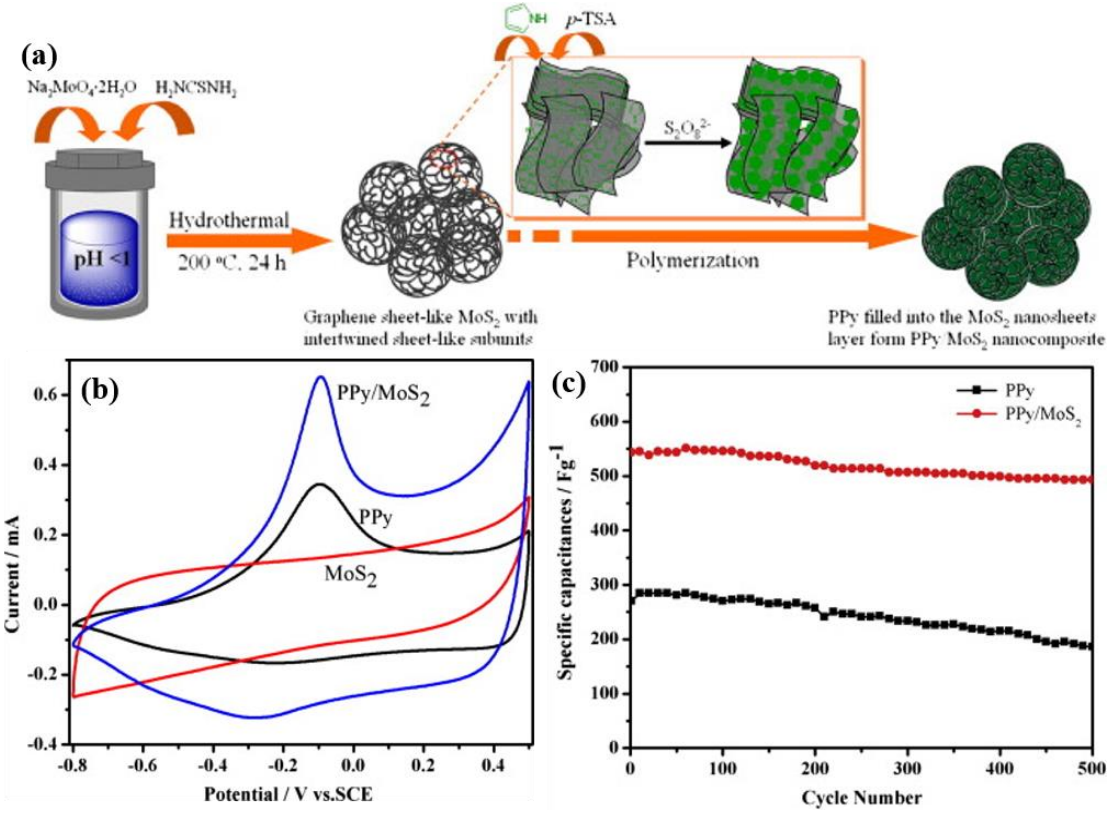

Figure 2.19 (a) The synthetic methods of PPy/MoS_2 nanocomposite, (b) CV and (c) the specific capacitance as a function of scan rate of pure and nanocomposite materials [186]. By Ma et al. © (2013) Elsevier.

2.3.2 Electrolytes

The electrolyte is another supercapacitor component which plays a key factor in supercapacitor performance. Two major types of electrolytes are liquid and solid-state electrolytes (Figure 2.20). A brief overview of these electrolytes and their effects on supercapacitor

performance are reviewed in this section. Considerations in selecting ideal electrodes for supercapacitors can be listed as follows:

- Wide operational voltage window
- High ionic conductivity
- Thermally, chemically and electrochemically stability
- Compatibility with electrode's active materials
- Wide operating temperature range
- Low cost
- Environmentally friendly

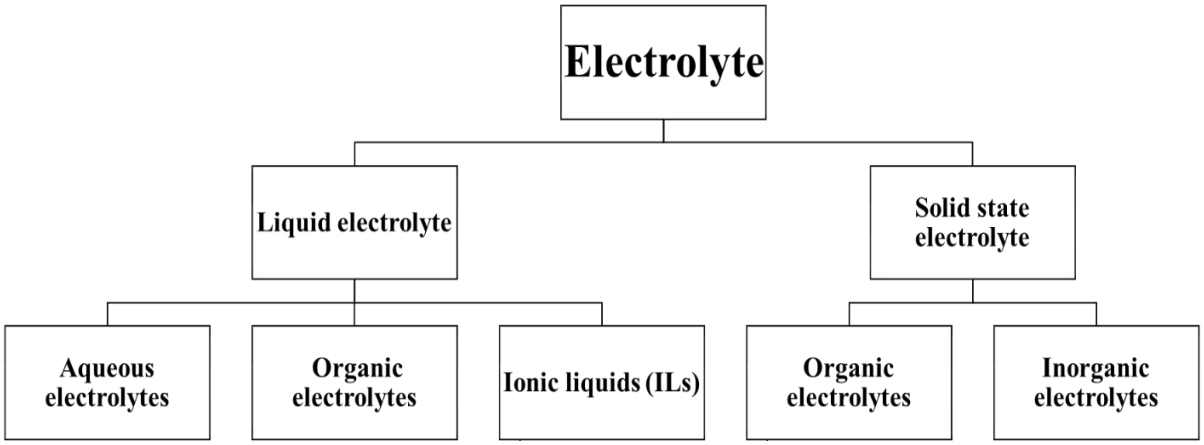

Figure 2.20 Classification of electrolytes for supercapacitors.

2.3.2.1 Liquid Electrolytes

The three types of liquid electrolytes that are being extensively investigated, fabricated, and commercially produced are: aqueous, organic, and ionic liquids. A comparison study between these electrolytes is listed in table 2.5 [190, 191]. The acid (HCl and H_2SO), base (KOH and NaOH) and neutral (KCl and Na_2SO_4) electrolytes are the main aqueous electrolytes which provide researchers many keys in order to enrich the performance of the supercapacitor. Also extensive academic studies have utilized aqueous electrolytes due to their extraordinary mechanism of

proton transport and high conductivity associated with the low cost and easy to synthesize and fabricate in an open environment.

Table 2.5 Liquid electrolytes comparison.

Type	Advantages	Disadvantages
Aqueous	High ionic conductivity, low internal resistance, inexpensive, abundance, environmentally friendly, low-toxicity and non-flammable.	Low working potential window (~ 1.2 V), low energy density. High corrosion and less cycle-life (concentrated acids)
Organic	Wider operating voltage windows (~ 2.7 V) which induce both the energy and power densities. Non-corrosive which is compatible with current collectors	More expensive, lower specific capacitance and ionic conductivity than aqueous electrolytes. Extreme purification processes. Toxicity and flammability
Ionic liquids	Widest voltage window (~ 2.7 V), high thermal, chemical and electrochemical stability.	Expensive, poor ionic conductivity compared to the previous types

2.3.2.2 Solid-State Electrolytes

Common classifications of solid-state electrolytes include organic (polymer) and inorganic electrolytes [192]. Solid-state electrolytes have attracted much interest for the advantages of higher operating voltage, high energy/power density, and excellent lifetime compared to aqueous electrolytes. In addition, solid-state electrolytes incorporated with aqueous electrolytes (such as: Poly(vinyl alcohol) (PVA) with HCl or H_2SO_4 or H_3PO_4 and poly vinylidene fluoride co-hexafluoropropylene (PVDF-HFP) with EMIM-BF4) can not only solve the encapsulation issue (liquid-leakage free) but also provide flexible supercapacitors with minimum potential leakage [193]. The major drawbacks when using solid-state electrolytes are the limited and permanent electrode/electrolyte interface and the need for proper packaging technologies in order to maintain wettability and avoid moisture resistance.

2.3.3 Separators

A Separator material is used to prevent contact, and short circuits between the two electrodes. The separator material is usually defined by the properties of the electrolyte type, for example: polymer membranes or paper are usually unitized with organic electrolytes whereas glass or cellulose fibers are used for aqueous electrolytes [194]. In order for optimum separator selection, the following properties should be considered [195, 196]:

- Highly-porous and high ionic conductivity, to increase the ion mobility
- Chemically and electrochemically inert, to avoid reaction and resistance with the electrodes and electrolyte materials
- Mechanically strong and with lower moisture, to inhibit pressure and volume changes
- Ultra-thin, to reduce equivalent series resistance (ESR)
- Thermally stable, to conserve the range of working temperature

2.3.4 Current Collectors

Current collectors play a role in the electrical charge transmission from/to the electrode's active materials as well as dissipate the heat generation within the electrical components, saving the supercapacitor against heat damage. Current collectors are electrically conductive, chemically and electrochemically stable. The most popular current collector's materials are: aluminum, steel, copper and graphite. Furthermore, synthesizing the active materials directly onto substrates works as current collectors in the system. In order to enhance the capacitive performance, electronic resistance at the current-collector/electrode interface should be reduced. The dislocation between the electrode and current collector could be problem over repeated doping and de-doping processes which not only maximizing the electronic resistance but also cause poor cycling and stability. One of the ways to mitigate this problem is using polymeric binding agents, such as Nafion and NMP,

to ensure thorough adhesion of the electrode materials onto the substrates. In many cases, the edges and back of the substrates need to be insulated to prevent of any reaction within the electrolytes.

2.4 Manufacturers

Table 2.6 Different products offered by manufacturers.

Manufacturer (Part Number)	Cs (F)	E (V)	ESR@ 1kHz (mΩ)	Lifetime @ Temp.	Specific Power (kW/kg)	Specific Energy (Wh/kg)	Operating Temp. (°C)	Unit Price (USD)
Maxwell Technologies Inc. [197]	3000	2.7	0.29	1×10^6 cycle. @ 25° C 1,500 hrs @ 65° C	5.9	6	-40 ~ 65	65. 9
AVX Corporation [198]	3000	2.7	0.29	5×10^5 cycle. @ 25° C 1,000 hrs @ 60° C	5.292	5.3	-40 ~ 65	60.8
Nichicon [199]	4000	2.5	2.2	2000 Hrs @ 60°C	-	-	-25 ~ 60	323.2
Eaton [200]	3000	2.7	0.23	1×10^6 cycle. @ 25° C 1500 hrs @ 65°C	7.9 kW	3 Wh	-40 ~ 65	73.6
KEMET [201]	3000	2.7	0.2	1×10^6 cycle. @ 25° C 1000 hrs @ 65°C	13.7	6	-40 ~ 65	100.1
NessCap Co Ltd [202]	650	2.7	0.6	1×10^6 cycle. @ 25° C 1500 hrs @ 65°C	7.1	3.2	-40 ~ 65	39.6
Illinois Capacitor [203]	350	2.7	3	5×10^5 cycle. @ 25° C 1000 hrs @ 65°C	3.845	5.452	-40 ~ 65	15.08

In recent years, the manufacturers and developers of supercapacitors are growing very fast. The recent trend has shown that 50% of manufacturers offer non-flammable and non-toxic based electrolytes, and are slowly replacing the propylene carbonate and/or acetonitrile based organic

solvents used in supercapacitor applications. Table 2.6 shows the different types of supercapacitors manufactured by various commercial companies.

CHAPTER 3: ELECTROCHEMICAL PARAMETERS, CHARACTERIZATION TECHNIQUES, TOOLS AND INSTRUMENTS USED TO EVALUATE THE SUPERCAPACITOR PERFORMANCE

3.1 Introduction

In the previous chapter, the fabrication and design of supercapacitor devices and their associated working principles were described. The capacitance, energy, power, internal resistance, and cycle stability are the main fundamental parameters to be considered in the evaluation of a supercapacitors' performance. Therefore, the basic electrochemical characterization methods including CV, CCCD and EIS are discussed in this chapter. Also, some advanced material characterization techniques used for studying morphologies, structures and physical properties of the electrodes are reviewed.

3.2 Electrochemical Cell Design for Performance Testing

Three-electrode and two-electrode configurations are the most electrochemical cell setups used in electrochemistry. Both configurations were used in this project.

3.2.1 Three-Electrode Configuration

This approach focuses on a basic analysis of the electrode materials. It also governs the potential across the electrode/electrolyte interface accurately. In this case, a reference/auxiliary electrode, counter electrode and working electrode are used in the electrochemical cell. For effective results, the reference electrode should be made with a material that has known redox potential in order to measure the working electrode potential without current flowing thought it.

Silver/silver chloride (Ag/AgCl) and copper/copper sulfate are the most common aqueous reference electrode materials [204].

The counter/auxiliary electrode is utilized to supply current and close the circuit in the electrochemical cell. An inert material should be used for the counter electrode, usually platinum meshes and larger in size than the working electrode to avoid current limitations [205]. The working electrode is the most important part in this system where the reaction of interest is taking place at electrode/electrolyte interface. In the preparation of the coated material, some binding agents (such as Nafion and NMP) need on be used to maintain the structural integrity and prevent the coated material diffusing away when entering in the electrolyte.

3.2.2 Two-Electrode Configuration

A two-electrode configuration is normally used for purposes of characterizing and testing two active electrodes as a complete device. The two active electrodes are cathode and anode, with a separator is located in between to avoid short circuits when the system is in operation. To collect the current that is created in the system, metal plates are used which are connected to the outer circuits. The two-electrode system can be similar to two capacitors that are placed in series.

On the above note, the projected area of the symmetric electrodes has to be twice as large as that of the single electrode [2]. The specific capacitance that is obtained from the two electrodes can be described as the device capacitance, whereas the material capacitance is referring to the three-electrode capacitance.

3.3 Capacitance

Capacitance (C) is defined as the ratio of the particular charge stored in the plates of a capacitor and the potential that exists between the plates. Capacitance is a significant parameter that is evaluated when carrying out an analysis of supercapacitors. The units of capacitance are

Farads, while specific capacitance is based on the mass contained within the active material and is calculated in order to compare the performance between two electrodes that have different masses. To calculate the capacitance of any materials, CV or CCCD techniques are used. The basics of these two techniques are explained in the next section.

3.3.1 Cyclic Voltammetry

Cyclic voltammetry is a technique that can be described as sweeping the voltage potential contained at the active materials of the working electrode back and forth through a potential window width (E_2-E_1) at a predefined scan rate. The current (I) of the system is recorded and plotted against the potential. In this case, the capacitance can be calculated by the use of equation 3.1 below:

$$C = \frac{\int_{E_1}^{E_2} i(E)\, dE}{2(E_2 - E_1)v} \tag{3.1}$$

where the capacitance is related to C (F), instantaneous current $i(E)$ is in (A), $\int_{E_1}^{E_2} i(E)\, dE$ is the integrated voltammetric charge for sweep in CVs, potential window width '(E_2-E_1)' and potential scan rate 'v' is in V s^{-1}.

An ideal capacitor during the positive voltage sweep would be when the current has a positive constant and the CV plot is a rectangle that is symmetric on the zero-current axis. Nevertheless, ideal supercapacitors do not exist and the ones that are available never exhibit the above-described conditions, although one can obtain results close to that under the idealized conditions, for instance when using extremely low scan rates. There are a number of non-idealities within realistic scenarios such as when operating at high scan rates. In this case, the interfacial double layers never have sufficient time for formation because of the transport limitations of both the electronic conductor (electrode) and the ionic conductor (electrolyte).

Electrolyte degradation is another case that happens in all supercapacitor devices because of a limited working potential window. For instance, the low working potential window (~ 1.2 V) of aqueous electrolytes will electrolyze and form oxygen and hydrogen when a higher or lower voltage is applied. This can have a negative effect on the device's cycle durability.

3.3.2 Constant Current Charge/Discharge

Constant current charge and discharge represent a situation where a constant charging current is applied until the maximum potential is achieved. After achieving the maximum potential, a constant discharging current is utilized to the point when the minimum potential is reached. During this time, the potential difference is monitored with respect to time. Data from charging-discharging capacitors can be used to estimate their capacitances using the following equation 3.2:

$$C = \frac{I \,.\, \Delta t}{\Delta E} \tag{3.2}$$

where discharge capacitance 'C' was expressed in (F), 'I' represents the current that is applied (in A), while $\Delta E/\Delta t$ presents the slope of that discharge curve (in unit of V s^{-1}). Dividing the mass of active materials (in unit of grams) to the capacitance calculated from equations 3.1 or 3.2 will yield the specific capacitance (C_s) in units of F g^{-1}. For the two-electrode configuration, the total of masses of active materials at electrodes need to be added as mass 1 + mass 2.

Equation 3.2 uses the slope of the voltage change to calculate the capacitance, but often the voltage profile shows a nonlinear response. When there is a decrease in the slope of the charge and discharge curve, is an indication of charge transfer that takes place at the electrode and electrolyte interfaces.

The charge transfer arises from the reactions that take place in the electrode and the electrolyte. A reaction that degrades the electrolyte reduces the potential window and lowers the

electrochemical stability of the electrolyte and the device. But the reaction that is used in a pseudocapacitor is reversible. When the reaction is irreversible, it results in electrode degradation, which is not desirable.

Another non-ideal behavior is the sudden voltage drop (IR_{drop}) at the point of shifting from charging to discharging, specifically under a high current charging. The above represents ohmic resistances, which are due to a combination of electrolyte and electrode resistances, as well as other contact resistances, such as contact between the currant collector and electrode. The supercapacitors DC equivalent series resistance (ESR) is estimated by using equation 3.3 below:

$$ESR = \frac{IR_{drop}}{2\,I} \tag{3.3}$$

The ESR value needs to be as low as it can be in order to maintain the high current and potential window width.

3.4 Energy Density

Analyzing the energy density of any supercapacitor is a key factor when it comes to estimating the amount of energy stored when the device is in use in real-life applications.

For any supercapacitor, the specific energy density is calculated by equation 3.4:

$$ED = \frac{1}{2}\,C_s(\Delta V)^2 \tag{3.4}$$

where specific discharge capacitance 'C_s' is in unit (F g^{-1}), and 'ΔV' was the voltage difference in (V). Watt hour per kilogram (W h kg^{-1}) is the unit of the energy density, therefore, dividing by 3600 to convert seconds to hours. As discussed in Section 2.3.2, the use of organic ionic liquid electrolytes is going to increase the potential window width and that will be key to resolving the

issue of supercapacitors lack of high energy densities. Utilizing the organic electrolytes that have a wider voltage window will definitely lead to the reduction of the supercapacitor's power density.

3.5 Power Density

To investigate a supercapacitors deliverable performance, the power density needs to be computed. The specific power density is expressed in watt per kilogram (W kg^{-1}) calculated as (equation 3.5):

$$PD = \frac{ED}{\Delta t} \tag{3.5}$$

where Δt (in unit of hour) represents the rate at which the cell is discharging or the discharge time, which is obtained through galvanostatic charge or discharge.

3.6 Internal Resistances

Supercapacitors never exhibit ideal conditions despite many improvements to ensure that they operate in an optimal way. The major contributor for the capacitors not to operate to their required standards is the issue of internal resistance. ESR forms the major resistance in capacitors. The devices include the electrolyte resistance as well as the contact resistance that exist between the current collectors and supercapacitor's electrodes. ESR affects the overall power that will be obtained from the supercapacitor since it restricts the rate of charge and discharge. One of the methods to compute the ESR has been already discussed in Section 3.3.2, whereas EIS is also another method.

3.6.1 Electrochemical Impedance Spectroscopy

Electrochemical Impedance Spectroscopy (EIS) is one of the techniques that is used to calculate the ESR. This method gives further information about the electric properties of both supercapacitor materials and devices. An alternating current with a wide frequency range is applied

to the system and then the amplitude and the phase shift of the resulting current is measured. The impedance data of the supercapacitor can be plotted either by the Nyquist or Bode plots. In order to compute the resistive component, the Nyquist plot should be used, which utilizes the imaginary component of the impedance against the real components. Within the Nyquist plot, the intersection of the x-axis, which corresponds to the ESR value, while the semicircle diameter is attributed to equivalent distributed resistance (EDR) or charge transfer resistance, which is the second type of resistive component. The charge transfer has particular speed and that depends on the type of reaction that is taking place in the cell, the concentration of the reacting products, temperature and the potential of the system. In general, the reaction taking place between the electrode, and electrolyte and the charge transfer is directly related to the number of pores in an active electrode. In this case, the real capacitance (C') and imaginary capacitance (C'') can be calculated as [206]:

$$C'(\omega) = \frac{-Z''(\omega)}{[\omega|Z'(\omega)|^2]} \tag{3.6}$$

$$C''(\omega) = \frac{-Z'(\omega)}{[\omega|Z(\omega)|^2]} \tag{3.7}$$

where ω is the angular frequency, which can be calculated by $\omega = 2\pi f$ and $Z'(\omega)$ and $Z''(\omega)$ are the respective real and imaginary parts of the complex impedance $Z(\omega)$.

3.7 Cycle Stability

Supercapacitors are preferred for having stable cycles. Commercial supercapacitors are known to have a long life through which they will operate with great stabilities at full capacity. Within a lab scale testing, 1000 to around 10,000 cycles are done for purposes of knowing the cell's durability. Stability test can be performed by comparing the first cycle to the final cycle of either cyclic voltammetry or charge/discharge using constant scan rate or current density. Extensive cycling has been noted to degrade the electrodes, that can induce corrosion of the cells,

and that could lead to the reduction of the capacitance, while the ESR will increase. On that note, making a comparison on the initial and final performance of any device offers clear vision into how various components will work in real life use where they will be subjected to the real conditions. On the other hand, the types of materials that are utilized have a great impact on the cycle durability. Supercapacitors have static storage mechanism, which leads to superior stability in comparison with batteries. Long cycle lifetime is one of the advantages of supercapacitors, hence it should be cycled many times.

3.8 Self-Discharge

Supercapacitors are known to suffer from self-discharge. Self-discharge entails the gradual decaying of its voltage when in full charge, resulting from constant leakage in the current within the open-circuit cell. This self-discharge is known to reduce the power delivered and energy that can be obtained from the supercapacitors, hence it is considered a big issue when it comes to commercial applications. Various studies have been done to determine the reason for self-discharge, such as Faradaic resistance, impurity reactions, and internal ohmic leakage pathways [207]. An effective way to measure self-discharge is when the supercapacitor held at full constant voltage then the voltage drop is recorded over time after the constant voltage supply is removed.

In order to develop an ideal electrode material for supercapacitors, suitable techniques were used to assess the performance of the electrode materials. Due to the nanostructure of most of the electrode materials that were used through these studies, a list of optical, physical, and structural and conductivity measurements must be carried out to evaluate the properties of these nanomaterials and further optimizing and validating the performance of the supercapacitor. The techniques include XRD, SEM, TEM, Raman spectroscopy, PSA, FTIR and conductivity measurements as shown in Figure 3.1 (a-h). Most of these techniques will be presented in the next

three chapters of this dissertation. In addition, other tools and instruments were used to accurately prepare the electrode samples. Figure 3.1 (h and i) shows all the measurement tools were used throughout the work of this study. In addition, the Radiometer Analytical Voltalab 40 was used for all electrochemical measurements (Figure 3.1 g).

3.9 Characterization Techniques of Materials for Supercapacitor Electrodes

Figure 3.1 Instruments were used for all the characterizations (a) XRD, (b) SEM, (c) TEM, (d) Raman spectroscopy, (e) PSA, (f) FTIR, (g) four-in-line probe setup, (h) Keithley source meter, (i) analytical balance and (j) Radiometer Analytical Voltalab 40.

CHAPTER 4: POLYETHYLENEDIOXYTHIOPHENE AND MOLYBDENUM DISULFIDE NANOCOMPOSITE ELECTRODES FOR SUPERCAPACITOR APPLICATIONS[1]

4.1 Introduction

Electrochemical supercapacitors have become a new and revolutionized energy storage field due to their specific capacitance, charging-discharging characteristics, compactness, power density and energy density applications [208, 209]. The recent advancement has shown that 2D-nanomaterials such as metal dichalcogenide nanosheets of MoS_2 or others could replace graphene as candidate for obtaining high energy based supercapacitor electrode material [210-212]. The 2D-dichalcogenide MoS_2 reveals high specific capacity and cycle stability when used as anode in lithium ion battery [140]. The 2D-layered MoS_2 shows double layer charge storage capacity, and provides excellent supercapacitive properties due to the large surface area [133-135]. MoS_2 also displays pseudocapacitance properties similar to ruthenium dioxide (RuO_2) due the +2 to +6 oxidation states of Mo in the structure [134].

Various conducting polymers (PANI, PPy, PEDO) and polythiophene 'PTh') have been used for supercapacitor applications due to their superior redox properties, high electrical conductivity and environmental stability [9, 18, 179-181, 213]. PEDOT possesses fast redox reactions, charging-discharging characteristics and stable conducting polymer, and it is used as an

---

[1] T. Alamro, M.K. Ram, "Polyethylenedioxythiophene and molybdenum disulfide nanocomposite electrodes for supercapacitor applications", published 16 March 2017, Electrochimica Acta, 235 (2017) 623-631

electrode material in various electrolytic solutions for supercapacitor applications [2, 214].However, conducting polymers also illustrate poor stability and recyclability due to the ohmic polarization in several solvents for supercapacitors applications [215]. The stability and recyclability of conducting polymers has been resolved by formation of nanocomposite with RuO_2, TiO_2, carbon nanotubes, graphite, activated carbon, graphene, etc. [215-218]. MoS_2 composites with CP have also been used as an electrode for supercapacitor applications [28, 189, 219].

The PEDOT/MoS_2 composite electrode materials are synthesized using exfoliation of MoS_2 and in-situ polymerization technique, and applied for supercapacitor and lithium battery applications [97, 220]. The surface analysis of the MoS_2-CP nanocomposites has shown high porosity and active surface area [221]. MoS_2 is a hydrophobic material, and its immiscibility in water creates an issue for the successful synthesis of nanocomposites in aqueous media. We have exploited the surface chemistry by using CTAB as surfactant for the presence of MoS_2 in the aqueous solution. The use of CTAB allowed MoS_2 to disperse uniformly in the resulting EDOT based polymerizing solution. The EDOT was dissolved in the aqueous solution in presence of PSS polyanions.

As demonstrated in this work, MoS_2-PEDOT nanocomposite materials were successfully synthesized using modified MoS_2 in aqueous media using surfactant. The simplistic synthesis, superior electrochemical redox properties and higher specific capacitance of electrode material are key in the foundation of practical supercapacitor applications for energy storage applications.

4.2 Experimental Details

4.2.1 Synthesis of MoS_2-PEDOT

The MoS_2-PEDOT was obtained by chemical oxidative polymerization technique using the monomer ‘ethylenedioxythiophene (EDOT)’ dissolved in a solution of 1 M HCl containing

2 mg ml^{-1} of polystyrene sulfonate salt. The MoS_2 was dispersed in water using surfactant CTAB before combining with dual oxidants containing a solution of 0.05 M ammonium peroxydisulfate [$(NH4)_2S_2O_8$)] and 0.05 iron chloride ($FeCl_3$) under controlled conditions.

Figure 4.1 shows 1:1 MoS_2-PEDOT, 2:1 MoS_2-PEDOT, and 1:2 MoS_2-PEDOT, nanocomposites which were synthesized by varying the ratio of EDOT to MoS_2. The reaction proceeded by mixing EDOT monomer with three ratios of MoS_2 in 1 M HCl containing PSS solution for two hours. The ice bath was used to compensate the heat of exothermic reaction of EDOT polymerization to PEDOT. The synthesized MoS_2-PEDOT nanocomposite was vacuum filtered, and washed thoroughly using deionized water, methanol & acetone and the nanocomposite filtrate powder was dried at 100° C [180, 222]. All the chemicals, including the EDOT monomer and MoS_2, were purchased from Sigma and used as received.

4.2.2 Optical Characterizations of Films

The nanocomposite at various ratios containing MoS_2-PEDOT were optically characterized using FTIR “Perkin Elmer spectrum one” and Raman “Renishaw inVia micro-Raman spectrometer” techniques. A potassium bromide pellet was made with MoS_2-PEDOT nanocomposite powders for FTIR measurement while the Raman Shift bands were measured for MoS_2-PEDOT nanocomposite film on a silicon substrate.

4.2.3 Surface/Structure Characterization

Field Emission Scanning Electron Microscopy (FE-SEM, S-800, Hitachi, Japan) was used to understand the surface morphology of the nanocomposites. TEM (Tecnai F20 high-resolution transmission electron microscopy (HRTEM)) measurement was used on various nanocomposite samples deposited on copper grid required for the measurement.

The crystalline structure was studied using Powder X-ray diffraction (XRD) technique (PANalytical X'Pert Pro MRD system with Cu Kα radiation (wavelength = 1.5442 Å) operated at 40 kV and 40 mA).

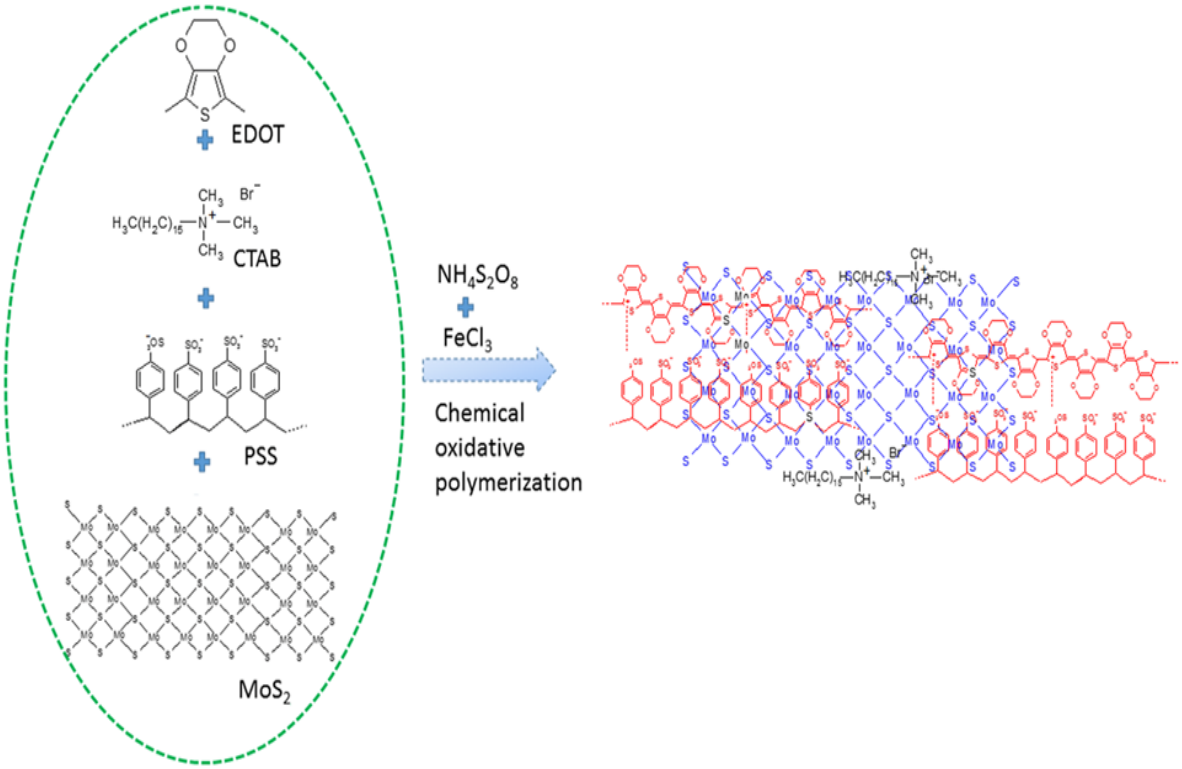

Figure 4.1 Schematic structures of molybdenum disulphide, PSS, EDOT and MoS_2-PEDOT nanocomposite.

4.2.4 Electrode Fabrication

The supercapacitor electrodes were made by mixing 1.5 mg of MoS_2-PEDOT powder with a 2–3% Nafion solution using a pastel and motor. Graphite, FTO and silicon substrates were used to deposit the Nafion mixed MoS_2-PEDOT nanocomposite. The MoS_2-PEDOT with Nafion coated substrates with defined area were dried at 100°C before insulating for any non-deposited substrate area. The symmetric MoS_2-PEDOT electrodes were used for supercapacitor study in both 2 M hydrochloric acid 'HCl' and 2 M sulfuric acid 'H_2SO_4' as electrolytes.

4.3 Results and Discussion

4.3.1 Physical and Structural Characterization

The porous structure of MoS_2-PEDOT nanocomposite is illustrated in SEM and TEM images. Figure 4.2 shows SEM pictures of 1:2, 2:1 and 1:1 based MoS_2-PEDOT nanocomposite samples. The SEM pictures show the platelet structure for MoS_2, while the PEDOT has wrapped around the MoS_2 similar to studies as shown in literature [97, 223]. The TEM pictures (Figure 4.3 a–c) depict that the PEDOT is wrapped with MoS_2 structure similar to the obtained SEM images. However, TEM images also reveal the lattice structure conforming to MoS_2. Figure 4.3 also shows magnified HRTEM images of lattice spacing of 0.160, 0.18 and 0.225 nm corresponding to 1:1 MoS_2-PEDOT, 1:2 MoS_2-PEDOT and 2:1 MoS_2-PEDOT nanocomposite structures, respectively. The TEM studies further proved the junction leading to efficient transfer of electrons between MoS_2 to PEDOT in the nanocomposite film on copper grid [142].

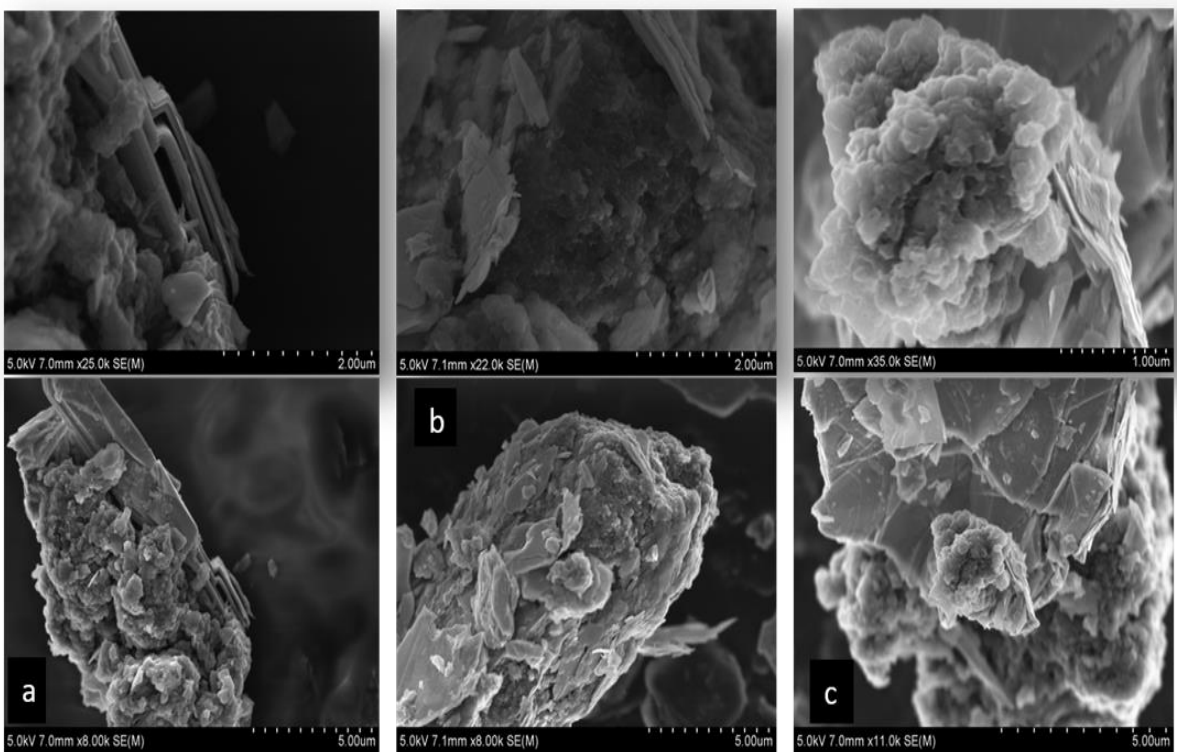

Figure 4.2 SEM pictures of (a) 1:2 MoS_2-PEDOT (b) 2:1 MoS_2-PEDOT (c) 1:1 MoS_2-PEDOT nanocomposite.

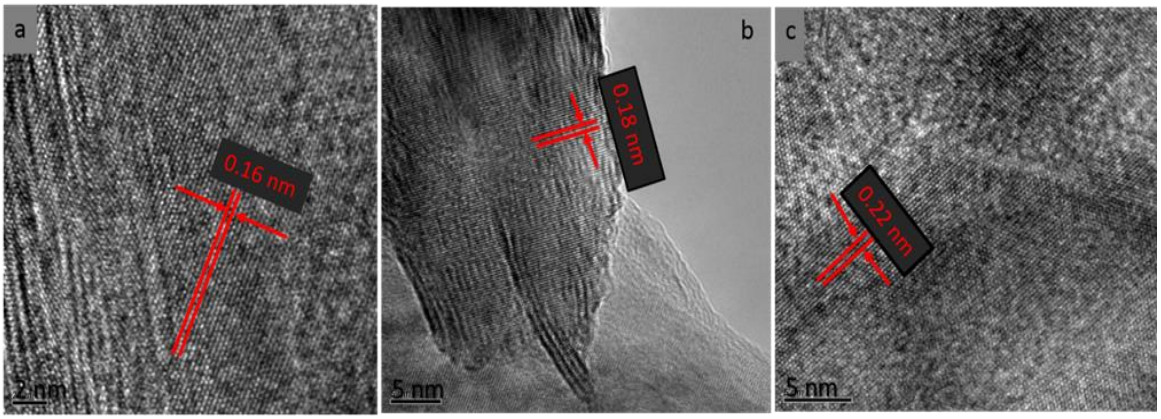

Figure 4.3 TEM pictures of MoS_2-PEDOT nanocomposites (a) 1:1 (b) 1:2 (c) 2:1 for MoS_2-PEDOT.

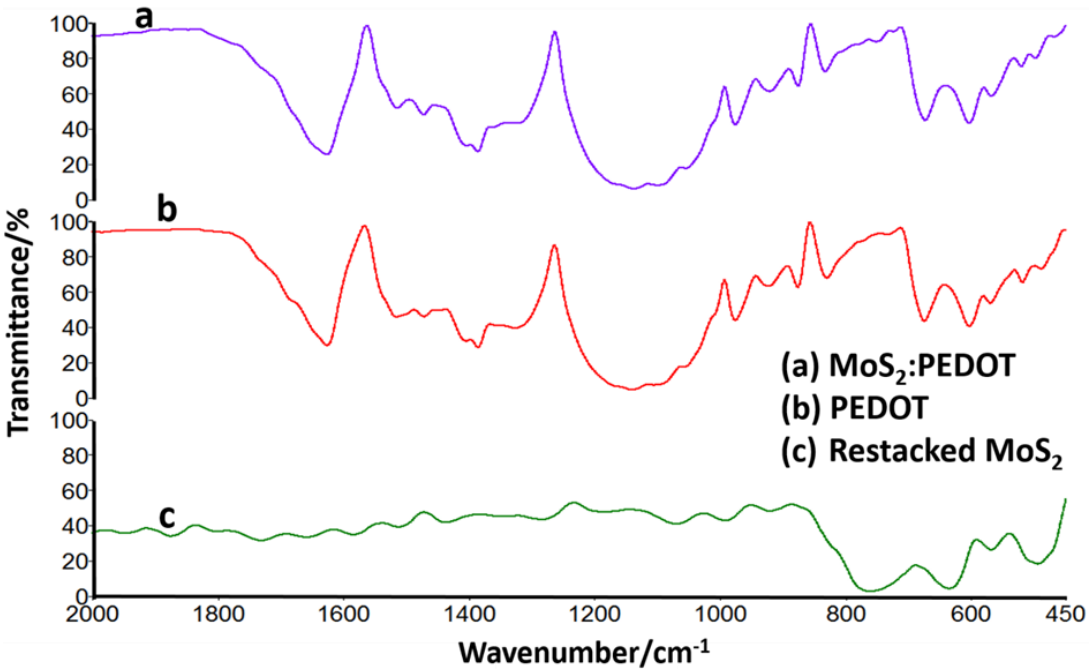

Figure 4.4 FTIR spectra of (a) MoS_2-PEDOT nanocomposite (b) PEDOT and (c) MoS_2 restacked from 600-2000 cm^{-1}.

Figure 4.4 (curves a–c) observes FTIR spectra of MoS_2-PEDOT nanocomposite, PEDOT and MoS_2 nanomaterial from 450–2000 cm^{-1}. The infrared bands at 1385 and 1328 cm^{-1} are due to C─C and C=C stretching vibrations for thiophene ring. The bands at 1138 and 1098 cm^{-1} are due to C─O─C stretching vibrations for ethylene oxide unit, and C─S stretching vibrations in thiophene ring was pertaining due to the bands 977 cm^{-1} and 673 cm^{-1}, and reveals the presence of PEDOT in MoS_2-PEDOT nanocomposite [224]. The infrared band at 493 cm^{-1} stretching

vibration depicted the presence of MoS_2. The shift of the band between 500–1500 cm^{-1} showed C─H vibrations [225]. The IR peak at 465 cm^{-1} implied the presence of MoS_2 in MoS_2-PEDOT nanocomposite material.

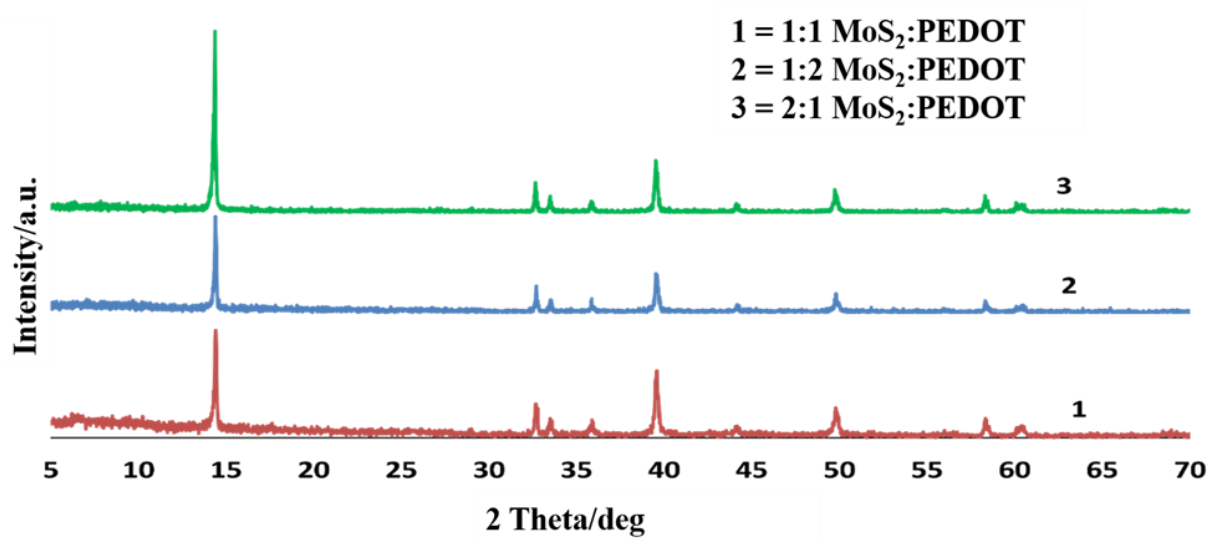

Figure 4.5 X-ray diffraction of (1) 2:1 MoS_2-PEDOT, (2) 1:1 MoS_2-PEDOT (3) 1:2 MoS_2-PEDOT nanocomposite.

The X-ray diffraction (XRD) patterns reveal angle 2θ peaks at 14.40, 32.69, 33.51, 35.88, 39.56, 44.16, 49.80, 58.34 and 60.46 degree (Figure 4.5). The angle 2θ in each composition 1:1, 1:2 and 2:1 for MoS_2-PEDOT have been assigned for their respective planes at (002), (100), (101), (102), (103), (006), (105), (110), and (112). The MoS_2-PEDOT nanocomposite displayed hexagonal structure regardless of any composition of MoS_2 and PEDOT in nanocomposite. The well-defined planes observed in X-ray diffraction indicated of crystallinity in MoS_2–PEDOT. However, no characteristics peaks have been observed for PEDOT revealing the amorphous nature of the material. The intensity of 2θ at (002) plane was decreased for the rise of MoS_2 in PEDOT in nanocomposite structure. The weight ratio of MoS_2 to PEDOT affected crystallinity of the nanocomposite. The average particle size of each ratio has been estimated to be 90, 102, 104 nm for MoS_2-PEDOT (1:2, 1:1 and 2:1) in nanocomposite using Scherrer equation [226].

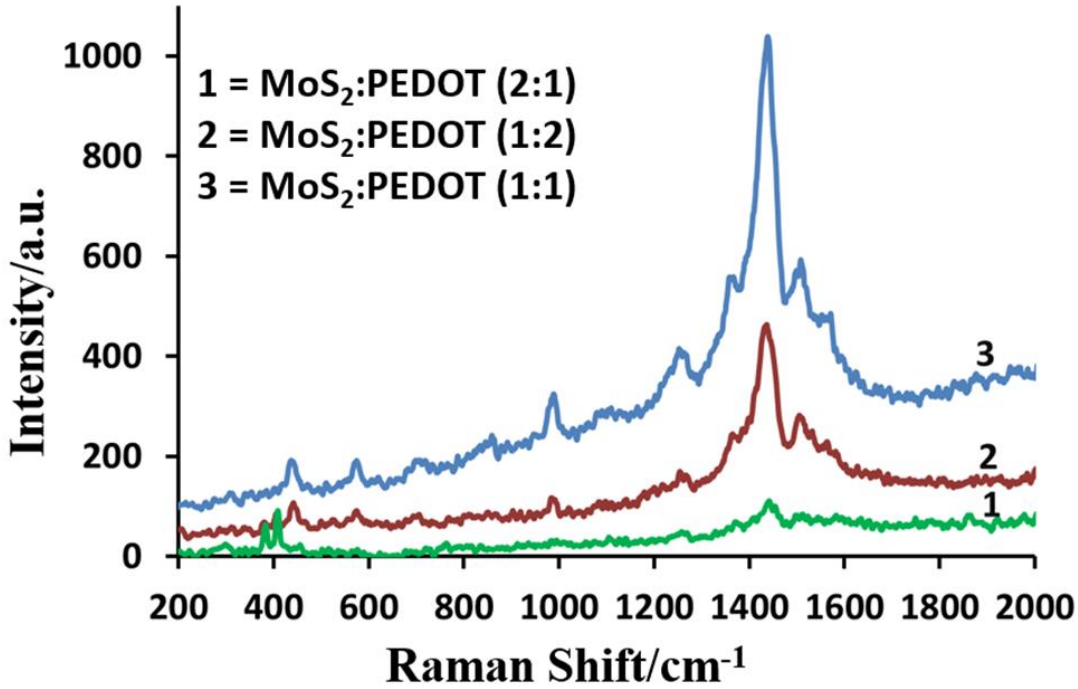

Figure 4.6 Raman spectroscopy of (1) 2:1 MoS_2-PEDOT, (2) 1:2 MoS_2-PEDOT (3) 1:1 MoS_2-PEDOT nanocomposite.

Figure 4.6 for all curves shows Raman shift at 383, 410, 440, 575, 710, 988, 1256, 1263, 1440, 1454, 1530, 1550, 1565 and 1572 cm^{-1} regardless of the ratio of MoS_2 to EDOT in MoS_2-PEDOT nanocomposite. Raman shift at 383 cm^{-1} and 410 cm^{-1} were due to the E^1_{2g} and A_{1g} modes for the presence of MoS_2 in the structure, as well as presence of the hexagonal structure of the MoS_2 [227]. The Raman shift for the E^1_{2g} mode also revealed the layer dislocations of Mo to S atoms. A_{1g} mode is the representative of out-of-plane vibrations due to S atoms in MoS_2 structure [228]. The Raman shifts at 1563 and 1531 cm^{-1} are assigned to the anti-symmetric C=C stretching, and could also be represented at polarization mode dispersion. The peaks at 1408, 1366, 1253 and 437 cm^{-1} are due to C=C stretching, C─C single stretching, inter-ring stretching C─C and SO_2 bending for PEDOT:PSS type in MoS_2-PEDOT nanocomposite thin films [229]. The band at 1442 cm^{-1} has been found to resemble the C=C symmetric band in MoS_2-PEDOT nanocomposite [230]. The bands at 1505 and 1571 cm^{-1} are due to C=C asymmetric stretching vibration of the thiophene rings [231]. The shift band at 1539 cm^{-1} is connected to asymmetric splitting vibrations

[231]. Besides, shift bands at 1257 and 1366 cm^{-1} are due to inter-ring stretching vibrations for 'Cα–Cα' and stretching deformations 'Cβ–Cβ' for MoS_2-PEDOT nanocomposite structures [232, 233].

Figure 4.7 shows the particle size measurement of MoS_2-PEDOT nanocomposite materials 1:2 (curve 1), 1:1 (curve 2) and 2:1 (curve 3) ratio of MoS_2-PEDOT obtained using Zetasizer Nano particle analyzer range. The Z-average size of the particles in liquid samples has been found to be 458 nm (1:2 ratio), 572 nm (1:1) and 882 nm (2:1) for MoS_2-PEDOT nanocomposite particle. The difference in the particle size determined through XRD and the particle size analyzer can be explained by the agglomeration of the nanoparticles in the aqueous solution. However, we have made the electrodes using Nafion, which is an organic based solution.

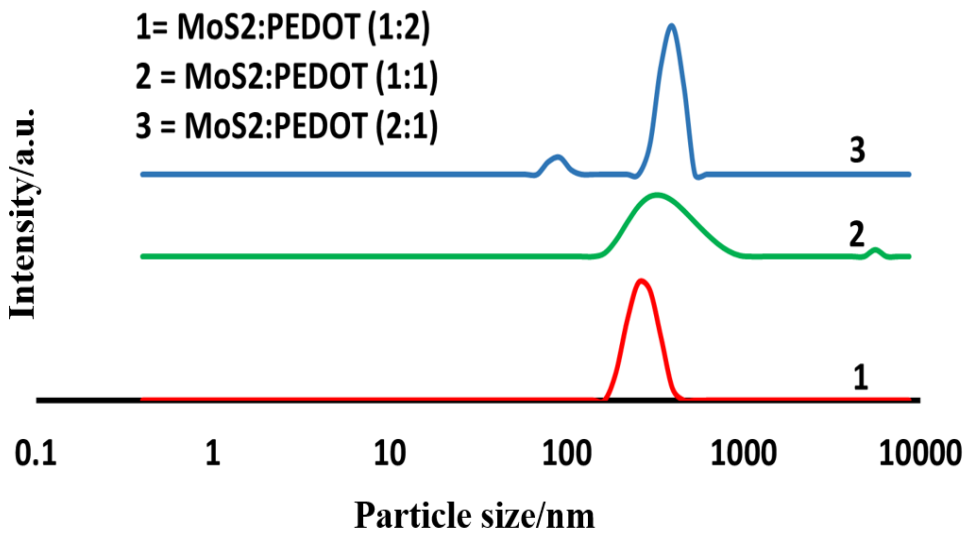

Figure 4.7 (a) Particle size and (b) raw correlation of (1) 1:2 MoS_2-PEDOT, (2) 1:1 MoS_2-PEDOT and (3) 2:1 MoS_2-PEDOT nanocomposite.

4.3.2 Electrochemical Responses of Supercapacitor

The electrochemical measurements on various samples were performed using electrochemical workstation (Volta lab). MoS_2-PEDOT nanocomposite electrodes were tested in both two and three electrode configuration using aqueous electrolytes at room temperature. In a

three electrode configuration, Nafion was mixed with MoS_2-PEDOT to coat a film onto the graphite as the working electrode, platinum was used as the counter electrode and Ag/AgCl as the reference electrode. Figure 4.8 (a and b) shows CV studies as a function of scan rates (5, 10, 20, 50 & 100 mV/s) for 1:2 MoS_2-PEDOT nanocomposite electrode in 2 M HCl electrolyte for three and two electrode configurations. Figure 4.8 (a) shows the oxidation peak at 0.55 V and reduction peak at 0.3 V for the three electrode configuration, while Figure 4.8 (b) shows the oxidation peak is at 0.8 V and the reduction peak at 0.7 V for the two electrode configuration, both at 5 mV/s. There is a marked difference in peak position in both three and two electrode configurations. However, there is a shift in both redox peaks as a function of scan rate and follows the typical trend of any nanocomposite structure [18].

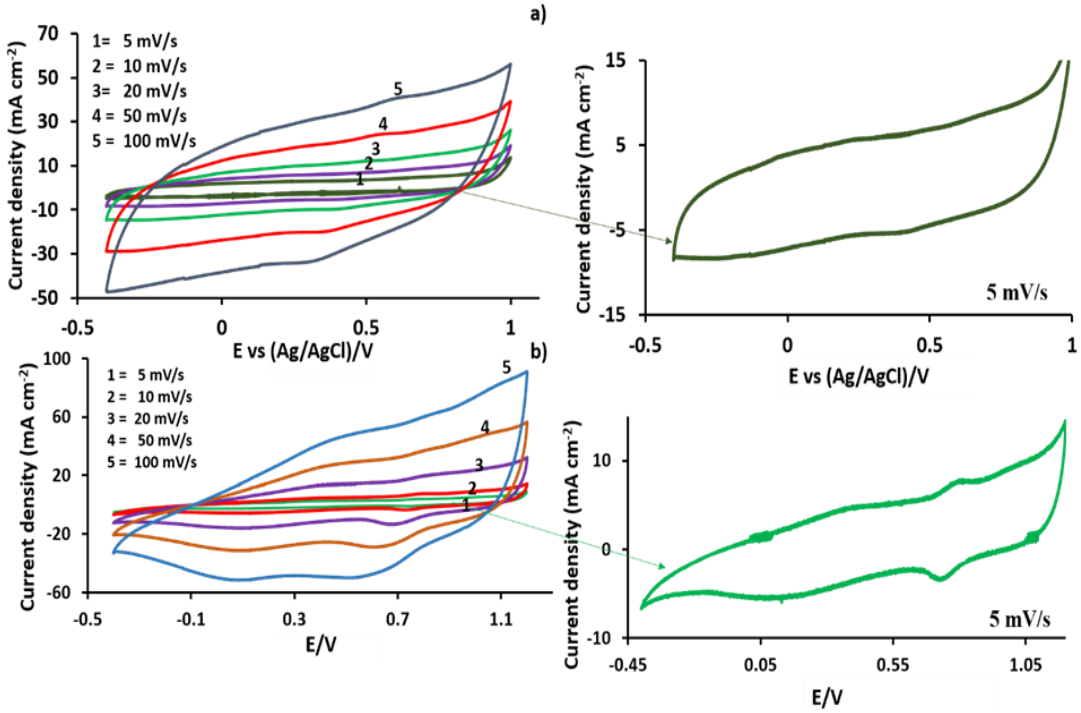

Figure 4.8 (a) Three (b) two configuration cells CV of 1:2 MoS_2-PEDOT nanocomposite electrodes in 2 M HCl as a function of scan rates (1) 10 (2) 20 (3) 50 and (4) 100 mV s^{-1}.

Figure 4.9 (a and b) shows CV at various scan rates (5, 10, 20, 50 & 100 mV s^{-1}) in 2 M H_2SO_4 for three and two electrode configurations. Figure 4.9 (a and b) shows a weak peak potential

at lower scan rate and no redox peak potential at higher scan rate due to the lower reaction kinetics in 2 M H_2SO_4 in MoS_2-PEDOT nanocomposite. At 5 mV/s, the weak redox peaks at 0 and −0.2 V as shown in Figure 4.9 (a) where in Figure 4.9 (b) the anodic peak is at 0.6 V and cathodic peak is at 0.3 V. The SO_4^{-2} is not able to replace any sulfur ions from the MoS_2 as well as the presence of sulphur in PEDOT makes H_2SO_4 a less reactive electrolyte in electrochemical studies. There was an increase in the current as a function of scan rate, suggesting a reversible process.

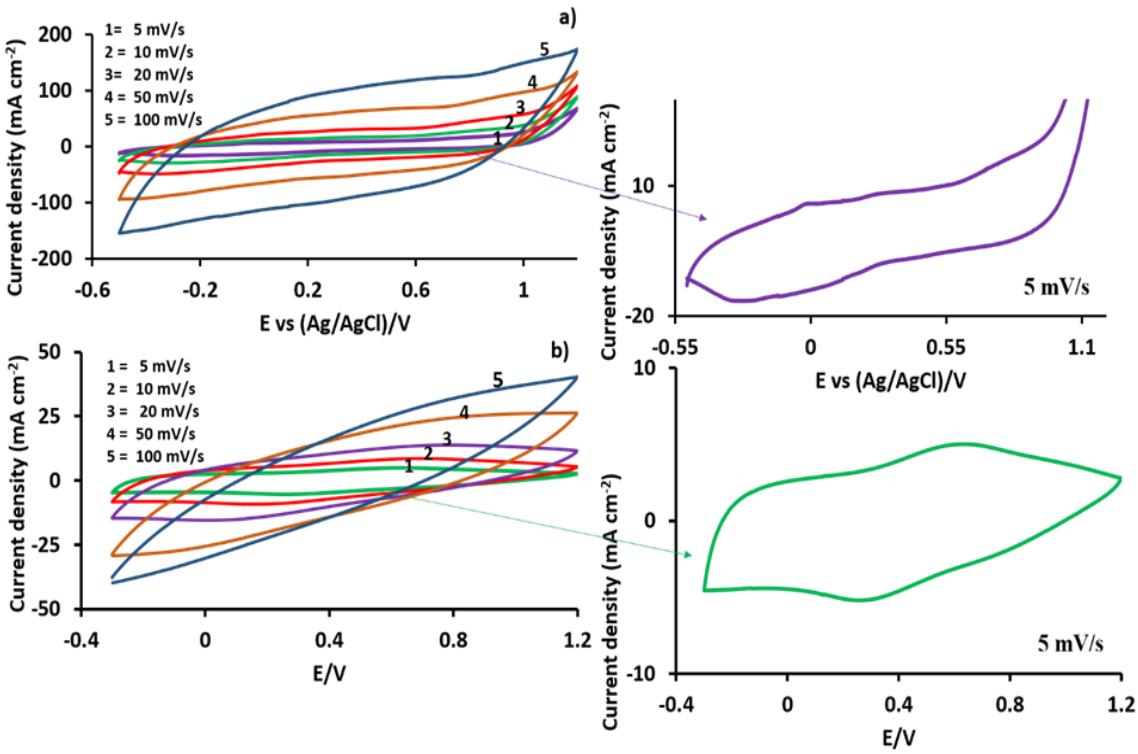

Figure 4.9 (a) Three (b) two configuration cells CV of MoS_2-PEDOT (1:2 ratio) nanocomposite electrodes in 2 M H_2SO_4 as a function of scan rates (1) 10 (2) 20 (3) 50 and (4) 100 mV s^{-1}.

The specific capacitance values of the supercapacitors from the respective cyclic voltammograms are listed in table 4.1 (a and b) which have been calculated, using equation (3.1). The estimated specific capacitance for MoS_2-PEDOT has been found to be 452 F g^{-1} and 360 F g^{-1} for three electrode and two electrode configurations in 2 M HCl acid. The specific capacitance obtained for MoS_2-PEDOT nanocomposite electrodes can be well compared with the results

obtained by Wang et. al who have shown 405 F g^{-1} for MoS_2-PEDOT composite synthesized using exfoliation and in-situ polymerization technique [97].

Table 4.1 Specific capacitance of MoS_2-PEDOT in aqueous electrolyte systems estimated using CV studies for (a) symmetric and (b) 3-electrode configurations.

a)

Aqueous Electrolyte	Electrode material	Scan rate (mV/s)	Specific capacitance (F g^{-1})
2 M HCl	2:1 MoS_2:PEDOT	5	209
		20	190
		100	142
2 M HCl	1:1 MoS_2:PEDOT	5	257
		20	230
		100	195
2 M HCl	1:2 MoS_2:PEDOT	5	360
		20	345
		100	311
2 M H_2SO_4	2:1 MoS_2:PEDOT	5	177.5
		20	160
		100	133
2 M H_2SO_4	1:1 MoS_2:PEDOT	5	214
		20	197
		100	161
2 M H_2SO_4	1:2 MoS_2:PEDOT	5	288
		20	264.5
		100	222

b)

Aqueous Electrolyte	Electrode material	Scan rate (mV/s)	Specific capacitance (F g^{-1})
2 M HCl	2:1 MoS_2:PEDOT	5	317.5
		20	303
		100	274
2 M HCl	1:1 MoS_2:PEDOT	5	369
		20	355
		100	212
2 M HCl	1:2 MoS_2:PEDOT	5	452
		20	445
		100	403
2 M H_2SO_4	2:1 MoS_2:PEDOT	5	261
		20	244
		100	207

Table 4.1 (Continued)

Aqueous Electrolyte	Electrode material	Scan rate (mV/s)	Specific capacitance ($F\ g^{-1}$)
2 M H_2SO_4	1:1 MoS_2:PEDOT	5	298
		20	277
		100	230.5
2 M H_2SO_4	1:2 MoS_2:PEDOT	5	367
		20	248
		100	212.5

Table 4.2 Specific capacitance of MoS_2-PEDOT in aqueous electrolyte systems estimated using charging and discharging mechanisms for 2 and 3 electrode configurations.

Aqueous Electrolyte	Electrode material	Device configuration	Discharging current (mA)	Specific capacitance (Fg^{-1})
2 M HCl	2:1 MoS_2:PEDOT	Symmetric	20	175
			10	150
2 M HCl	1:1 MoS_2:PEDOT	Symmetric	20	204
			10	177
2 M HCl	1:2 MoS_2:PEDOT	Symmetric	20	285
			10	250
2 M H_2SO_4	2:1 MoS_2:PEDOT	Symmetric	20	145
			10	122
2 M H_2SO_4	1:1 MoS_2:PEDOT	Symmetric	20	181
			10	158
2 M H_2SO_4	1:2 MoS_2:PEDOT	Symmetric	20	220
			10	198
2 M HCl	2:1 MoS_2:PEDOT	Symmetric	20	290
			10	275
2 M HCl	1:1 MoS_2:PEDOT	Symmetric	20	330
			10	304
2 M HCl	1:2 MoS_2:PEDOT	Symmetric	20	418
			10	394
2 M H_2SO_4	2:1 MoS_2:PEDOT	Symmetric	20	238
			10	208
2 M H_2SO_4	1:1 MoS_2:PEDOT	Symmetric	20	265
			10	230
2 M H_2SO_4	1:2 MoS_2:PEDOT	Symmetric	20	333
			10	301

Figure 4.10 shows the charging and discharging behaviors of 1:2 MoS_2-PEDOT in a 2 M HCl aqueous solution. The charging and discharging is symmetric in the HCl electrolyte.

Figure 4.11 shows the charging and discharging behavior of MoS_2-PEDOT in a 2 M H_2SO_4 electrolyte. Unlike the case with the HCl electrolyte, the charging and discharging in H_2SO_4 electrolyte is not symmetrical due to the slower electrochemical reaction kinetics for the presence of $SO4^{-2}$ ions in the solution. Data from charging-discharging the capacitors can be used to estimate their specific capacitances using equation (3.2).

The specific capacitance has been estimated as a function of scan rate for the MoS_2-PEDOT nanocomposite electrodes as shown in tables 4.1 and 4.2. The specific capacitance of each nanocomposite is greater in the HCl than H_2SO_4 based electrolyte due to faster electrochemical kinetics in the HCl than H_2SO_4 electrolyte.

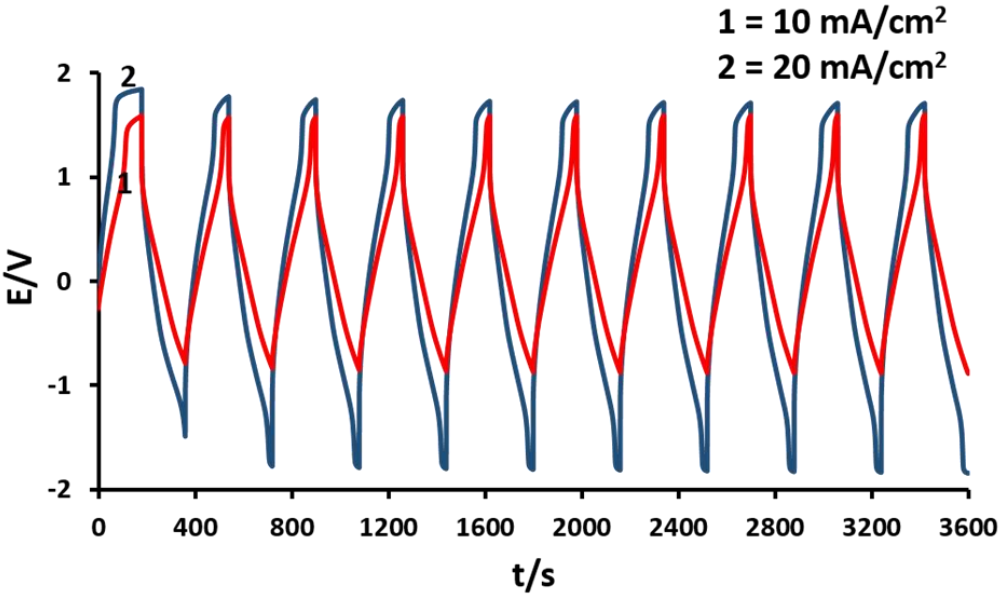

Figure 4.10 Charging and discharging mechanism in MoS_2-PEDOT (1:2 ratio) supercapacitor in 2 M HCl electrolytic media at different discharging currents: (1) 10 mA and (2) 20 mA.

Figure 4.12 (curve 1-2) shows Nyquist plots of MoS_2-PEDOT based supercapacitor containing (1:2 ratio) in both (1) 2 M HCl, and (2) 2 M H_2SO_4 electrolytic systems. The electrode/electrolyte conductivity for H_2SO_4 was 0.4 ohm (Ω) whereas HCl based electrolyte shows 0.5 Ω resistance. However, there is a variation in the Nyquist plot for H_2SO_4, but little

variation has been observed for the impedance value for 2 M HCl cells. That is also consistent with CV and charging-discharging characteristics of the nanocomposite electrodes.

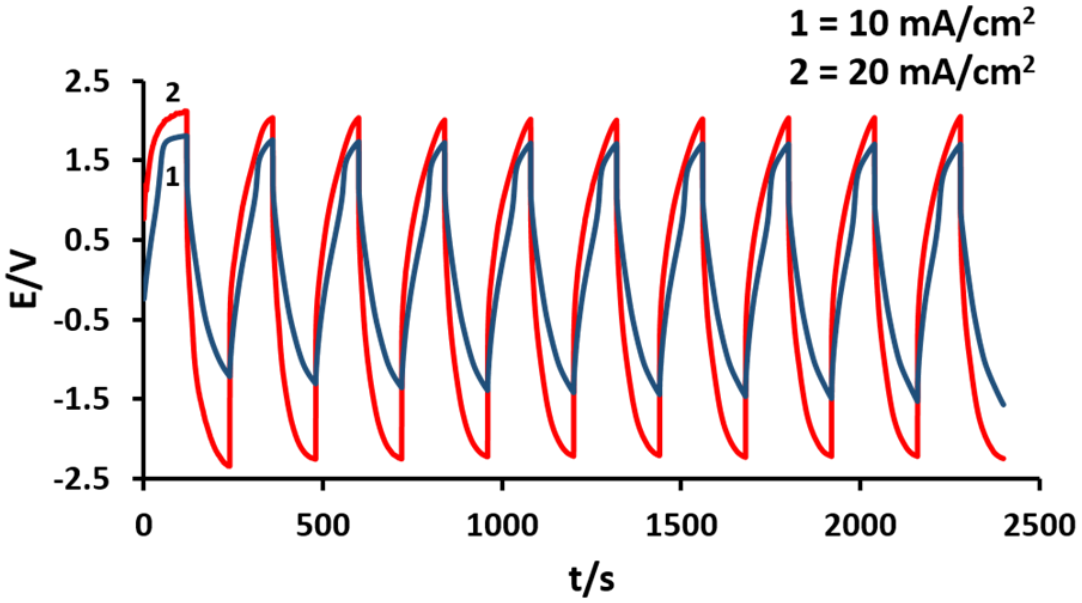

Figure 4.11 Charging and discharging mechanism in MoS_2-PEDOT (1:2 ratio) supercapacitor in 2 M H_2SO_4 electrolytic media at different discharging currents: (1) 10 mA and (2) 20 mA.

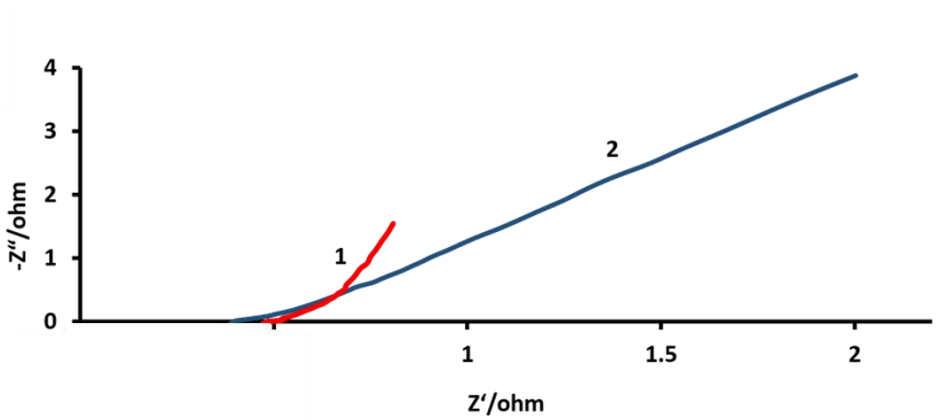

Figure 4.12 Nyquist plots of MoS_2- PEDOT (1:2 ratio) supercapacitor in (1) 2 M HCl, and (2) 2 M H_2SO_4.

Figure 4.13 shows the schematic diagram of three electrodes based electrochemical cell configuration which shows the charged state (left) and discharged state (right) of supercapacitor. The positive ions adsorption along with the large electrode surface area is illustrated in enlarged view in Figure 4.13. There is clear charge separation between the working and counter electrodes

due to the double layer and the positive charges in MoS_2-PEDOT due to pseudocapacitive effect in three electrodes based supercapacitor configuration.

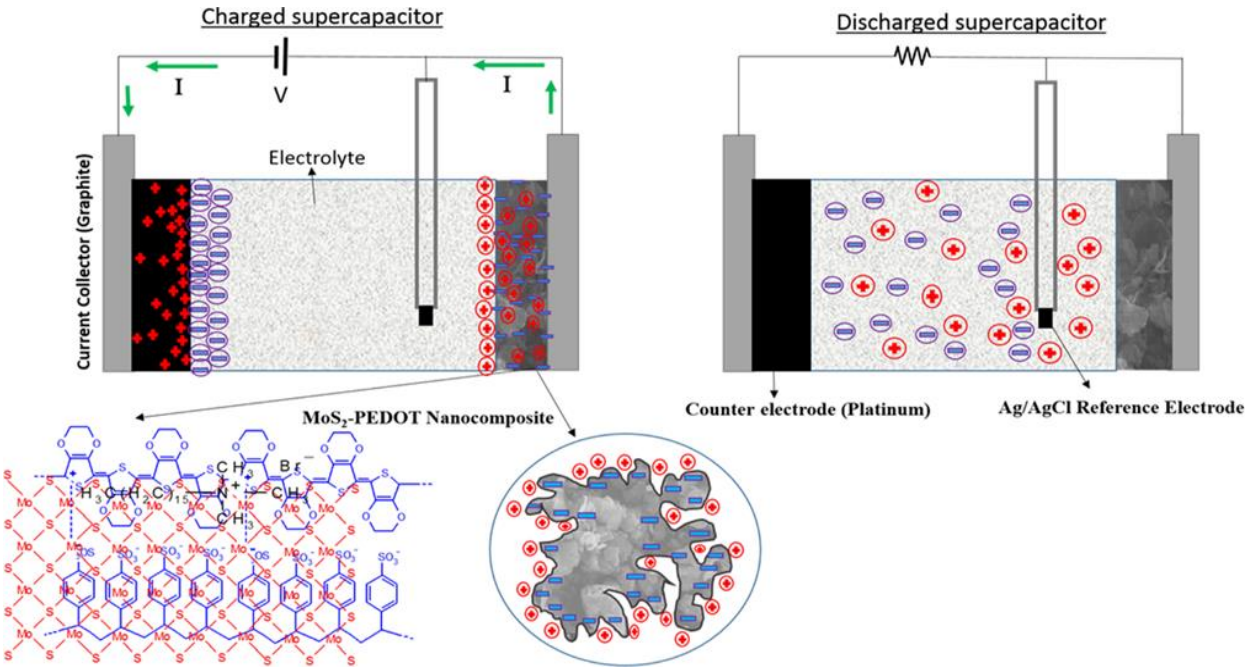

Figure 4.13 Schematic diagrams of an electrochemical pseudocapacitive supercapacitor showing the charged (left) and discharged (right) states.

4.4 Conclusions

The MoS_2-PEDOT nanocomposite was chemically synthesized by oxidative polymerization of ethylenedioxythiophene (EDOT) and MoS_2 using PSS polyanions and surfactant CTAB under controlled conditions. The MoS_2-PEDOT composite showed uniform structure with plate like MoS_2 structure wrapped in PEDOT. The infrared spectrum was sensitive to CH vibrations and showed shifts to identify the prominent changes in the polymer structure. The Raman study has shown the CC asymmetric stretching vibration due to thiophene rings in the middle and the latter due to those at the end of the chains. The XRD curves have revealed sharp and defined peaks of MoS_2 indicating crystallinity in MoS_2–PEDOT composite materials. The specific capacitance for MoS_2-PEDOT has been shown around 452 F g^{-1} and 360 F g^{-1} for three

electrode and two electrode configurations in 2 M HCl acid, respectively. Based on charging discharging behavior of MoS_2-PEDOT nanocomposite, it seems that higher concentration of MoS_2 to EDOT causes better pseudocapacitive behavior for supercapacitor applications. 2 M HCl-based supercapacitors exhibit an energy density of 52 W h kg^{-1}, and a power density of 4.8 kW kg^{-1} at the constant current density of 10 mA g^{-1} for MoS_2-PEDOT based supercapacitor electrodes.

CHAPTER 5: PROCESSED POLYANILINE-MOLYBDENUM DISULFIDE NANOCOMPOSITE ELECTRODES FOR SUPERCAPACITOR APPLICATIONS

5.1 Introduction

The rapidly increasing demand for energy storage devices has promoted further development of electrochemical supercapacitors due to their unique high power density, charge-discharge mechanism and superior stability. Recently, 2-dimensional (2D) materials (molybdenum disulfide (MoS_2)) layered nanocomposite with carbon materials (activated carbon fibers tows [234], carbon aerogel [235], carbon nanotubes [236-239], graphene [70, 240-242]) and/or conducting polymer (polyethylenedioxythiophene [26], polypyrrole [28, 189], polyaniline (PANI) [67, 243] and so on) have been synthesized to obtain high specific power and specific energy in asymmetric or symmetric electrodes for supercapacitors. Among them, conjugated PANI/ 2D-layered MoS_2 nanocomposite materials have shown high stability, cost-efficiency and larger surface area as well as reinforcement during the doping and undoping of counter ions in PANI structure [141]. The specific power and specific energy in a supercapacitor are largely dependent on the electrode material, its synthesis processes of obtaining nanocomposites, the electrode fabrication process, its electrical conductivity and redox electrochemical properties [1, 244].

Conducting polymers (CPs) are promising electrode materials for supercapacitor applications due to ease in synthesis, excellent electrochemical reversibility, high conductivity and mechanical flexibility [157, 245-247]. However, the agglomeration and solubility of CPs can influence their application in nanocomposites [248]. Among various CPs, PANI is one of the promising materials for energy storage applications in pseudocapacitors due its multiple oxidation

states. However, it is found that not only the electrical conductivity but also the solubility of PANI for fabricating nanocomposites depends on the oxidation state of the polymer [249, 250].

Previous studies have employed different approaches to cover uniformly MoS_2 nanosheets with a PANI coating layer to obtain nanocomposite electrodes for supercapacitor applications [72, 92, 251, 252]. Fabrication of PANI emeraldine salt (ES) two nanocomposites is challenging due to insolubility of the polymer [253]. Therefore, we have introduced a new method in which first MoS_2/PANI ES I nanocomposite is synthesized, then the polymer is undoped to the emeraldine base (EB) form. After mixing the material with N-Methyl-2-pyrrolidone (NMP), it is treated with HCl to produce MoS_2/PANI ES II nanocomposite (Figure 5.1). The presented results show that a very high specific capacitance can be achieved for a certain concentration of polymer in the nanocomposite material.

5.2 Experimental

5.2.1 Synthesis of MoS_2/PANI ES State One (ESI) Nanocomposites

By choosing appropriate oxidant (ammonium peroxydisulfate, $(NH_4)_2S_2O_8$), chemical oxidative polymerization technique was used to synthesis MoS_2/PANI nanocomposite as illustrates in Figure 5.1. In order to achieve the optimal nanocomposite electrode materials, various amounts of aniline monomer (1, 5 and 10 ml) were used and labeled as MoS_2 PANI-1, PANI-5 and PANI-10, respectively.

The aniline was first mixed in 60 ml of a solution of 1 M HCl and 0.025 M of $(NH_4)_2S_2O_8$ in an ice bath while the MoS_2 (1 gm) was dissolved in deionized water using 100 mg of surfactant cetrimonium bromide (CTAB). Simultaneously, 40 ml a solution of 0.025 M ammonium peroxydisulfate in 1 M HCl was prepared for 2 hours before it was slowly mixed together with aniline and MoS_2 solution to dedope the polymer. After stirring the final reaction for 12 hours in

an ice-water bath, a dark green MoS_2-PANI nanocomposite was obtained as ESI. Next, the MoS_2/PANI ESI nanocomposite was vacuum filtered, and washed using low-boiling solvents such as acetone, methanol and deionized water then was dried at 100° C for 3 hours [179, 181].

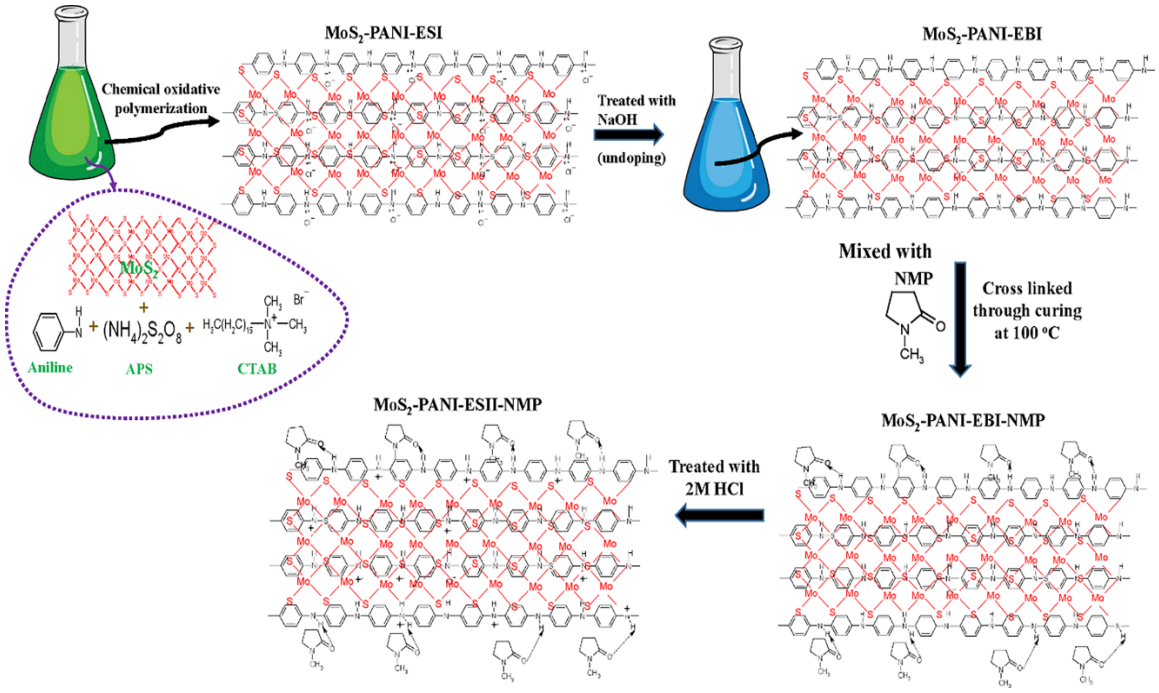

Figure 5.1 Schematic of MoS_2/PANI ESI and ESII nanocomposite synthesis.

5.2.2 Synthesis of MoS_2 ES State Two (ESII) Nanocomposites

As shown in Figure 5.1, the dried powder samples of MoS_2/PANI ESI have been undoped by using 50ml aqueous solution of 1 M sodium hydroxide (NaOH) to remove HCl and unreacted organic constituents. The solution was stirred for 24 hours. The synthesized EB of PANI and MoS_2 nanocomposite (MoS_2/PANI EB) was washed, and filtered in a filter paper. The MoS_2/PANI EBI nanocomposite powder were dried at 100° C for 3 hours then mixed with NMP as binder prior to depositing onto graphite substrate.

The MoS_2-PANI nanocomposite was dedoped in 2 M of HCl for 2-minutes for attaining MoS_2 and ESII of PANI nanocomposite material. All the chemicals, including the aniline monomer and MoS_2, were purchased from Sigma and used as received.

5.2.3 Optical Characterizations of Films

The vibrational bands of PANI (ESI & ESII) and MoS_2, MoS_2/PANI (ESI & ESII) nanocomposite powders were characterized using FTIR "Perkin Elmer spectrum one" spectrophotometer. Potassium bromide (KBr) powder was mixed with 1% of nanocomposite powders for obtaining pressed pellets for the FTIR spectra. Films of above materials were deposited on a silicon substrate for the Raman measurement.

5.2.4 Surface/Structure Characterization

The morphology and structure of (PANI ESI & ESII), MoS_2 and MoS_2/PANI (ESI & ESII) samples was investigated by field emission scanning electron microscopy (FE-SEM, SU70, at accelerating voltage of 5kV) where transmission electron microscopy (TEM) and high resolution transmission electron microscopy (HRTEM) images of MoS_2/PANI (ESI & ESII) nanocomposites were collected using Tecnai F20. The crystalline structure of all above materials were studied using Philips Panalytical Xpert Pro MRD X-ray diffraction (XRD) technique with Cu Kα radiation (wavelength = 1.5442 Å) and 2θ range from 10° to 70° where the Zetasizer Nano particle analyzer range model was used for the average particle size measurement.

5.2.5 Electrical and Electrochemical Characterization

The four-point probe method was used to investigate the electrical conductivity of the pure MoS_2 and PANI ESI & ESII, as well as their nanocomposites. All conductivity measurements were performed by placing a thin pellet (1 mm) under a custom-made four-probe setup connected to a Kiethley (2602) source-measure unit. Whereas, the Radiometer Analytical Voltalab 40 was used for all electrochemical measurements, the three-electrode configuration cell setup was adopted with silver (Ag)/ silver chloride (AgCl) and platinum (Pt) wires as reference and counter electrodes, respectively.

5.2.6 Electrode Fabrication

Most of the supercapacitor studies on PANI nanocomposite are based on ESI. Since the ES state of PANI is not processable, binder materials such as 'Nafion' or 'camphorsulfonic acid', should be used to mix with the composite material to fabricate supercapacitor electrodes. In this work, we have used NMP as a solvent and binder to EB form of PANI. The synthesized PANI EB and MoS_2 nanocomposite powders were mixed with 0.1 M NMP and stirred thoroughly before deposition onto graphite substrates (1 cm ×1 cm). The edges and back of the substrates were insulated before coating films. The coated substrates were dedoped in 2 M HCl for 2 minutes then dried at 100° C. The electrolytic solutions was 1 M sulfuric acid 'H_2SO_4' in DI water.

5.3 Results and Discussion

5.3.1 Physical and Structural Characterization

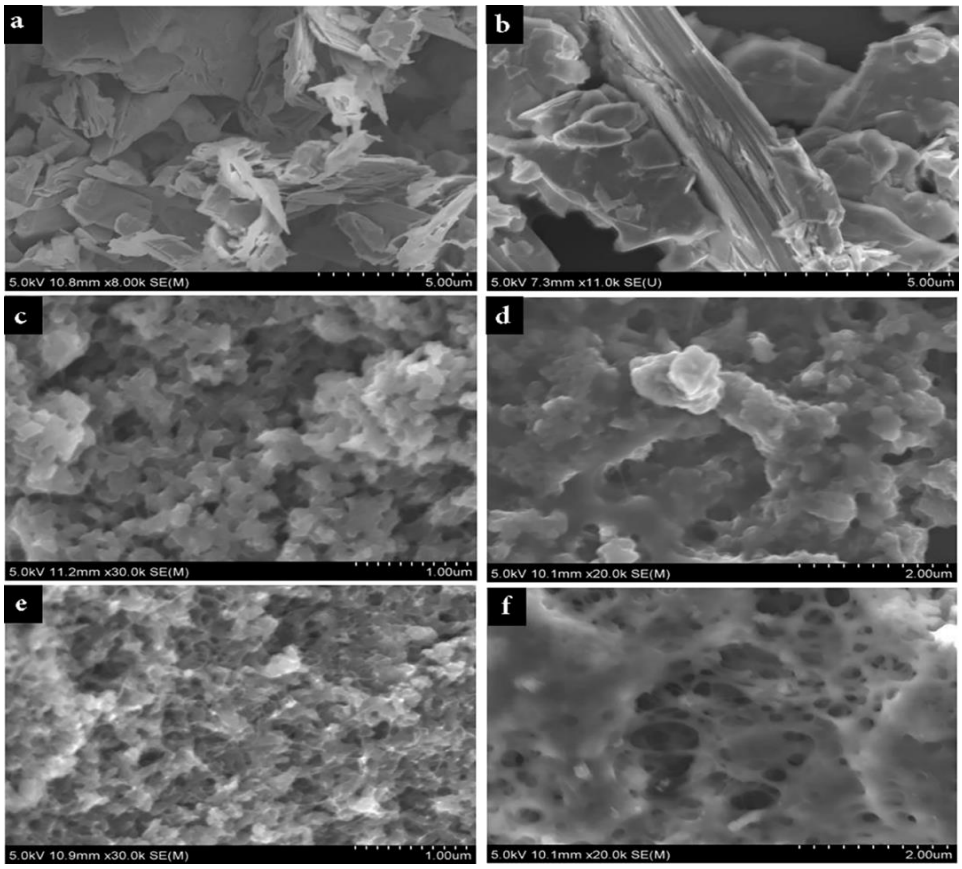

Figure 5.2 SEM images of pure: (a & b) MoS_2, (c & d) ESI and (e & f) ESII samples.

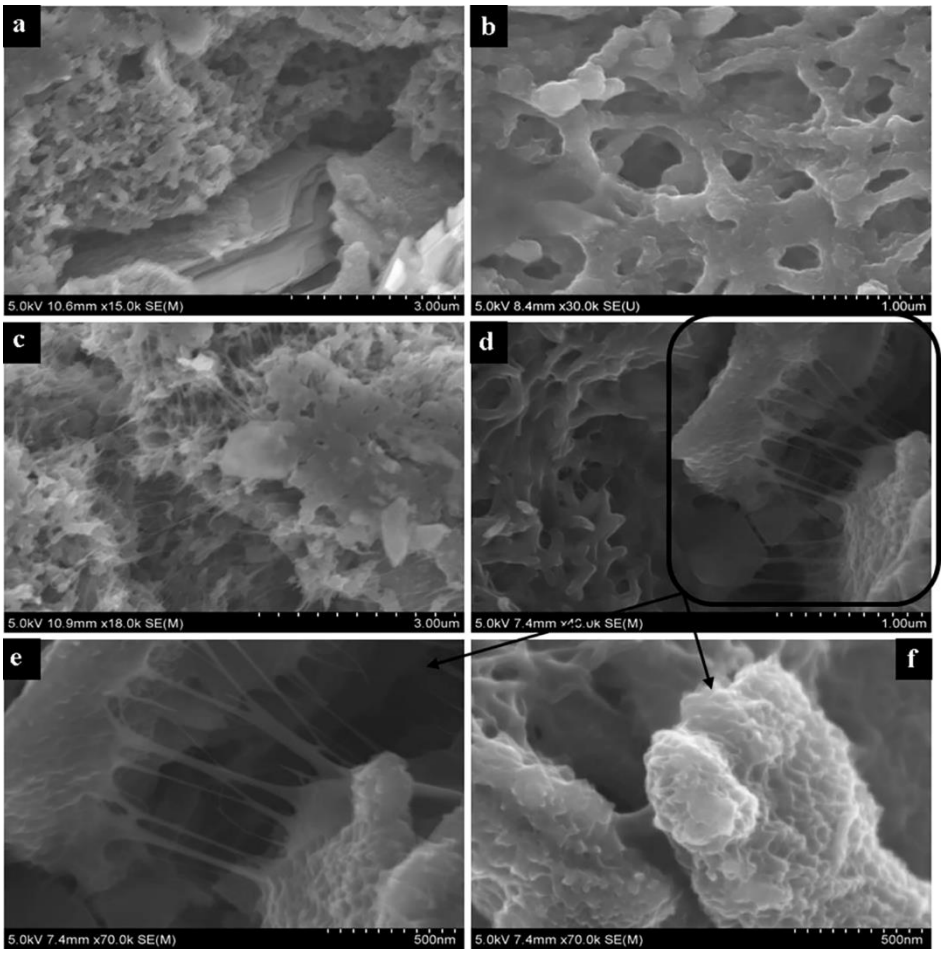

Figure 5.3 SEM images of (a & b) MoS_2-ESI and (c-f) MoS_2-ESII nanocomposites.

To explore the nanostructure and intercalation of the porous network of PANI into MoS_2 flakes, SEM was used. The FE-SEM images of the MoS_2, pure PANI (ESI & ESI) and nanocomposites of MoS_2-PANI-ESI/ESII samples are shown in Figure 5.2 and 5.3. Smooth surface of MoS_2 nanosheets was observed in Figure 5.2 (a & b). A continuous porous network due to PANI dendritic nanofibers was obtained in Figure 5.2 and 5.3. As shown in Figure 5.3, PANI was coated homogenously and acted as the conductive, connective and protective coating layer on MoS_2. Figure 5.3 (e and f) illustrates that PANI nanofibers were connected with each other, consisting of porous networks formed by PANI, which could exhibit enhanced conductivity of supercapacitor electrodes. In contrast, MoS_2/PANI ESII nanocomposite shows that the PANI ESII nanowire arrays on the top of MoS_2 could facilitate the electrolyte ions diffusion, resulting in high

utilization of PANI's surface and fast doping and undoping processes. The SEM studies confirm that PANI was wrapping homogenously over entire surfaces of MoS_2 nanosheets.

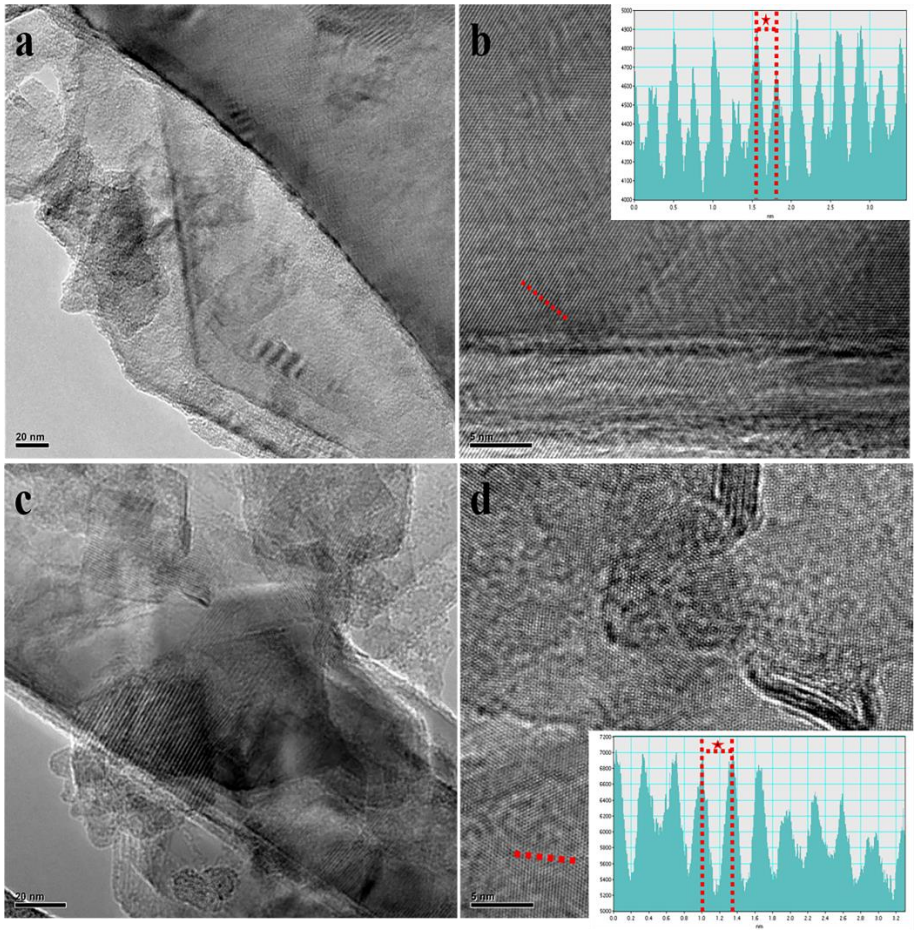

Figure 5.4 Low and high-magnification TEM images of: (a & b) MoS_2/PANI ESI and (c & d) MoS_2/PANI ESII nanocomposites. Inset of (b & d) showing the interlayer spacing along the red line.

The TEM images (Figure 5.4) further confirm that uniform hexagonal MoS_2 nanosheets were embedded in PANI layers with some well-defined edges and parallel lines due to the multi-layered MoS_2 nanosheets. The unique interaction between PANI and MoS_2 was further recognized using the high-resolution TEM (HRTEM). The contrast between the dark umps/edges of MoS_2 and ultrathin PANI amorphous layers suggests a fine dispersion and uniform distribution of ESII in the nanocomposite which is potentially beneficial for the supercapacitor applications The HRTEM images in figure 5.4 (b and c) exhibit lattice fringes with the same clear interlayer spacing

of 0.274 corresponding to the (110) plane of crystalline MoS_2 [254], consistent with the XRD results.

To confirm the composition of the resultant nanocomposite material, the FTIR spectra of the pure MoS_2, PANI ESI and ESII as well as the MoS_2-ESI/ESII nanocomposite materials are provided in Figure 5.5. The absorption signals of PANI at 1639 and 1457 cm^{-1} can be assigned to the C═C stretching of the stretching vibration of the quinonoid ring and benzenoid deformation, respectively [255, 256]. The peak at 1167 cm^{-1} is attributed to the N═Q═N, where Q represents the quinoid ring while the bends at 795 and 673 cm^{-1} are due to the out of plane bending vibrations of C-H [245]. The presence of MoS_2 is confirmed by bands at 669 and 468 cm^{-1} which can be ascribed due to S═S and Mo─S, respectively [225, 257].

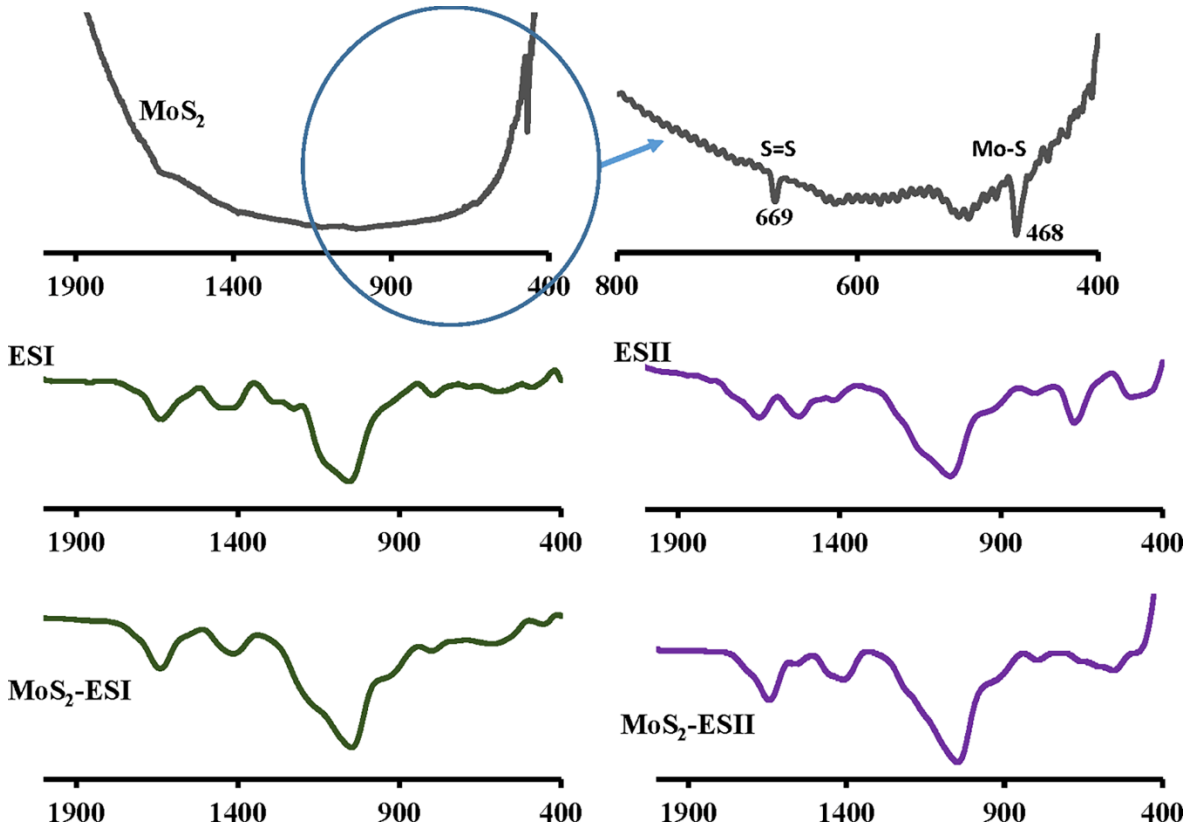

Figure 5.5 FTIR spectra of MoS_2, ESI, ESII, MoS_2-ESI and MoS_2-ESII nanocomposites (from 400 to 2000 cm^{-1}).

The interference of PANI into the MoS_2 nanosheets is further affirmed by Raman spectra (Figure 5.6). The two broad bands at 384 and 409 cm^{-1} are very characteristic of MoS_2, which can be attributed to E^1_{2g} (in-plane vibration of Mo and S atoms) mode and A_{1g} (out-of-plane vibration of S atoms) modes [258, 259]. Raman shifts of pure PANI ESI and ESII and their composites with MoS_2 show same peak positons at: 1177, 1245, 1344, 1414, 1482 and 1622 cm^{-1} are due to C-H bending (benzenoid ring), C-N stretching (benzenoid ring), C–N stretching (quinoid ring), C–C stretching (quinoid ring), C═N stretching (quinoid ring) and C–C stretching (benzenoid ring) of PANI [260, 261][40, 41].

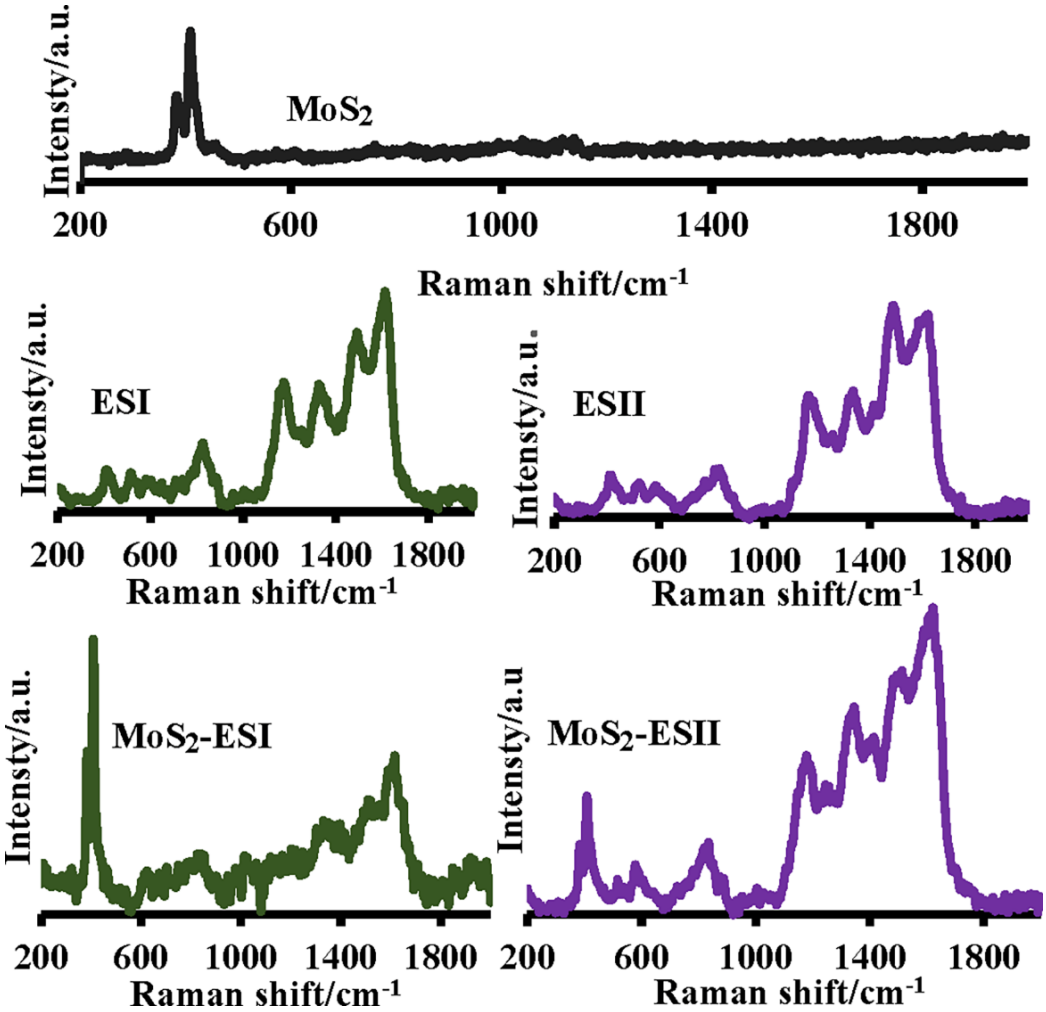

Figure 5.6 Raman spectra of MoS_2, ESI, ESII, MoS_2-ESI and MoS_2-ESII nanocomposites.

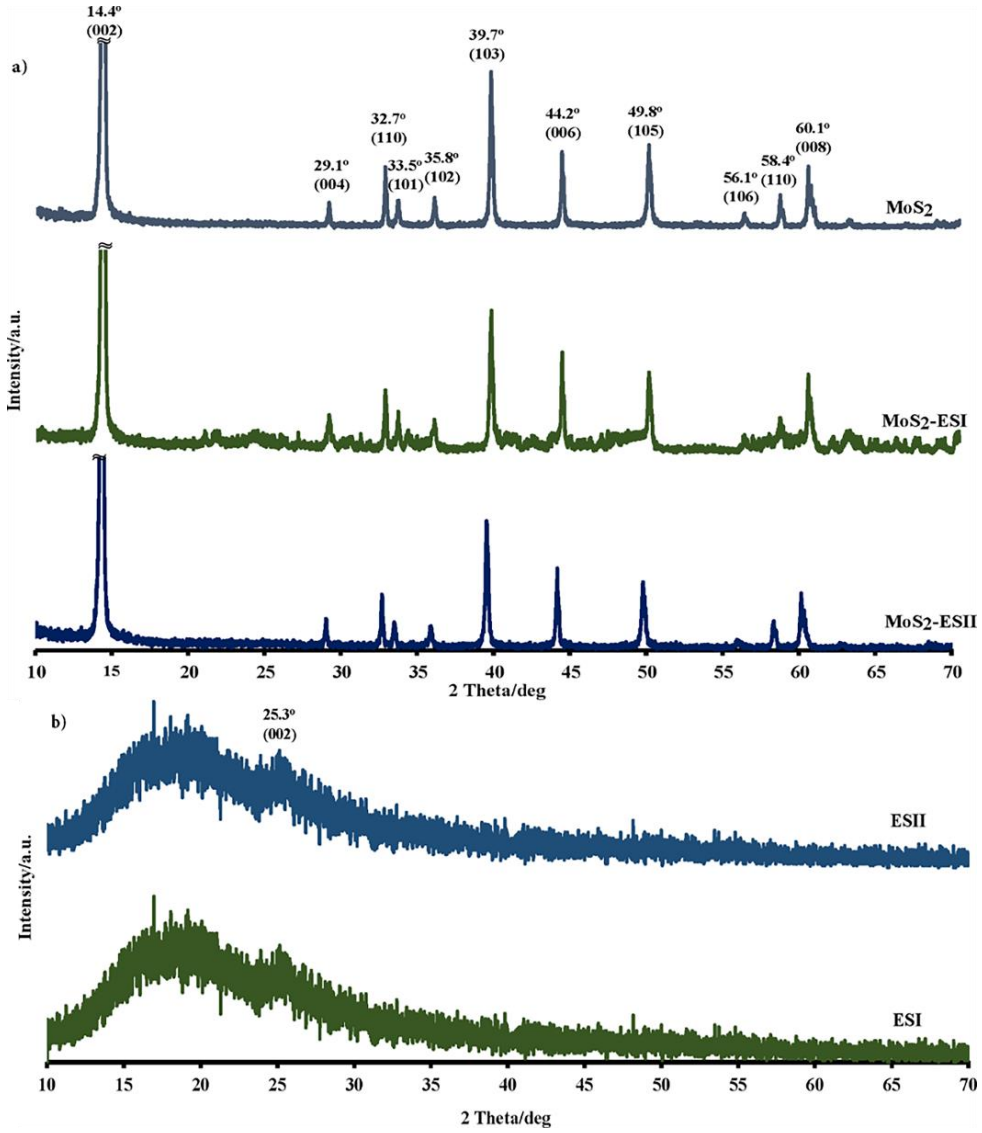

Figure 5.7 X-ray diffraction of (a) pure MoS_2 and MoS_2-ESI, MoS_2-ESII nanocomposites and (b) pure ESI & ESII.

The XRD measurement was carried out to investigate the crystal structure of the synthesized materials. The XRD pattern shown in Figure 5.7(a), displays 2θ peaks at 14.4°, 29.1°, 32.7°, 33.5°, 35.8°, 39.7°, 44.2°, 49.8°, 56.1°, 58.4° and 60.1°, which are designated to the (002), (004), (100), (101), (102), (103), (006), (105), (106), (110), and (112) diffraction planes. Whereas, the XRD pattern for pure PANI ESI/ESII (Figure 5.7b) has revealed trivial peak at 25.3° corresponding to the (002) diffraction planes, suggesting the polymer amorphous phase [262]. Furthermore, the XRD patterns of MoS_2-PANI ESI/ESII nanocomposites exhibit the similar peaks

of MoS_2 alone, confirming the presence of MoS_2, and no additional peaks has been presented. However, the diffraction peaks intensities are lower than the pure MoS_2 indicating a homogeneous mixture between PANI and MoS_2.

In order to comprehend the particle distribution of the nanocomposites in water solution, the particle size measurements were investigated. Figure 5.8 shows the particle size of the MoS_2-PANI ESI/ESII nanocomposites. MoS_2/PANI ESII nanocomposite presented smaller particle size which is key feature to gain higher electrochemical interface of the material in a supercapacitor application [7].

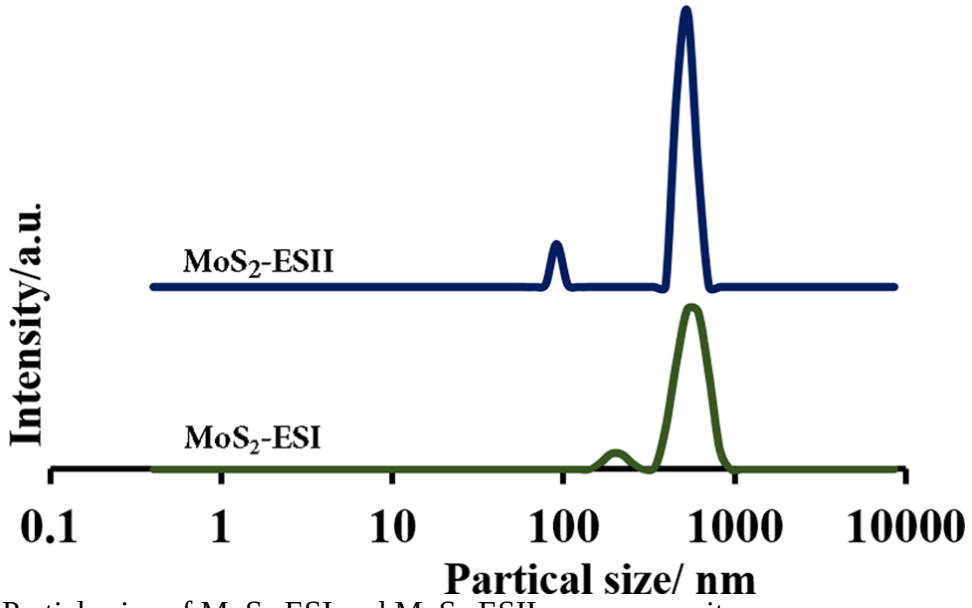

Figure 5.8 Particle size of MoS_2-ESI and MoS_2-ESII nanocomposites.

The electrical conductivity was tested using four-point probe test. As table 5.1 illustrates, electrical conductivity as high as 19.6 $S.cm^{-1}$ was achieved of MoS_2-PANI ESII. While the electrical conductivities of MoS_2, ESI, ESII and MoS_2-ESI were 4.5×10^{-5}, 1.3, 4.5 and 10 $S.cm^{-1}$, respectively. This clearly implies that the electrical conductivity of PANI was improved by adding nanocomposite materials. A reason could be that MoS_2 had cross-linked many PANI chains and also formed a more compact form of PANI.

Table 5.1 Electrical conductivity of ESI, ESII, MoS_2, MoS_2-PANI-10 ESI and ESII.

Samples	ESI	ESII	MoS_2	MoS_2 PANI-10 ESI	MoS_2 PANI-10 ESII
Conductivity ($S\ m^{-1}$)	1.3	4.5	4.5×10^{-5}	10	19.5

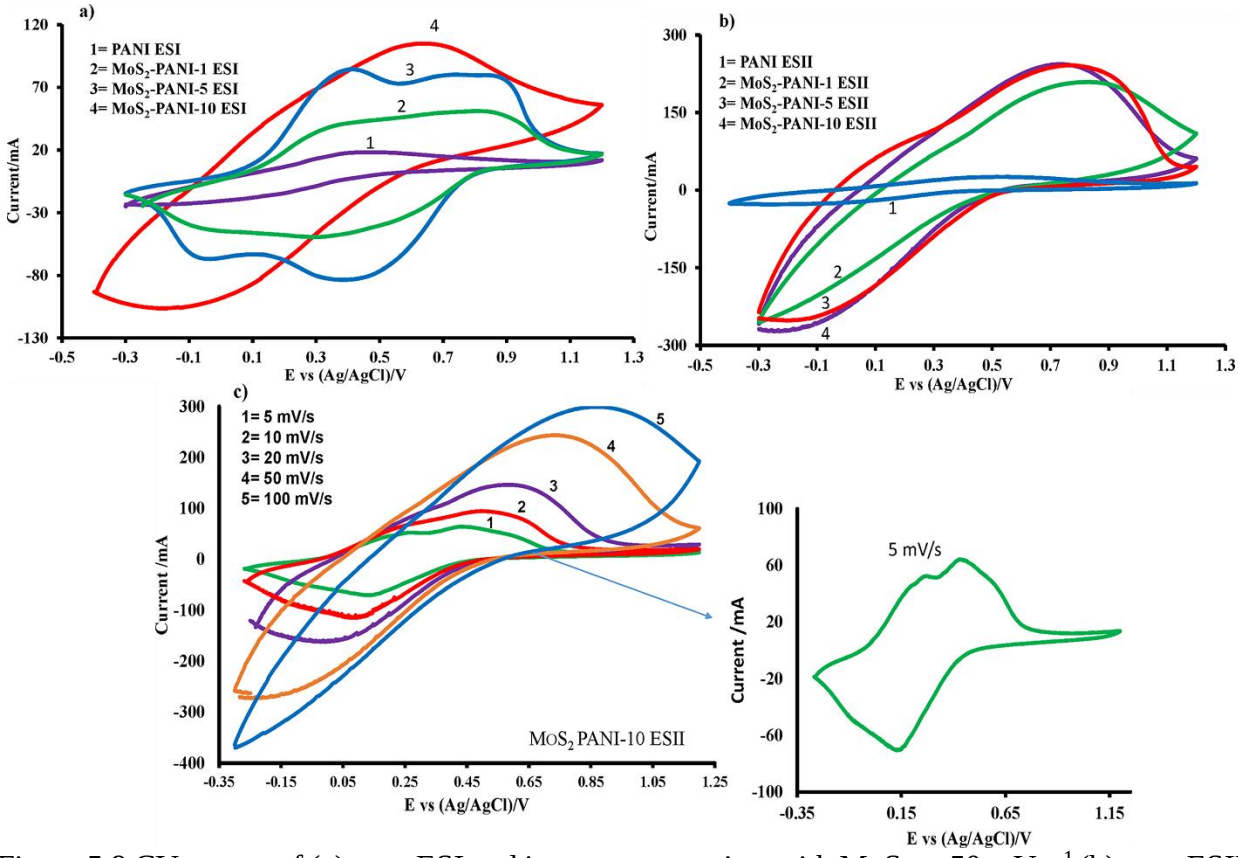

Figure 5.9 CV curves of (a) pure ESI and its nanocomposites with MoS_2 at 50 mV s^{-1} (b) pure ESII and its nanocomposites with MoS_2 at 50 mV s^{-1} and (c) MoS_2-ESII-10 nanocomposite at 5, 10, 20, 50 and 100 mV s^{-1} all in 1 M H_2SO_4 electrolytic media.

5.3.2 Electrochemical Responses of Supercapacitor

The electrochemical properties of the active material were measured, using the techniques of CV, CCCD and EIS techniques. Figure 5.9 (a & b) exhibits the CV studies of MoS_2, PANI ESI/ESII and MoS_2 with different PANI content obtained by electrochemical workstation (Volta lab) at a scan rate of 50 mV.s^{-1} in 1 M H_2SO_4 while the current is normalized to the mass of the

electrodes Even with a wide potential window from E_1 = -0.3 to E_2 = 1.2 V (vs. AgCl/Ag), the electrolyte did not show any breakdown. Yet, because of the high value of scan rate (50 mV.s^{-1}), no redox peaks were observed in most of the curves. In contrast, the nanocomposites have much higher CV loop area than the pure PANI, suggesting much higher capacitance in the composite material. More specifically, it is found that the loop area of MoS_2/PANI ESII nanocomposite is higher than that in the electrode with MoS_2/PANI ESI (Figure 5.9 a&b) [134]. Figure 5.9 (b) shows that MoS_2/PANI-10 ESII was the best among other ESII nanocomposites. Further study of MoS_2/PANI-10 ESII was carried out by testing the sample at a very low scan rate (5 mV.s^{-1}) which revealed a reversible redox system with peaks at 0.45, 0.27 and 0.13 V. This can be assigned to the transformation of emeraldine to pernigraniline form of PANI (Figure 5.9 c). The peaks clearly indicate a pseudocapacitive charge storage mechanism for all studied electrodes, as expected.

Using the CV results the materials specific capacitance (C) can be governed by equation (3.1). At a scan rate of 50 mV.s^{-1}, the specific capacitances of PANI ESI and ESII, MoS_2 PANI-1 ESI and ESII, MoS_2 PANI-5 ESI and ESII and MoS_2 PANI-10, ESI and ESII were experimentally estimated to be 203, 251, 321, 430, 384, 476, 430 and 480 F.g^{-1}, respectively (table 5.2). Since MoS_2 PANI-10 ESII has the highest capacitance, Figure 5.9 (c) shows its CV curves at scan rates from 5 to 100 mV.s^{-1}.

Table 5.2 Specific capacitance of pure ESI and ESII and their nanocomposites with MoS_2 in 1 M H_2SO_4 estimated using CV studies and charging and discharging mechanisms at a scan rate of 50 mV s^{-1} and 20 mA discharging current, respectively.

Electrode material	Specific capacitance C_s (F g^{-1})	Specific capacitance C_m (F g^{-1})
PANI ESI	203	224
PANI ESII	251	267
1:1 MoS_2:PANI ESI	321	354
1:1 MoS_2:PANI ESII	430	449
1:5 MoS_2:PANI ESI	384	441
1:5 MoS_2:PANI ESII	476	488

Table 5.2 (Continued)

Electrode material	Specific capacitance C_s (F g^{-1})	Specific capacitance C_m (F g^{-1})
1:10 MoS_2:PANI ESI	430	471
1:10 MoS_2:PANI ESII	480	512

The plots of pure ESI and ESII and their nanocomposites with MoS_2 galvanostatic charging–discharging behaviors at constant current are shown in Figure 5.10a. The faradaic reaction mechanism could be occurring in charging and discharging processes due to nonlinear shaped curves. The MoS_2-PANI-10 ESII electrode exhibits a lower internal resistance than MoS_2-PANI-10 ESI sample due to the lower resistive drop and higher discharge time. That can be attributed to the incorporation of MoS_2 nanoparticles into the processed PANI (ESII) which tended to endow the nanocomposite with a fine dispersion and uniform distribution of nanoparticles achieving a fast ion movement through the porous nanostructure. The electrode specific capacitance (C_m) can be calculated using equation (3.2). As table 5.2 illustrates, the specific capacitances of MoS_2 PANI-10 ESII was 512 F.g^{-1} which is slightly higher than calculated capacitance from the CV results (481 F.g^{-1}). The obtained specific capacitance from MoS_2 PANI-10 ESII nanocomposite (512 F g^{-1}) in this work is at least ×2.5 higher than the results achieved by Khawaja et. al (203 F.g^{-1}) who have used PANI ESI and NMP as the binder [47].

EIS measurements were carried out to understand the electrode/electrolyte interface properties of the nanocomposite materials. The Nyquist plots of MoS_2 PANI-10 ESI and ESII are shown in Figure 5.10 (b). Both curves consist of a small diameter semicircle and straight-line behavior at the high and low frequency regions, respectively. Both devices presented a series resistance of about R_S=0.6 Ω. The charge transfer resistance (R_{ct}) was estimated through the diameter of the semicircles. The MoS_2 PANI-10 ESII electrode showed an R_{ct} of 1.9 Ω, while the R_{ct} was about twice larger in the MoS_2 PANI-10 ESI electrode.

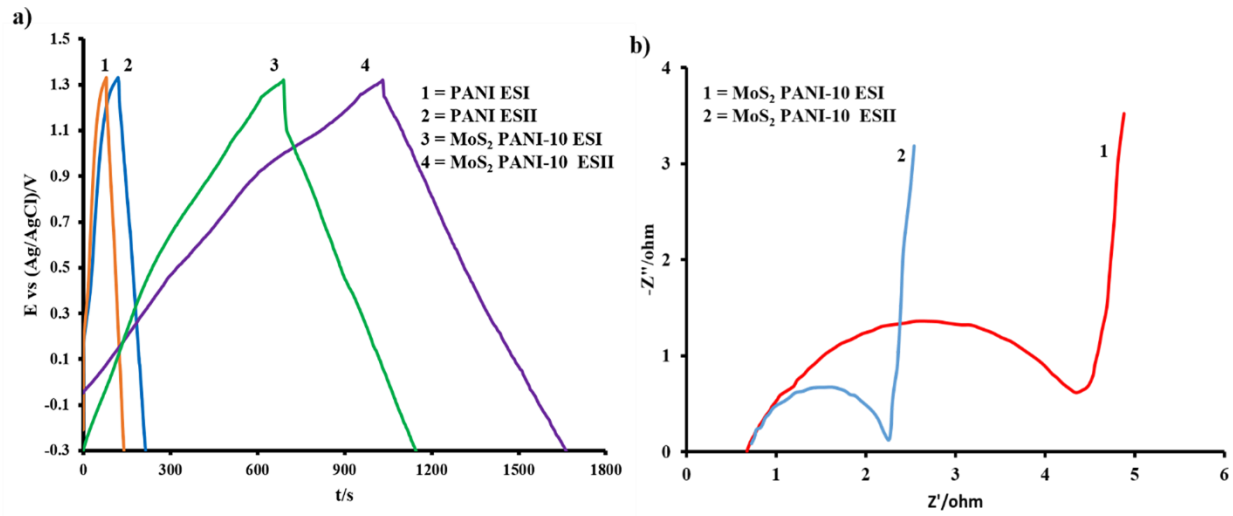

Figure 5.10 (a) Galvanostatic charge/discharge curves of pure ESI and ESII and their nanocomposites with MoS_2 in 1 M H_2SO_4 electrolytic media at 20 mA discharging current and (b) Nyquist plots of (1) MoS_2-ESI-10 and (2) MoS_2-ESII-10 nanocomposites in 1 M H_2SO_4 electrolyte.

The presented electrochemical results clearly show that the composite of MoS_2 PANI is superior to the PANI films alone for the supercapacitor applications. Additionally, it is found that MoS_2 PANI-10 ESII shows the highest electrical conductivity and specific capacitance among all other nanocomposites, which is likely due to the structure of the composite. The simple fabrication process of the electrode materials for MoS_2 and PANI nanocomposites and their high specific capacitance are encouraging for their use in commercial supercapacitors.

5.4 Conclusions

The MoS_2-PANI nanocomposite was synthesized via oxidative chemical polymerization method. However, the processing of MoS_2-PANI nanocomposite materials were realized to acquire MoS_2-ESI, MoS_2-EBI and MoS_2-ESII states using doping and undoping processes. The MoS_2/PANI EBI nanocomposite soluble in NMP allowed to coat over conducting substrates and the heat treatment was made to obtain the electrode needed to measure the supercapacitance properties. The MoS_2/PANI EBI nanocomposite film coated over the conducting substrates were dedoped in 2 M HCl to form MoS_2/PANI ESII nanocomposite. The MoS_2-PANI ESII

nanocomposite revealed nanowire arrays of PANI wrapped in MoS_2 nanosheet indicating rapid doping undoping processes. The presence of MoS_2 and PANI in the nanocomposites were emphasized using the infrared and Raman spectrum while the XRD measurement revealed crystallinity in MoS_2-PANI nanocomposite materials. The higher specific capacitances and electrical conductivity of MoS_2-ESII nanocomposite are indicative of cross-linking of PANI, and further enhancing of compactness in composite structure. The specific capacitance was realized experimentally to be 512 F g^{-1} at current density of 20 A g^{-1} in 1 M H_2SO_4 when the content of aniline was 10 ml. The stability in electrodes, high specific capacitance, cost-effectiveness, and changing-discharging behavior on MoS_2/PANI ESII nanocomposite are indicative of practical application in commercial supercapacitors.

CHAPTER 6: HIGH SPECIFIC CAPACITANCE IN SOLID-STATE SUPERCAPACITOR

6.1 Introduction

Supercapacitors have been one of the emerging energy storage technologies, with potential applications in small electronics, hybrid vehicles, solar and wind farms [37, 263, 264]. The key factors in a supercapacitor are specific capacitance, power, and energy densities, which are all largely depending on the nature of electrode materials [265]. To obtain high performance in a supercapacitor, the electrodes of the device have to be porous with a high surface to volume ratio and high conductivity. Also, for employing the pseudocapacitive effect for enhancing a device's capacitance, the electrode material should present excellent electrochemical redox stability at a wide potential window [263]. High specific capacitances have been reported in devices made of nanocomposites of a conducting polymer with graphene, MoS_2, and carbon nanotubes [18, 26, 179-182].

A practical method to enhance the porosity of the electrodes is to coat the composite materials on the surface of a cellulose or sponge structure. Kang et al [266] fabricated a solid-state supercapacitor with high surface area based carbon nanotubes on bacterial nanocellulose in poly(styrene-block-ethylene oxide-block-styrene) based ionic liquid electrolyte. The electrodes based on carbon nanotubes on bacterial nanocellulose had a specific capacitance of 50 F g^{-1}. Porous nitrogen doped carbon fibers made by Chen et al showed a specific capacitance of 202 F g^{-1} by [267]. Xiao et al. measured a volumetric capacitance of 2.5 F cm^{-3} in a solid-state supercapacitor based on carbon fiber and manganese oxide core-shell fiber [268].

Graphene aerogels showed specific capacitance of 325 F g^{-1} in a sulfuric-based electrolyte [269]. The supercapacitor fabricated by Xu et al. on a 3D sponge like nano-structure coated with functionalized multi-walled carbon nanotubes had an energy density of 7.1 Wh kg^{-1} and power density of 48 kW kg^{-1} in an ionic liquid-based electrolyte [270]. Chen et al. reported power density of 63 kW kg^{-1} and energy density of 31 Wh kg^{-1} with a manganese oxide and carbon nanotube sponge-based supercapacitor [271]. Xu et al. have fabricated supercapacitors by coating graphene oxide on polyurethane based sponge and achieved energy density of 89 W h kg^{-1} [272].

The common approach with aerogel or sponge based substrates is to dip the substrate in a conductive ink or mechanically pressing a conductive powder (e.g. carbon nanotubes or graphene) to the substrate to make conductive porous electrodes. Despite the simplicity of the process, the electrode conductivity may vary at different parts of the substrate, influencing the properties of supercapacitors.

In this work, we present a multilayer electrode being built on a sponge substrate. That electrode was used to fabricate solid-state supercapacitor with a polyvinyl alcohol (PVA) gel-based electrolyte. To build the electrode, in-situ self-assembled polymerization of both PPy and PANI were used to make a conductive surface for subsequent electrochemical polymerization of molybdenum disulfide (MoS_2)-PANI nanocomposite to obtain the supercapacitor electrodes. The electrochemical results are promising towards a practical application of the multilayer electrode structure for high power and energy density supercapacitors.

6.2 Experimental Details

6.2.1 Electrode Fabrication

A commercial kitchen sponge (Carrand/high density foam) was washed in deionized water, and dipped in polyanions solution of polystyrene sulfonate (PSS) (2 mg ml^{-1}) for 24 hours. The

PSS treatment allowed the sponge surface to absorb negative charges of anions. Initially, pyrrole was polymerized by in-situ self-assembly polymerization over the PSS treated sponge [273, 274]. 0.1 M pyrrole, 0.1 M para-toluene sulfonic acid were added in 1 M HCl solution, and later 0.05 M iron chloride was added in a solution and stirred for few second. Then the sponge was dipped in the solution and kept for 3 hours. The sponge/PSS/PPy was cleaned and kept in 1 M HCl solution. The second layer of PANI on sponge/PSS/PPy was deposited by in-situ self-assembled technique using a solution of 0.2 M aniline, 0.1 M of an oxidizing agent (ammonium persulfate, APS) in 1 M HCl for 3 hours. The third layer of PANI was deposited by electrochemical technique in 0.2 M aniline in 1 M HCl at a potential of 1.5 V for 2 hours for each side of the sponge. The 4th layer of MoS_2-PANI was electrochemically deposited over sponge/PSS/PPy/PANI in an electrochemical cell at 1.5 V in a solution containing 0.2 M aniline, 0.5 g MoS_2 and 1 g cetrimonium bromide 'CTAB' for 2 hours [275-278]. The sponge/PSS/PPy/PANI-MoS_2 substrate was turned upside down, and further deposition was also made at 1.5 V for another 2 hours to complete the deposition process. This allowed nearly metallic conductivity in the sponge/PSS/PPy/ PANI-MoS_2 layers.

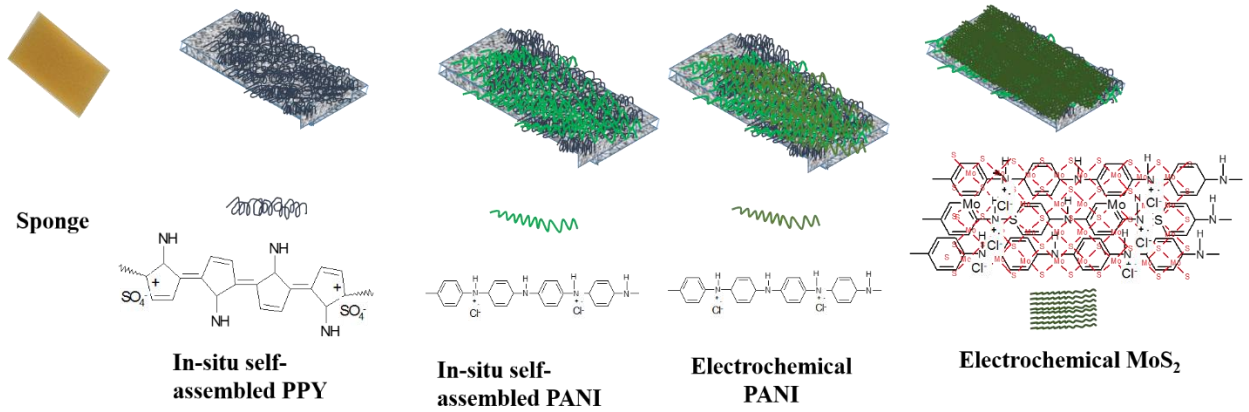

Figure 6.1 Schematic of an electrode fabrication.

Figure 6.1 shows the schematic of electrode fabrication process, chemical structures of the conducting polymer, and its composite materials. Later the sponge/PSS/PPy/PANI-MoS_2 was cleaned using deionized water, 1 M HCl, and gently squeezed to remove the acid, and left drying

for 24 hours in a room temperature. The sponge/PSS/PPy/PANI-MoS_2 was used to characterize and fabricate a solid supercapacitor. Figure 6.1 shows the schematic of PPy, PANI and PANI-MoS_2 deposited on the sponge.

6.2.2 Preparation of PVA-Gel

Initially, 10 g of poly(vinyl alcohol) (PVA) was added in 100 ml of 1 M HCl at 80 °C and stirred under for 24 hours. The gel was aged a week before fabrication of supercapacitor. Figure 6.2 shows structure of PVA-gel.

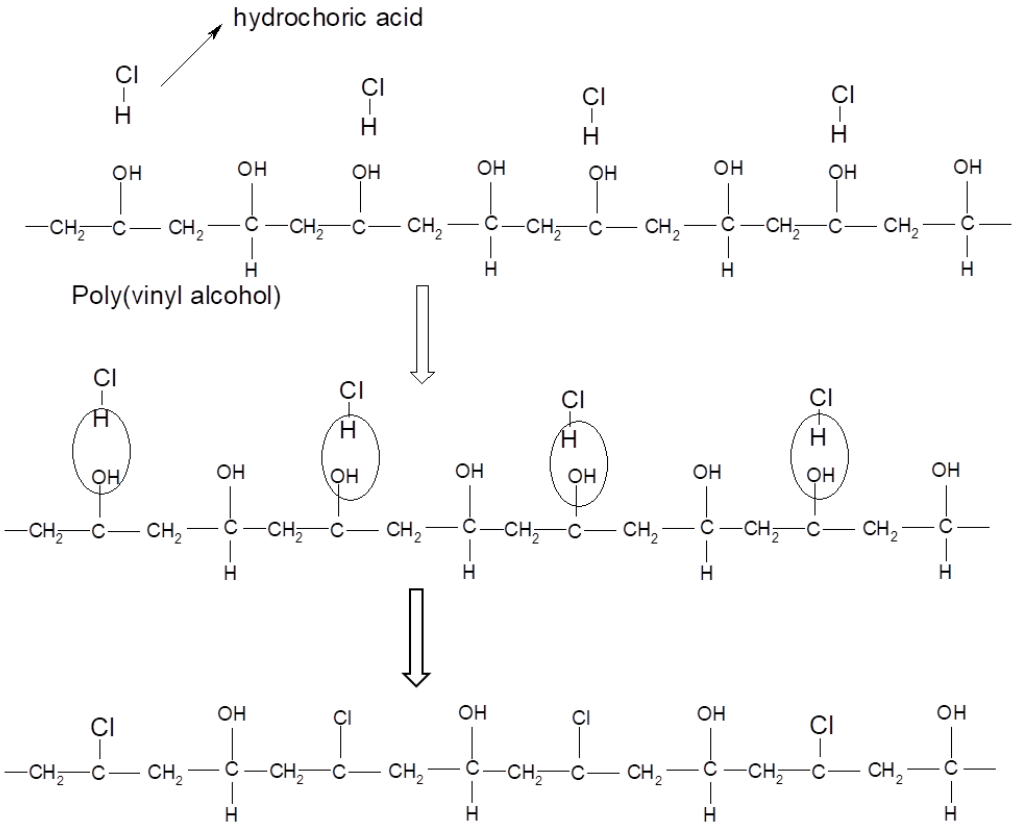

Figure 6.2 Formation of PVA based gel electrolyte.

6.2.3 Preparation of Supercapacitor

The sponge/PSS/PPy/PANI-MoS_2 was used for both electrodes in a symmetric supercapacitor structure. The PVA gel electrolyte was applied to the sponge/PSS/PPy/PANI-MoS_2 and a porous filter paper that was used as the separator. Copper tape was used as the current

collector for each electrode. The device was assembled by sandwiching two electrodes and the separator between the two pieces of plexiglass tightened with one screw on each of the four corners. Figure 6.3 shows the schematic of the fabrication of the sponge-based solid supercapacitor.

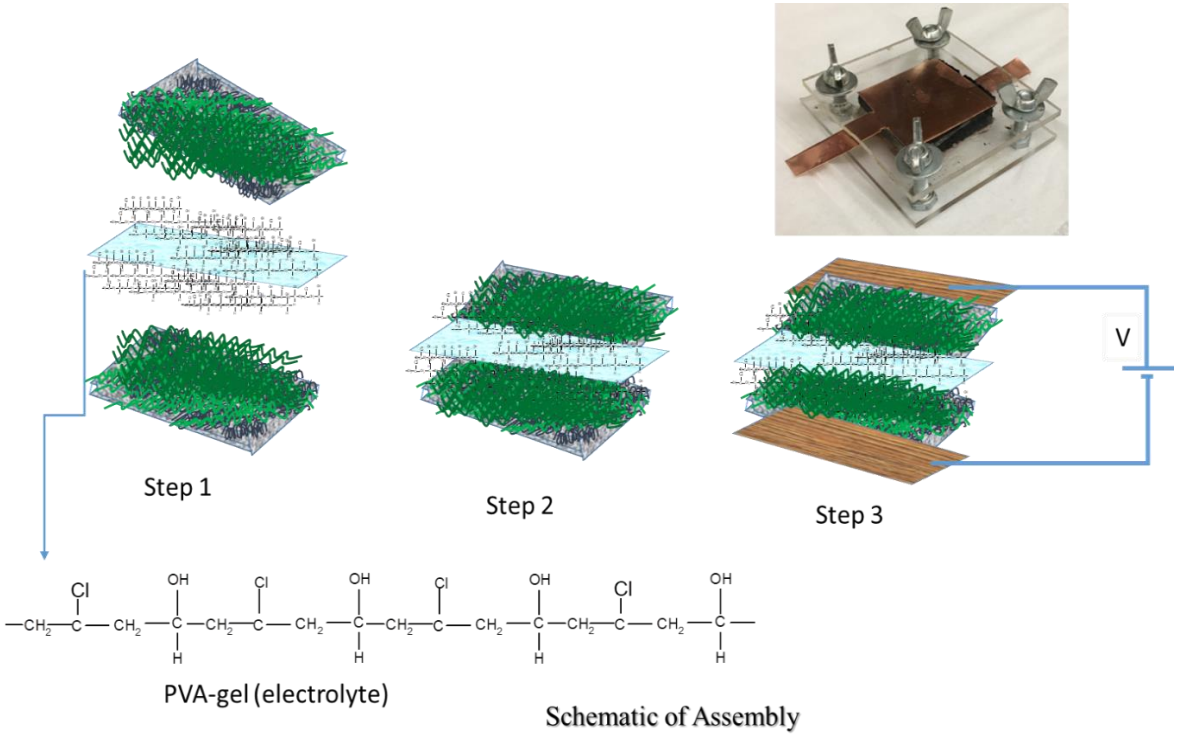

Figure 6.3 Fabrication schematics of sponge based solid supercapacitor.

6.3 Results and Discussion

6.3.1 Physical and Structural Characterization

SEM was use to image the sponge, each of the deposited conducting polymers, and the composite structure on the sponge. Figure 4 (a) shows a picture of the sponge at higher magnification, while the lower magnification shows the large surface area. The structure of the sponge was different before and after the PPy layer as shown in figure 4 (c and d). The lower magnification shows equally distributed PPy particles with diameters of approximately 1000 to 3500 nm. Further, the PANI deposition over PPy changed the structure again. Nanostructures are

clearly visible over the sponge surface as shown in figure 4 (d) and (e). The PANI-MoS_2 is again a clearly distinguishable structure, and different than both PPy and PANI after the electrochemical deposition. The MoS_2 platelets are observed in the PANI network in the SEM pictures in figure 4 (g and h).

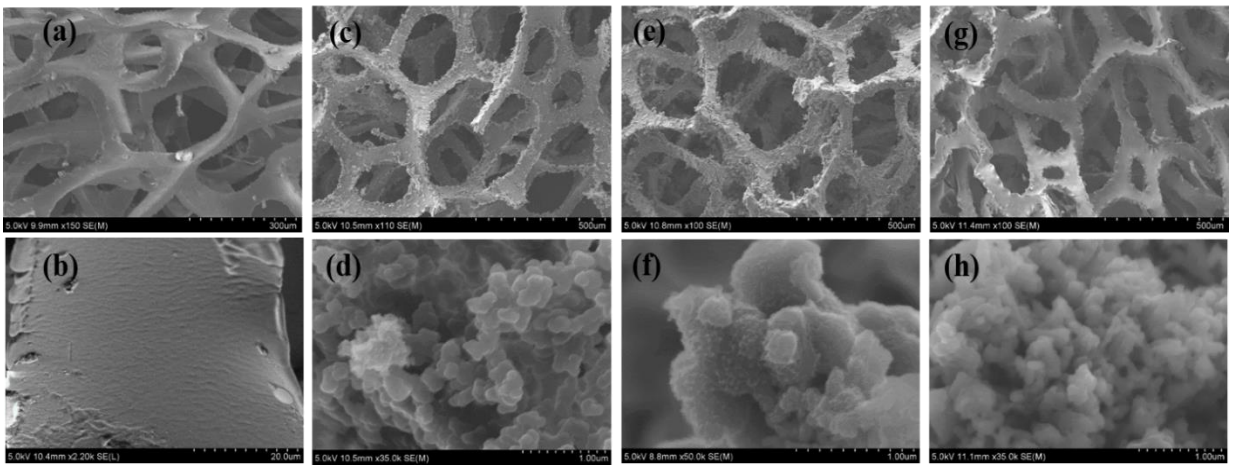

Figure 6.4 SEM pictures of (a & b) pure sponge, (c & d) sponge/PPy, (e & f) sponge/PPy/PANI (via in-situ self-assembly) and (g & h) sponge/PPy/PANI/MoS_2 (via electrochemical deposition).

A Philips Panalytical Xpert Pro MRD with Cu Kα radiation and 2θ range from 5° to 45° was used to study the X-ray diffraction (XRD) of sponge/PSS/PPy/PANI-MoS_2. As shown in figure 5(a), peaks for diffraction angle '2θ' at 6.8, 11, 14.4, 33.6, 38 and 40.7 degrees were found in the results. Generally, the emeraldine salt of PANI is quasi crystalline and PPY is amorphous in nature. However, the composite with MoS_2 structure is a more ordered state than the conventional PANI as well as PPy structure [279][29, 30].

FTIR spectra of sponge/PSS/PPy, sponge/PSS/PPy/PANI and sponge/PSS/PPy/PANI-MoS_2 were measured using a Perkin Elmer spectrometer from 600-2000 cm^{-1} in reflectance mode. Curve 1 in Figure 5(b) shows the infrared peaks at 1936, 1824, 1726 ((C=N, C-N)), 1586 (C=C stretching), 1494, 1332 (C=N, C-N) bonds, 1242 (N-H plane mode), 1114 (C-H in plane mode), 972 (C-H wag), 833 (C-H waging), 749 and 694 cm^{-1} [280]. Curve 2 in Figure 5(b) shows the vibrational bands at 1933, 1821, 1722, 1595, 1406, 1332, 1233, 1114, 969, 824, 728, 627 cm^{-1}.

Curve 3 in Figure 5(b) show infrared peaks at 1940, 1822, 1729, 1600, 1490, 1394, 1338, 1215, 1114, 962, 846, 742, 867, 665 and 643 cm^{-1}. There is a decrease in the wavenumber in the IR spectra after PANI was polymerized over PPy; which could be due to formation of some hydrogen bonds in the doped form of PANI [281]. The peak around 663 cm^{-1} is the characteristic peak of MoS_2 [282].

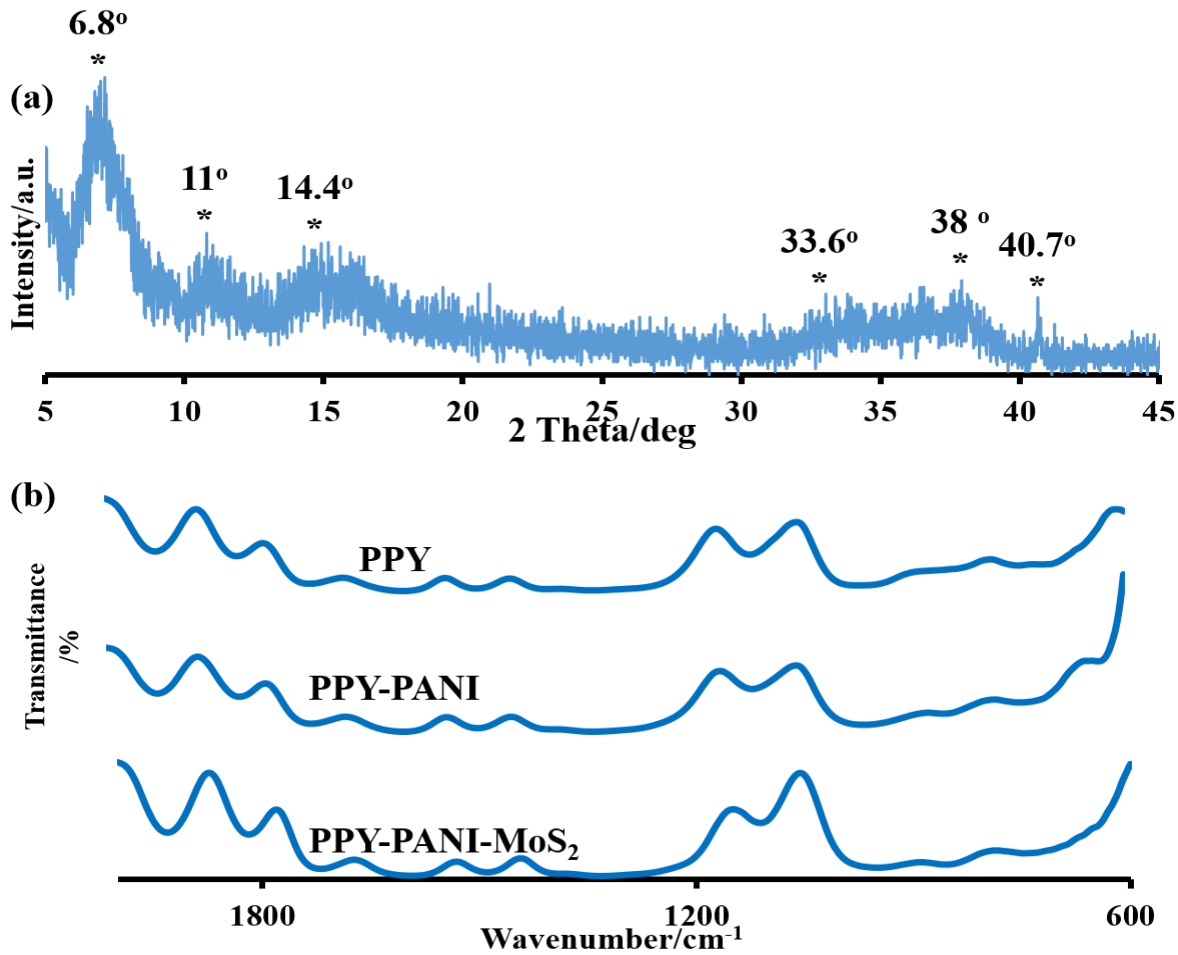

Figure 6.5 (a) X-ray diffraction of PPy/PANI/MoS_2 and (b) FTIR spectra of PPy, PPy/PANI and PPy/PANI/MoS_2 deposited on sponges from 600-2000 cm^{-1}.

6.3.2 Electrochemical Characterization

Electrochemical tests, including CV, CCCD and EIS, were conducted using the two-electrode configuration. Figure 6.6 (a) illustrations the CV curves of the device at different scan rates (5-100 mV s^{-1}). Oxidation and reduction peaks are observed at 0.34V and -0.37V,

respectively, for the scan rate of 10 mV s^{-1}. The peaks were shifted to 0.8 V (oxidation) and -0.74V (reduction) at 100 mV s^{-1} scan rate.

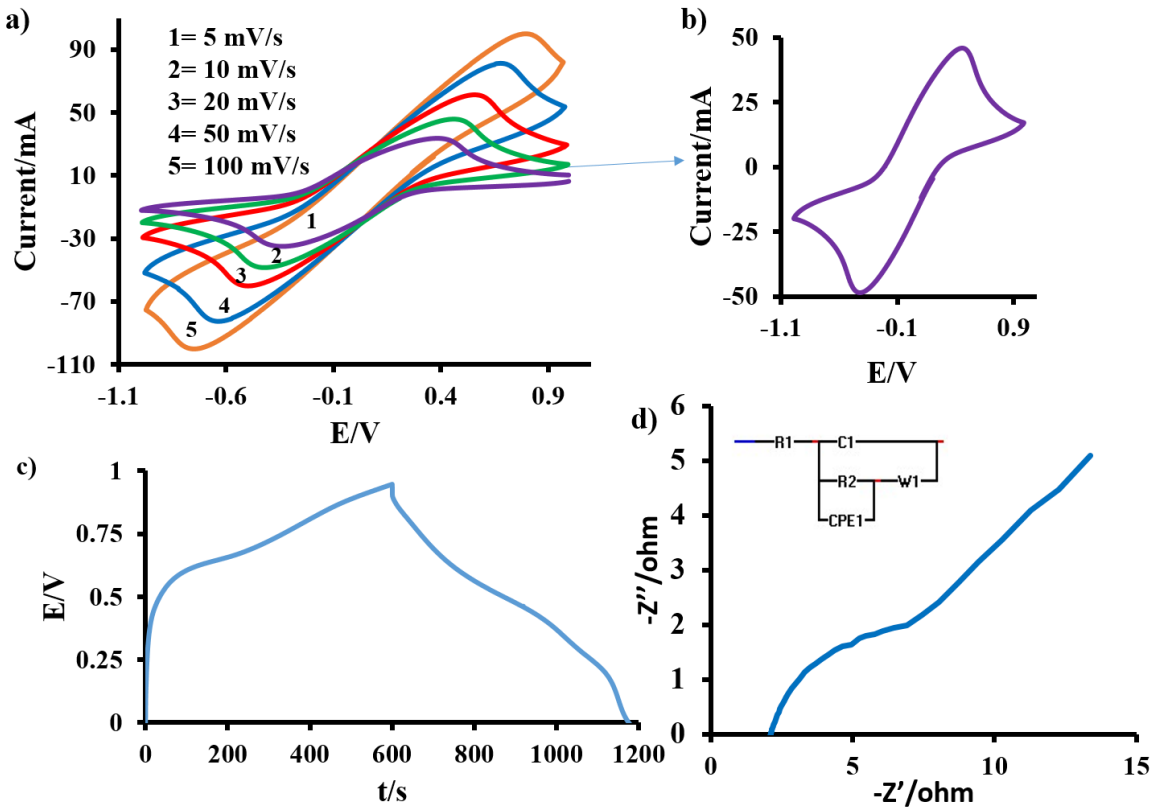

Figure 6.6 (a) CV as a function of scan rates (1) 5 (2) 10 (3) 20 (4) 50 and (5) 100 mV s^{-1}, (b) at 10 mV s^{-1}, (c) charge/discharge cycling curves at 5 mA and (d) Nyquist plot. (Inset) the applied equivalent circuit of the sponge supercapacitor

Figure 6.6 (b) shows the CV plot at 10 mV s^{-1} scan rate to show the redox peaks. The visible redox peaks at different scan rates imply the strong charge storage via the pseudo-capacitive effect in addition to the double layer effect. The highest specific capacitance of ~569 F g^{-1} has been calculated from the 5 mV s^{-1} CV result. Figure 6.6 (c) shows the charging and discharging behaviors of the sponge/PSS/PPy/PANI/PANI/PANI-MoS_2 supercapacitor with the PVA-gel electrolyte. The specific capacitance, specific power density and specific energy density have been calculated to be 631.6 Fg^{-1}, 475 W kg^{-1} and 79.17 Wh kg^{-1} considering the weight of only electrode material. Figure 6.6 (d) shows the Nyquist plot of sponge/PSS/PPy/PANI/PANI./PANI-MoS_2

based supercapacitor fabricated using PVA-gel. The value of R_1, C_1, R_2 and CPE_1 has been estimated 2.0817 Ω, 297.7 μF, 5.180 Ω and Aw_1=3.041, P_1= 0.05 and n_1= 0.5889. In order to test the stability of the device in multiple cycles, CV results of 1500 cycles were collected when the scan rate was 100 mV s^{-1}. Figure 6.7 shows a retention of ~95.5 %.

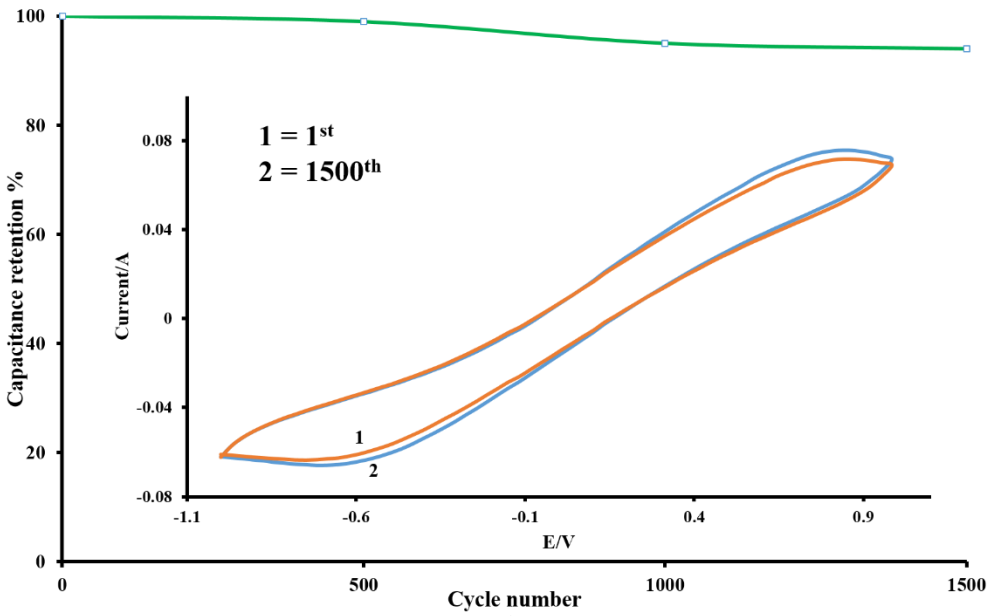

Figure 6.7 CV cycling performance at 1000 mV s^{-1} for 1500 cycles (inset) CV curves collected at the 1st and the 1000th cycle.

6.4 Conclusions

A multilayer electrode with conducting polymers and a composite material of molybdenum disulfide (MoS_2) was designed and fabricated on a kitchen sponge substrate to make a solid-state supercapacitor with high specific capacitance of 631.6 F g^{-1}. The electrode was fabricated first by in-situ self-assembled polymerization of a layer of polypyrrole (PPy) and a layer of polyaniline (PANI) on a sponge substrate. The two layers of PPy and PANI converted the sponge surface to a conductive surface that was used to electrochemical deposition of thicker layers of PANI and another layer of MoS_2-PANI composite. The polyvinyl alcohol (PVA) gel was synthesized and further, PANI was polymerized in PVA gel to obtain highly conducting electrolyte.

The PANI-MoS_2 is a clearly distinguishable structure and different than both PPy and PANI for electrochemical deposition. The MoS_2 platelets are observed in the PANI network in the SEM pictures. There is a decrease in the wavenumber in IR spectra after polyaniline is polymerized over polypyrrole; which could be due to formation of some hydrogen bonds in the doped form of PANI. Generally, the emeraldine salt of PANI is quasi crystalline and PPy is amorous in nature. However, the composite with MoS_2 structure is in a more ordered state than the conventional PANI as well as PPy structure. The fabrication, characterization and results of this study demonstrate that high surface area based sponge PSS/PPy/ PANI/MoS_2 sponge could find potential use as supercapacitor electrode materials for a promising low-cost supercapacitor that exhibited good electrochemical performance with great cycle durability, time stability and shelf life.

CHAPTER 7: CONCLUSIONS AND FUTURE WORK

7.1 Conclusions

Although supercapacitors have been on the market since 1966, their performance is far lower than batteries. Nevertheless, there have been a lot of advancements in technology that had big influence on how supercapacitors work. Today they can be a great replacement for other electrical energy storage devices. The main benefit of supercapacitors is that they store energy in an electric field. In addition, the energy can be delivered quickly because there is no chemical reaction happening in the device. Contrary to batteries, supercapacitors can survive thousands of charge-discharge cycles. They also last longer than batteries, because they do not have to lose energy on charge and discharge cycles as well they do not undergo ware and tare which are normally caused by chemical reaction in batteries. There is, however, a great future for supercapacitors in many industries. It has been said that they can be a big hit in the micro-hybrid car business, because they can supply the car in the power during stop and rest/restart as well. This means that it can be recharged during the travel time. Some improvements have to be made in the amount of plate that needs to be used as well as in increasing the amount of voltage that it can carry.

As part of this work, we have shown an innovative nanocomposite electrode which was chemically synthesized using MoS_2/PEDOT to understand the charge mechanism in a symmetric supercapacitor. The MoS_2/PEDOT nanocomposite was produced at various ratios of MoS_2 to EDOT in an aqueous medium of PSS and CTAB at controlled conditions. The morphology, crystallinity and optical properties of MoS_2/PEDOT nanocomposite materials were characterized

using different techniques. The specific capacitance was estimated to be 452 F g^{-1} and 360 F g^{-1} for three electrode and two electrode configurations in 2 M HCl acid, respectively. Chemical oxidative polymerization along with reduction/oxidation synthesis techniques, characterization and supercapacitor properties of processed polyaniline (PANI)-MoS_2 based nanocomposite materials were applied to fabricate the supercapacitor electrode. Further, comprehensive characterizations, analysis and calculations were carried out to demonstrate the outstanding electrical and electrochemical properties of the supercapacitor. At the highest value, a specific capacitance of MoS_2/PANI ESII of 512 F g^{-1} was obtained using symmetric supercapacitor configuration. The nanocomposite based on a sponge as electrodes was made by deposition of in-situ self-assembled polymerization of both monomers 'pyrrole and aniline' over the sponge and followed by electrochemical polymerization of MoS_2-CPs nanocomposite to obtain the supercapacitor electrodes. Further, polyvinyl alcohol (PVA) gel was synthesized to obtain highly conducting electrolyte to fabricate the solid-state supercapacitor. The sponge type supercapacitor construction consists of two porous sponge electrodes, gel electrolytes, and membrane of paper that is sandwiched between the two sponge electrodes. A multilayer electrode structure with CPs and a composite material of molybdenum disulfide (MoS_2) was designed and fabricated on a kitchen sponge substrate to make solid-state supercapacitors with high specific capacitance of 632 F.g^{-1}.

7.2 Recommendations for Future Work

Various polyanilines (poly(o-anisidine), poly (o-toluidine), poly-ethoxy-aninile, polyethyanilne etc.) show excellent electrochemical properties and could be associated with MoS_2 for nanocomposite formation of high energy and high power based supercapacitors. The sponge was used to fabricate the large surface area based electrodes for obtaining high specific capacitance

based supercapacitor, however, an aerogel based material and carbon cloth based material could be used for fabrication of high specific capacitance based supercapacitor. In addition, understanding the mass loading of electrodes using nanocomposites will give a new dimension in fabrication of high energy density and power density based supercapacitors. The nanocomposites should be integrated with photovoltaic cells (e.g. silicon solar cells or dye sensitized solar cells) for a more sustainable energy storage device. Lastly, the packaging is important in order to prevent leakage and enhance stability in the supercapacitor devices which is recommended to be studied in future works.

REFERENCES

[1] Y. Zhang, H. Feng, X. Wu, L. Wang, A. Zhang, T. Xia, H. Dong, X. Li, L. Zhang, Progress of electrochemical capacitor electrode materials: A review, International journal of hydrogen energy 34(11) (2009) 4889-4899.

[2] R. Kötz, M. Carlen, Principles and applications of electrochemical capacitors, Electrochimica acta 45(15-16) (2000) 2483-2498.

[3] P. Simon, Y. Gogotsi, Materials for electrochemical capacitors, Nanoscience And Technology: A Collection of Reviews from Nature Journals, World Scientific2010, pp. 320-329.

[4] S. Sarangapani, B. Tilak, C.P. Chen, Materials for electrochemical capacitors theoretical and experimental constraints, Journal of the Electrochemical Society 143(11) (1996) 3791-3799.

[5] J.P. Holdren, Population and the energy problem, Population and environment 12(3) (1991) 231-255.

[6] I. Hadjipaschalis, A. Poullikkas, V. Efthimiou, Overview of current and future energy storage technologies for electric power applications, Renewable and sustainable energy reviews 13(6-7) (2009) 1513-1522.

[7] P. Simon, Y. Gogotsi, B. Dunn, Where do batteries end and supercapacitors begin?, Science 343(6176) (2014) 1210-1211.

[8] P. Simon, Y. Gogotsi, Materials for electrochemical capacitors, Nature Materials 7 (2008) 845.

[9] E. Frackowiak, V. Khomenko, K. Jurewicz, K. Lota, F. Béguin, Supercapacitors based on conducting polymers/nanotubes composites, Journal of Power Sources 153(2) (2006) 413-418.

[10] G.A. Snook, P. Kao, A.S. Best, Conducting-polymer-based supercapacitor devices and electrodes, Journal of Power Sources 196(1) (2011) 1-12.

[11] M. Mastragostino, C. Arbizzani, F. Soavi, Conducting polymers as electrode materials in supercapacitors, Solid state ionics 148(3-4) (2002) 493-498.

[12] I. Shown, A. Ganguly, L.C. Chen, K.H. Chen, Conducting polymer-based flexible supercapacitor, Energy Science & Engineering 3(1) (2015) 2-26.

[13] K.D. Fong, T. Wang, S.K. Smoukov, Multidimensional performance optimization of conducting polymer-based supercapacitor electrodes, Sustainable Energy & Fuels 1(9) (2017) 1857-1874.

[14] V. Khomenko, E. Frackowiak, V. Barsukov, F. Béguin, Development of supercapacitors based on conducting polymers, New carbon based materials for electrochemical energy storage systems: batteries, supercapacitors and fuel cells, Springer2006, pp. 41-50.

[15] H. Sun, X. You, Y. Jiang, G. Guan, X. Fang, J. Deng, P. Chen, Y. Luo, H. Peng, Self-Healable Electrically Conducting Wires for Wearable Microelectronics, Angewandte Chemie 126(36) (2014) 9680-9685.

[16] C. Peng, S. Zhang, D. Jewell, G.Z. Chen, Carbon nanotube and conducting polymer composites for supercapacitors, Progress in Natural science 18(7) (2008) 777-788.

[17] K.H. An, K.K. Jeon, J.K. Heo, S.C. Lim, D.J. Bae, Y.H. Lee, High-capacitance supercapacitor using a nanocomposite electrode of single-walled carbon nanotube and polypyrrole, Journal of the Electrochemical Society 149(8) (2002) A1058-A1062.

[18] H. Gómez, M.K. Ram, F. Alvi, P. Villalba, E.L. Stefanakos, A. Kumar, Graphene-conducting polymer nanocomposite as novel electrode for supercapacitors, Journal of Power Sources 196(8) (2011) 4102-4108.

[19] M.M. Islam, S.H. Aboutalebi, D. Cardillo, H.K. Liu, K. Konstantinov, S.X. Dou, Self-assembled multifunctional hybrids: toward developing high-performance graphene-based architectures for energy storage devices, ACS central science 1(4) (2015) 206-216.

[20] K. Zhang, L.L. Zhang, X. Zhao, J. Wu, Graphene/polyaniline nanofiber composites as supercapacitor electrodes, Chemistry of Materials 22(4) (2010) 1392-1401.

[21] C. Xia, W. Chen, X. Wang, M.N. Hedhili, N. Wei, H.N. Alshareef, Highly stable supercapacitors with conducting polymer core-shell electrodes for energy storage applications, Advanced Energy Materials 5(8) (2015) 1401805.

[22] C.J. Zhang, T.M. Higgins, S.-H. Park, S.E. O'Brien, D. Long, J.N. Coleman, V. Nicolosi, Highly flexible and transparent solid-state supercapacitors based on RuO2/PEDOT: PSS conductive ultrathin films, Nano Energy 28 (2016) 495-505.

[23] Y. Hou, Y. Cheng, T. Hobson, J. Liu, Design and synthesis of hierarchical MnO2 nanospheres/carbon nanotubes/conducting polymer ternary composite for high performance electrochemical electrodes, Nano letters 10(7) (2010) 2727-2733.

[24] G. Yu, L. Hu, N. Liu, H. Wang, M. Vosgueritchian, Y. Yang, Y. Cui, Z. Bao, Enhancing the supercapacitor performance of graphene/MnO2 nanostructured electrodes by conductive wrapping, Nano letters 11(10) (2011) 4438-4442.

[25] X. Hu, W. Xiong, W. Wang, S. Qin, H. Cheng, Y. Zeng, B. Wang, Z. Zhu, Hierarchical manganese dioxide/poly (3, 4-ethylenedioxythiophene) core–shell nanoflakes on ramie-derived carbon fiber for high-performance flexible all-solid-state supercapacitor, ACS Sustainable Chemistry & Engineering 4(3) (2016) 1201-1211.

[26] T. Alamro, M.K. Ram, Polyethylenedioxythiophene and molybdenum disulfide nanocomposite electrodes for supercapacitor applications, Electrochimica Acta 235 (2017) 623-631.

[27] L. Ren, G. Zhang, Z. Yan, L. Kang, H. Xu, F. Shi, Z. Lei, Z.-H. Liu, Three-dimensional tubular MoS2/PANI hybrid electrode for high rate performance supercapacitor, ACS applied materials & interfaces 7(51) (2015) 28294-28302.

[28] H. Tang, J. Wang, H. Yin, H. Zhao, D. Wang, Z. Tang, Growth of Polypyrrole Ultrathin Films on MoS2 Monolayers as High-Performance Supercapacitor Electrodes, Advanced materials 27(6) (2015) 1117-1123.

[29] R. Lv, J.A. Robinson, R.E. Schaak, D. Sun, Y. Sun, T.E. Mallouk, M. Terrones, Transition metal dichalcogenides and beyond: synthesis, properties, and applications of single-and few-layer nanosheets, Accounts of chemical research 48(1) (2014) 56-64.

[30] H. Li, J. Wu, Z. Yin, H. Zhang, Preparation and applications of mechanically exfoliated single-layer and multilayer MoS2 and WSe2 nanosheets, Accounts of chemical research 47(4) (2014) 1067-1075.

[31] T.A. Skotheim, Handbook of conducting polymers, CRC press1997.

[32] L. Pan, H. Qiu, C. Dou, Y. Li, L. Pu, J. Xu, Y. Shi, Conducting polymer nanostructures: template synthesis and applications in energy storage, International journal of molecular sciences 11(7) (2010) 2636-2657.

[33] A. Burke, Ultracapacitors: why, how, and where is the technology, Journal of power sources 91(1) (2000) 37-50.

[34] S.-M. Chen, R. Ramachandran, V. Mani, R. Saraswathi, Recent advancements in electrode materials for the high-performance electrochemical supercapacitors: a review, Int. J. Electrochem. Sci 9(8) (2014) 4072-4085.

[35] A.S. Arico, P. Bruce, B. Scrosati, J.-M. Tarascon, W. Van Schalkwijk, Nanostructured materials for advanced energy conversion and storage devices, Materials For Sustainable Energy: A Collection of Peer-Reviewed Research and Review Articles from Nature Publishing Group, World Scientific2011, pp. 148-159.

[36] Y.G. Guo, J.S. Hu, L.J. Wan, Nanostructured materials for electrochemical energy conversion and storage devices, Advanced Materials 20(15) (2008) 2878-2887.

[37] B.E. Conway, Electrochemical supercapacitors: scientific fundamentals and technological applications, Springer Science & Business Media2013.

[38] A. Yu, V. Chabot, J. Zhang, Electrochemical supercapacitors for energy storage and delivery: fundamentals and applications, CRC press2013.

[39] F. Bonaccorso, L. Colombo, G. Yu, M. Stoller, V. Tozzini, A.C. Ferrari, R.S. Ruoff, V. Pellegrini, Graphene, related two-dimensional crystals, and hybrid systems for energy conversion and storage, Science 347(6217) (2015) 1246501.

[40] L. Zubieta, R. Bonert, Characterization of double-layer capacitors for power electronics applications, IEEE Transactions on industry applications 36(1) (2000) 199-205.

[41] H. Wu, L. Cheng, Y. Zhang, W. Yuan, L. Zheng, Free-standing activated flax fabrics with tunable meso/micropore ratio for high-rate capacitance, Carbon 116 (2017) 518-527.

[42] J.M. Rosas, T. Cordero-Lanzac, F.J. García-Mateos, J. Rodriguez-Mirasol, T. Cordero, Flexible and low-cost binderless capacitors based on p-and n-containing fibrous activated carbons from denim cloth wastes, (2018).

[43] D. Zhang, J. Zhao, C. Feng, R. Zhao, Y. Sun, T. Guan, B. Han, N. Tang, J. Wang, K. Li, Scalable synthesis of hierarchical macropore-rich activated carbon microspheres assembled by carbon nanoparticles for high rate performance supercapacitors, Journal of Power Sources 342 (2017) 363-370.

[44] D. Wang, Z. Geng, B. Li, C. Zhang, High performance electrode materials for electric double-layer capacitors based on biomass-derived activated carbons, Electrochimica Acta 173 (2015) 377-384.

[45] S. Zhang, Q. Weng, F. Zhao, H. Gao, P. Chen, X. Chen, Z. An, High electrocapacitive performance of bowl-like monodispersed porous carbon nanoparticles prepared with an interfacial self-assembly process, Journal of colloid and interface science 496 (2017) 35-43.

[46] E. Redondo, W.-Y. Tsai, B. Daffos, P.-L. Taberna, P. Simon, E. Goikolea, R. Mysyk, Outstanding room-temperature capacitance of biomass-derived microporous carbons in ionic liquid electrolyte, Electrochemistry Communications 79 (2017) 5-8.

[47] Y. Zhu, S. Murali, M.D. Stoller, K. Ganesh, W. Cai, P.J. Ferreira, A. Pirkle, R.M. Wallace, K.A. Cychosz, M. Thommes, Carbon-based supercapacitors produced by activation of graphene, Science 332(6037) (2011) 1537-1541.

[48] B. Chen, Y. Jiang, X. Tang, Y. Pan, S. Hu, Fully packaged carbon nanotube supercapacitors by direct ink writing on flexible substrates, ACS applied materials & interfaces 9(34) (2017) 28433-28440.

[49] T. Kim, M.K. Kim, Y. Park, E. Kim, J. Kim, W. Ryu, H.M. Jeong, K. Kim, Cutting-Processed Single-Wall Carbon Nanotubes with Additional Edge Sites for Supercapacitor Electrodes, Nanomaterials (Basel, Switzerland) 8(7) (2018).

[50] D. Deng, N. Chen, Y. Li, X. Xing, X. Liu, X. Xiao, Y. Wang, Cerium oxide nanoparticles/multi-wall carbon nanotubes composites: Facile synthesis and electrochemical performances as supercapacitor electrode materials, Physica E: Low-dimensional Systems and Nanostructures 86 (2017) 284-291.

[51] A. Roy, A. Ray, S. Saha, S. Das, Investigation on energy storage and conversion properties of multifunctional PANI-MWCNT composite, International Journal of Hydrogen Energy 43(14) (2018) 7128-7139.

[52] K. Xia, Q. Li, L. Zheng, K. You, X. Tian, B. Han, Q. Gao, Z. Huang, G. Chen, C. Zhou, Controllable fabrication of 2D and 3D porous graphene architectures using identical thermally exfoliated graphene oxides as precursors and their application as supercapacitor electrodes, Microporous and Mesoporous Materials 237 (2017) 228-236.

[53] R.P. Panmand, P. Patil, Y. Sethi, S.R. Kadam, M.V. Kulkarni, S.W. Gosavi, N. Munirathnam, B.B. Kale, Unique perforated graphene derived from Bougainvillea flowers for high-power supercapacitors: a green approach, Nanoscale 9(14) (2017) 4801-4809.

[54] R.-R. Bi, X.-L. Wu, F.-F. Cao, L.-Y. Jiang, Y.-G. Guo, L.-J. Wan, Highly dispersed RuO2 nanoparticles on carbon nanotubes: facile synthesis and enhanced supercapacitance performance, The Journal of Physical Chemistry C 114(6) (2010) 2448-2451.

[55] L. Miao, H. Duan, M. Liu, W. Lu, D. Zhu, T. Chen, L. Li, L. Gan, Poly (ionic liquid)-derived, N, S-codoped ultramicroporous carbon nanoparticles for supercapacitors, Chemical Engineering Journal 317 (2017) 651-659.

[56] J. Yan, J. Liu, Z. Fan, T. Wei, L. Zhang, High-performance supercapacitor electrodes based on highly corrugated graphene sheets, Carbon 50(6) (2012) 2179-2188.

[57] S. Zhai, C. Wang, H.E. Karahan, Y. Wang, X. Chen, X. Sui, Q. Huang, X. Liao, X. Wang, Y. Chen, Nano-RuO2-Decorated Holey Graphene Composite Fibers for Micro-Supercapacitors with Ultrahigh Energy Density, Small (2018) 1800582.

[58] R. Zarrougui, R. Hachicha, R. Rjab, O. Ghodbane, 1-Allyl-3-methylimidazolium-based ionic liquids employed as suitable electrolytes for high energy density supercapacitors based on graphene nanosheets electrodes, Journal of Molecular Liquids 249 (2018) 795-804.

[59] E. Gomibuchi, T. Ichikawa, K. Kimura, S. Isobe, K. Nabeta, H. Fujii, Electrode properties of a double layer capacitor of nano-structured graphite produced by ball milling under a hydrogen atmosphere, Carbon 44(5) (2006) 983-988.

[60] K. Gurunathan, A.V. Murugan, R. Marimuthu, U. Mulik, D. Amalnerkar, Electrochemically synthesised conducting polymeric materials for applications towards technology in electronics, optoelectronics and energy storage devices, Materials Chemistry and Physics 61(3) (1999) 173-191.

[61] K. Krishnamoorthy, P. Pazhamalai, S.J. Kim, Ruthenium sulfide nanoparticles as a new pseudocapacitive material for supercapacitor, Electrochimica Acta 227 (2017) 85-94.

[62] S. Sahoo, P. Pazhamalai, K. Krishnamoorthy, S.-J. Kim, Hydrothermally prepared α-MnSe nanoparticles as a new pseudocapacitive electrode material for supercapacitor, Electrochimica Acta 268 (2018) 403-410.

[63] M. Aghazadeh, I. Karimzadeh, M.R. Ganjali, Electrochemical evaluation of the performance of cathodically grown ultra-fine magnetite nanoparticles as electrode material for supercapacitor applications, Journal of Materials Science: Materials in Electronics 28(18) (2017) 13532-13539.

[64] X.-h. Yang, Y.-g. Wang, H.-m. Xiong, Y.-y. Xia, Interfacial synthesis of porous MnO2 and its application in electrochemical capacitor, Electrochimica Acta 53(2) (2007) 752-757.

[65] S.S. Karade, D.P. Dubal, B.R. Sankapal, MoS 2 ultrathin nanoflakes for high performance supercapacitors: room temperature chemical bath deposition (CBD), RSC Advances 6(45) (2016) 39159-39165.

[66] K.-J. Huang, J.-Z. Zhang, G.-W. Shi, Y.-M. Liu, Hydrothermal synthesis of molybdenum disulfide nanosheets as supercapacitors electrode material, Electrochimica Acta 132 (2014) 397-403.

[67] K.-J. Huang, L. Wang, Y.-J. Liu, H.-B. Wang, Y.-M. Liu, L.-L. Wang, Synthesis of polyaniline/2-dimensional graphene analog MoS2 composites for high-performance supercapacitor, Electrochimica Acta 109 (2013) 587-594.

[68] L. Wang, Y. Ma, M. Yang, Y. Qi, Hierarchical hollow MoS2 nanospheres with enhanced electrochemical properties used as an electrode in supercapacitor, Electrochimica Acta 186 (2015) 391-396.

[69] X. Wang, J. Ding, S. Yao, X. Wu, Q. Feng, Z. Wang, B. Geng, High supercapacitor and adsorption behaviors of flower-like MoS 2 nanostructures, Journal of Materials Chemistry A 2(38) (2014) 15958-15963.

[70] K.-J. Huang, L. Wang, Y.-J. Liu, Y.-M. Liu, H.-B. Wang, T. Gan, L.-L. Wang, Layered MoS2–graphene composites for supercapacitor applications with enhanced capacitive performance, International journal of hydrogen energy 38(32) (2013) 14027-14034.

[71] B.S. Singu, U. Male, P. Srinivasan, K.R. Yoon, Preparation and performance of polyaniline–multiwall carbon nanotubes–titanium dioxide ternary composite electrode material for supercapacitors, Journal of Industrial and Engineering Chemistry 49 (2017) 82-87.

[72] J. Wang, Z. Wu, K. Hu, X. Chen, H. Yin, High conductivity graphene-like MoS2/polyaniline nanocomposites and its application in supercapacitor, Journal of Alloys and Compounds 619 (2015) 38-43.

[73] L. Tang, F. Duan, M. Chen, Silver nanoparticle decorated polyaniline/multiwalled super-short carbon nanotube nanocomposites for supercapacitor applications, RSC Advances 6(69) (2016) 65012-65019.

[74] Y. Xie, D. Wang, J. Ji, Preparation and supercapacitor performance of freestanding polypyrrole/polyaniline coaxial nanoarrays, Energy Technology 4(6) (2016) 714-721.

[75] D. Dubal, S. Patil, W. Kim, C. Lokhande, Supercapacitors based on electrochemically deposited polypyrrole nanobricks, Materials Letters 65(17-18) (2011) 2628-2631.

[76] C. Bora, J. Sharma, S. Dolui, Polypyrrole/sulfonated graphene composite as electrode material for supercapacitor, The Journal of Physical Chemistry C 118(51) (2014) 29688-29694.

[77] Y. Chen, W. Ma, K. Cai, X. Yang, C. Huang, In Situ Growth of Polypyrrole onto Three-Dimensional Tubular MoS2 as an Advanced Negative Electrode Material for Supercapacitor, Electrochimica Acta 246 (2017) 615-624.

[78] W. Li, J. Chen, J. Zhao, J. Zhang, J. Zhu, Application of ultrasonic irradiation in preparing conducting polymer as active materials for supercapacitor, Materials Letters 59(7) (2005) 800-803.

[79] J. Jang, J. Bae, E. Park, Selective Fabrication of Poly (3, 4-ethylenedioxythiophene) Nanocapsules and Mesocellular Foams Using Surfactant-Mediated Interfacial Polymerization, Advanced Materials 18(3) (2006) 354-358.

[80] R. Liu, S.I. Cho, S.B. Lee, Poly (3, 4-ethylenedioxythiophene) nanotubes as electrode materials for a high-powered supercapacitor, Nanotechnology 19(21) (2008) 215710.

[81] K. Naoi, 'Nanohybrid capacitor': the next generation electrochemical capacitors, Fuel cells 10(5) (2010) 825-833.

[82] T. Aida, K. Yamada, M. Morita, An advanced hybrid electrochemical capacitor that uses a wide potential range at the positive electrode, Electrochemical and solid-state letters 9(12) (2006) A534-A536.

[83] G. Yu, X. Xie, L. Pan, Z. Bao, Y. Cui, Hybrid nanostructured materials for high-performance electrochemical capacitors, Nano Energy 2(2) (2013) 213-234.

[84] T. Tevi, S.W. Saint Birch, S.W. Thomas, A. Takshi, Effect of Triton X-100 on the double layer capacitance and conductivity of poly (3, 4-ethylenedioxythiophene): poly (styrenesulfonate)(PEDOT: PSS) films, Synthetic Metals 191 (2014) 59-65.

[85] X. Hong, B. Zhang, E. Murphy, J. Zou, F. Kim, Three-dimensional reduced graphene oxide/polyaniline nanocomposite film prepared by diffusion driven layer-by-layer assembly for high-performance supercapacitors, Journal of Power Sources 343 (2017) 60-66.

[86] M. Li, H. He, Study on electrochemical performance of multi-wall carbon nanotubes coated by iron oxide nanoparticles as advanced electrode materials for supercapacitors, Vacuum 143 (2017) 371-379.

[87] F. Meng, Y. Ding, Sub-Micrometer-Thick All-Solid-State Supercapacitors with High Power and Energy Densities, Advanced Materials 23(35) (2011) 4098-4102.

[88] X. Li, Y. Wu, F. Zheng, M. Ling, F. Lu, Preparation and characterization of RuO2/polypyrrole electrodes for supercapacitors, Solid State Communications 197 (2014) 57-60.

[89] P. Tang, L. Han, L. Zhang, Facile synthesis of graphite/PEDOT/MnO2 composites on commercial supercapacitor separator membranes as flexible and high-performance supercapacitor electrodes, ACS applied materials & interfaces 6(13) (2014) 10506-10515.

[90] D. Liu, H. Wang, P. Du, W. Wei, Q. Wang, P. Liu, Flexible and robust reduced graphene oxide/carbon nanoparticles/polyaniline (RGO/CNs/PANI) composite films: excellent candidates as free-standing electrodes for high-performance supercapacitors, Electrochimica Acta 259 (2018) 161-169.

[91] Z. Liu, W. Chen, X. Fan, J. Yu, Y. Zhao, Preparation of 3D MnO2/Polyaniline/Graphene Hybrid Material via Interfacial Polymerization as High-Performance Supercapacitor Electrode, Chinese Journal of Chemistry 34(8) (2016) 839-846.

[92] C. Sha, B. Lu, H. Mao, J. Cheng, X. Pan, J. Lu, Z. Ye, 3D ternary nanocomposites of molybdenum disulfide/polyaniline/reduced graphene oxide aerogel for high performance supercapacitors, Carbon 99 (2016) 26-34.

[93] Y. Wang, L. Jiang, Y. Wang, Development of candle soot based carbon nanoparticles (CNPs)/polyaniline electrode and its comparative study with CNPs/MnO2 in supercapacitors, Electrochimica Acta 210 (2016) 190-198.

[94] Y. He, Y. Bai, X. Yang, J. Zhang, L. Kang, H. Xu, F. Shi, Z. Lei, Z.-H. Liu, Holey graphene/polypyrrole nanoparticle hybrid aerogels with three-dimensional hierarchical porous structure for high performance supercapacitor, Journal of Power Sources 317 (2016) 10-18.

[95] X. Gu, Y. Yang, Y. Hu, M. Hu, J. Huang, C. Wang, Facile fabrication of graphene–polypyrrole–Mn composites as high-performance electrodes for capacitive deionization, Journal of Materials Chemistry A 3(11) (2015) 5866-5874.

[96] P. Sen, A. De, Electrochemical performances of poly (3, 4-ethylenedioxythiophene)–NiFe2O4 nanocomposite as electrode for supercapacitor, Electrochimica Acta 55(16) (2010) 4677-4684.

[97] J. Wang, Z. Wu, H. Yin, W. Li, Y. Jiang, Poly (3, 4-ethylenedioxythiophene)/MoS 2 nanocomposites with enhanced electrochemical capacitance performance, RSC Advances 4(100) (2014) 56926-56932.

[98] H. Gong, F. Zheng, J. Xu, C. Sun, L. Gao, P. Hu, Y. Li, Y. Gong, Q. Zhen, S. Bashir, Preparation and supercapacitive property of molybdenum disulfide (MoS2) nanoflake arrays-tungsten trioxide (WO3) nanorod arrays composite heterojunction: A synergistic effect of one-dimensional and two-dimensional nanomaterials, Electrochimica Acta 263 (2018) 409-416.

[99] Y. Zhao, L. Xu, J. Yan, W. Yan, C. Wu, J. Lian, Y. Huang, J. Bao, J. Qiu, L. Xu, Facile preparation of NiFe2O4/MoS2 composite material with synergistic effect for high performance supercapacitor, Journal of Alloys and Compounds 726 (2017) 608-617.

[100] M. Majumder, R.B. Choudhary, S.P. Koiry, A.K. Thakur, U. Kumar, Gravimetric and volumetric capacitive performance of polyindole/carbon black/MoS2 hybrid electrode material for supercapacitor applications, Electrochimica Acta 248 (2017) 98-111.

[101] B. Hu, X. Qin, A.M. Asiri, K.A. Alamry, A.O. Al-Youbi, X. Sun, Synthesis of porous tubular C/MoS2 nanocomposites and their application as a novel electrode material for supercapacitors with excellent cycling stability, Electrochimica Acta 100 (2013) 24-28.

[102] M.D. Stoller, S. Park, Y. Zhu, J. An, R.S. Ruoff, Graphene-based ultracapacitors, Nano letters 8(10) (2008) 3498-3502.

[103] N. Liu, W. Li, M. Pasta, Y. Cui, Nanomaterials for electrochemical energy storage, Frontiers of Physics 9(3) (2014) 323-350.

[104] M.R. Benzigar, S.N. Talapaneni, S. Joseph, K. Ramadass, G. Singh, J. Scaranto, U. Ravon, K. Al-Bahily, A. Vinu, Recent advances in functionalized micro and mesoporous carbon materials: synthesis and applications, Chemical Society Reviews 47(8) (2018) 2680-2721.

[105] F. Ran, X. Yang, L. Shao, Recent progress in carbon-based nanoarchitectures for advanced supercapacitors, Advanced Composites and Hybrid Materials (2018) 1-24.

[106] T. Otowa, Y. Nojima, T. Miyazaki, Development of KOH activated high surface area carbon and its application to drinking water purification, Carbon 35(9) (1997) 1315-1319.

[107] M. Zhi, F. Yang, F. Meng, M. Li, A. Manivannan, N. Wu, Effects of pore structure on performance of an activated-carbon supercapacitor electrode recycled from scrap waste tires, ACS Sustainable Chemistry & Engineering 2(7) (2014) 1592-1598.

[108] L. Wei, G. Yushin, Nanostructured activated carbons from natural precursors for electrical double layer capacitors, Nano Energy 1(4) (2012) 552-565.

[109] M. Sevilla, W. Gu, C. Falco, M.-M. Titirici, A. Fuertes, G. Yushin, Hydrothermal synthesis of microalgae-derived microporous carbons for electrochemical capacitors, Journal of Power Sources 267 (2014) 26-32.

[110] R.H. Baughman, A.A. Zakhidov, W.A. De Heer, Carbon nanotubes--the route toward applications, Science 297(5582) (2002) 787-792.

[111] M. Kaempgen, C.K. Chan, J. Ma, Y. Cui, G. Gruner, Printable thin film supercapacitors using single-walled carbon nanotubes, Nano letters 9(5) (2009) 1872-1876.

[112] Y.J. Kang, H. Chung, C.-H. Han, W. Kim, All-solid-state flexible supercapacitors based on papers coated with carbon nanotubes and ionic-liquid-based gel electrolytes, Nanotechnology 23(6) (2012) 065401.

[113] G. Wang, Y. Ling, F. Qian, X. Yang, X.-X. Liu, Y. Li, Enhanced capacitance in partially exfoliated multi-walled carbon nanotubes, Journal of Power Sources 196(11) (2011) 5209-5214.

[114] K.S. Novoselov, V. Fal, L. Colombo, P. Gellert, M. Schwab, K. Kim, A roadmap for graphene, nature 490(7419) (2012) 192.

[115] C.e.N.e.R. Rao, A.e.K. Sood, K.e.S. Subrahmanyam, A. Govindaraj, Graphene: the new two-dimensional nanomaterial, Angewandte Chemie International Edition 48(42) (2009) 7752-7777.

[116] C. Bussy, H. Ali-Boucetta, K. Kostarelos, Safety considerations for graphene: lessons learnt from carbon nanotubes, Accounts of chemical research 46(3) (2012) 692-701.

[117] L. Yan, F. Zhao, S. Li, Z. Hu, Y. Zhao, Low-toxic and safe nanomaterials by surface-chemical design, carbon nanotubes, fullerenes, metallofullerenes, and graphenes, Nanoscale 3(2) (2011) 362-382.

[118] M. Agharkar, S. Kochrekar, S. Hidouri, M.A. Azeez, Trends in green reduction of graphene oxides, issues and challenges: a review, Materials Research Bulletin 59 (2014) 323-328.

[119] A. Bianco, Graphene: safe or toxic? The two faces of the medal, Angewandte Chemie International Edition 52(19) (2013) 4986-4997.

[120] A.M. Jastrzębska, P. Kurtycz, A.R. Olszyna, Recent advances in graphene family materials toxicity investigations, Journal of Nanoparticle Research 14(12) (2012) 1320.

[121] X. Cao, Z. Yin, H. Zhang, Three-dimensional graphene materials: preparation, structures and application in supercapacitors, Energy & Environmental Science 7(6) (2014) 1850-1865.

[122] Y. Huang, J. Liang, Y. Chen, An overview of the applications of graphene-based materials in supercapacitors, Small 8(12) (2012) 1805-1834.

[123] Z.-S. Wu, G. Zhou, L.-C. Yin, W. Ren, F. Li, H.-M. Cheng, Graphene/metal oxide composite electrode materials for energy storage, Nano Energy 1(1) (2012) 107-131.

[124] Y. Wang, Z. Shi, Y. Huang, Y. Ma, C. Wang, M. Chen, Y. Chen, Supercapacitor devices based on graphene materials, The Journal of Physical Chemistry C 113(30) (2009) 13103-13107.

[125] W. Deng, X. Ji, Q. Chen, C.E. Banks, Electrochemical capacitors utilising transition metal oxides: an update of recent developments, Rsc Advances 1(7) (2011) 1171-1178.

[126] T. Brousse, M. Toupin, R. Dugas, L. Athouël, O. Crosnier, D. Bélanger, Crystalline MnO2 as possible alternatives to amorphous compounds in electrochemical supercapacitors, Journal of the Electrochemical Society 153(12) (2006) A2171-A2180.

[127] N.-L. Wu, Nanocrystalline oxide supercapacitors, Materials Chemistry and Physics 75(1-3) (2002) 6-11.

[128] P. Kulal, D. Dubal, C. Lokhande, V. Fulari, Chemical synthesis of Fe2O3 thin films for supercapacitor application, Journal of Alloys and Compounds 509(5) (2011) 2567-2571.

[129] P. Yang, X. Xiao, Y. Li, Y. Ding, P. Qiang, X. Tan, W. Mai, Z. Lin, W. Wu, T. Li, Hydrogenated ZnO core–shell nanocables for flexible supercapacitors and self-powered systems, ACS nano 7(3) (2013) 2617-2626.

[130] C.-C. Hu, K.-H. Chang, M.-C. Lin, Y.-T. Wu, Design and tailoring of the nanotubular arrayed architecture of hydrous RuO2 for next generation supercapacitors, Nano letters 6(12) (2006) 2690-2695.

[131] J. Zheng, P. Cygan, T. Jow, Hydrous ruthenium oxide as an electrode material for electrochemical capacitors, Journal of the Electrochemical Society 142(8) (1995) 2699-2703.

[132] H. Xia, Y.S. Meng, G. Yuan, C. Cui, L. Lu, A symmetric RuO2/RuO2 supercapacitor operating at 1.6 V by using a neutral aqueous electrolyte, Electrochemical and Solid-State Letters 15(4) (2012) A60-A63.

[133] K.-K. Liu, W. Zhang, Y.-H. Lee, Y.-C. Lin, M.-T. Chang, C.-Y. Su, C.-S. Chang, H. Li, Y. Shi, H. Zhang, Growth of large-area and highly crystalline MoS2 thin layers on insulating substrates, Nano letters 12(3) (2012) 1538-1544.

[134] J. Kibsgaard, Z. Chen, B.N. Reinecke, T.F. Jaramillo, Engineering the surface structure of MoS 2 to preferentially expose active edge sites for electrocatalysis, Nature materials 11(11) (2012) 963.

[135] J.M. Soon, K.P. Loh, Electrochemical double-layer capacitance of MoS2 nanowall films, Electrochemical and Solid-State Letters 10(11) (2007) A250-A254.

[136] H. Dong, S. Tang, Y. Hao, H. Yu, W. Dai, G. Zhao, Y. Cao, H. Lu, X. Zhang, H. Ju, Fluorescent MoS2 quantum dots: ultrasonic preparation, up-conversion and down-conversion bioimaging, and photodynamic therapy, ACS applied materials & interfaces 8(5) (2016) 3107-3114.

[137] J. Brivio, D.T. Alexander, A. Kis, Ripples and layers in ultrathin MoS2 membranes, Nano letters 11(12) (2011) 5148-5153.

[138] H.I. Karunadasa, E. Montalvo, Y. Sun, M. Majda, J.R. Long, C.J. Chang, A molecular MoS2 edge site mimic for catalytic hydrogen generation, Science 335(6069) (2012) 698-702.

[139] G.S. Bang, K.W. Nam, J.Y. Kim, J. Shin, J.W. Choi, S.-Y. Choi, Effective liquid-phase exfoliation and sodium ion battery application of MoS2 nanosheets, ACS applied materials & interfaces 6(10) (2014) 7084-7089.

[140] J. Xiao, D. Choi, L. Cosimbescu, P. Koech, J. Liu, J.P. Lemmon, Exfoliated MoS2 nanocomposite as an anode material for lithium ion batteries, Chemistry of Materials 22(16) (2010) 4522-4524.

[141] W.-J. Zhang, K.-J. Huang, A review of recent progress in molybdenum disulfide-based supercapacitors and batteries, Inorganic Chemistry Frontiers 4(10) (2017) 1602-1620.

[142] H. Liu, D. Su, R. Zhou, B. Sun, G. Wang, S.Z. Qiao, Highly ordered mesoporous MoS2 with expanded spacing of the (002) crystal plane for ultrafast lithium ion storage, Advanced Energy Materials 2(8) (2012) 970-975.

[143] P. Poizot, S. Laruelle, S. Grugeon, L. Dupont, J. Tarascon, Nano-sized transition-metal oxides as negative-electrode materials for lithium-ion batteries, Nature 407(6803) (2000) 496.

[144] K. Novoselov, D. Jiang, F. Schedin, T. Booth, V. Khotkevich, S. Morozov, A. Geim, Two-dimensional atomic crystals, Proceedings of the National Academy of Sciences 102(30) (2005) 10451-10453.

[145] W.T. Neo, Q. Ye, S.-J. Chua, J. Xu, Conjugated polymer-based electrochromics: materials, device fabrication and application prospects, Journal of Materials Chemistry C 4(31) (2016) 7364-7376.

[146] D. Kumar, R. Sharma, Advances in conductive polymers, European polymer journal 34(8) (1998) 1053-1060.

[147] C. Meng, C. Liu, L. Chen, C. Hu, S. Fan, Highly flexible and all-solid-state paperlike polymer supercapacitors, Nano letters 10(10) (2010) 4025-4031.

[148] A. Elschner, S. Kirchmeyer, W. Lovenich, U. Merker, K. Reuter, PEDOT: principles and applications of an intrinsically conductive polymer, CRC Press2010.

[149] K. Lota, V. Khomenko, E. Frackowiak, Capacitance properties of poly (3, 4-ethylenedioxythiophene)/carbon nanotubes composites, Journal of Physics and Chemistry of Solids 65(2-3) (2004) 295-301.

[150] K.S. Ryu, Y.-G. Lee, Y.-S. Hong, Y.J. Park, X. Wu, K.M. Kim, M.G. Kang, N.-G. Park, S.H. Chang, Poly (ethylenedioxythiophene)(PEDOT) as polymer electrode in redox supercapacitor, Electrochimica acta 50(2-3) (2004) 843-847.

[151] G.A. Snook, G.Z. Chen, The measurement of specific capacitances of conducting polymers using the quartz crystal microbalance, Journal of Electroanalytical Chemistry 612(1) (2008) 140-146.

[152] F. Jonas, J. Morrison, 3, 4-polyethylenedioxythiophene (PEDT): Conductive coatings technical applications and properties, Synthetic Metals 85(1-3) (1997) 1397-1398.

[153] A. Laforgue, All-textile flexible supercapacitors using electrospun poly (3, 4-ethylenedioxythiophene) nanofibers, Journal of Power Sources 196(1) (2011) 559-564.

[154] H. Ghenaatian, M. Mousavi, S. Kazemi, M. Shamsipur, Electrochemical investigations of self-doped polyaniline nanofibers as a new electroactive material for high performance redox supercapacitor, Synthetic Metals 159(17-18) (2009) 1717-1722.

[155] F. Fusalba, P. Gouérec, D. Villers, D. Bélanger, Electrochemical characterization of polyaniline in nonaqueous electrolyte and its evaluation as electrode material for electrochemical supercapacitors, Journal of the Electrochemical Society 148(1) (2001) A1-A6.

[156] M. Delvaux, J. Duchet, P.-Y. Stavaux, R. Legras, S. Demoustier-Champagne, Chemical and electrochemical synthesis of polyaniline micro-and nano-tubules, Synthetic Metals 113(3) (2000) 275-280.

[157] K.S. Ryu, K.M. Kim, N.-G. Park, Y.J. Park, S.H. Chang, Symmetric redox supercapacitor with conducting polyaniline electrodes, Journal of Power Sources 103(2) (2002) 305-309.

[158] L.Z. Fan, Y.S. Hu, J. Maier, P. Adelhelm, B. Smarsly, M. Antonietti, High electroactivity of polyaniline in supercapacitors by using a hierarchically porous carbon monolith as a support, Advanced Functional Materials 17(16) (2007) 3083-3087.

[159] S. Tripathi, A. Kumar, S. Hashmi, Electrochemical redox supercapacitors using PVdF-HFP based gel electrolytes and polypyrrole as conducting polymer electrode, Solid state ionics 177(33-34) (2006) 2979-2985.

[160] L.-Z. Fan, J. Maier, High-performance polypyrrole electrode materials for redox supercapacitors, Electrochemistry communications 8(6) (2006) 937-940.

[161] A. Hussain, D. Saikia, F. Singh, D. Avasthi, A. Kumar, Effects of 160 MeV Ni12+ ion irradiation on polypyrrole conducting polymer electrode materials for all polymer redox supercapacitor, Nuclear Instruments and Methods in Physics Research Section B: Beam Interactions with Materials and Atoms 240(4) (2005) 834-841.

[162] J.-H. Sung, S.-J. Kim, K.-H. Lee, Fabrication of microcapacitors using conducting polymer microelectrodes, Journal of Power Sources 124(1) (2003) 343-350.

[163] L. Yuan, B. Yao, B. Hu, K. Huo, W. Chen, J. Zhou, Polypyrrole-coated paper for flexible solid-state energy storage, Energy & Environmental Science 6(2) (2013) 470-476.

[164] Y. Shi, L. Pan, B. Liu, Y. Wang, Y. Cui, Z. Bao, G. Yu, Nanostructured conductive polypyrrole hydrogels as high-performance, flexible supercapacitor electrodes, Journal of Materials Chemistry A 2(17) (2014) 6086-6091.

[165] D. Wang, Y.-X. Li, Z. Shi, H.-L. Qin, L. Wang, X.-F. Pei, J. Jin, Spontaneous growth of free-standing polypyrrole films at an air/ionic liquid interface, Langmuir 26(18) (2010) 14405-14408.

[166] M. Inagaki, H. Konno, O. Tanaike, Carbon materials for electrochemical capacitors, Journal of power sources 195(24) (2010) 7880-7903.

[167] J. Li, X. Cheng, A. Shashurin, M. Keidar, Review of electrochemical capacitors based on carbon nanotubes and graphene, Graphene 1(01) (2012) 1.

[168] I.-H. Kim, K.-B. Kim, Ruthenium oxide thin film electrodes for supercapacitors, Electrochemical and Solid-State Letters 4(5) (2001) A62-A64.

[169] R.Y. Song, J.H. Park, S. Sivakkumar, S.H. Kim, J.M. Ko, D.-Y. Park, S.M. Jo, D.Y. Kim, Supercapacitive properties of polyaniline/Nafion/hydrous RuO2 composite electrodes, Journal of power sources 166(1) (2007) 297-301.

[170] J. Zang, S.-J. Bao, C.M. Li, H. Bian, X. Cui, Q. Bao, C.Q. Sun, J. Guo, K. Lian, Well-aligned cone-shaped nanostructure of polypyrrole/RuO2 and its electrochemical supercapacitor, The Journal of Physical Chemistry C 112(38) (2008) 14843-14847.

[171] L.-M. Huang, H.-Z. Lin, T.-C. Wen, A. Gopalan, Highly dispersed hydrous ruthenium oxide in poly (3, 4-ethylenedioxythiophene)-poly (styrene sulfonic acid) for supercapacitor electrode, Electrochimica acta 52(3) (2006) 1058-1063.

[172] S.H. Mujawar, S.B. Ambade, T. Battumur, R.B. Ambade, S.-H. Lee, Electropolymerization of polyaniline on titanium oxide nanotubes for supercapacitor application, Electrochimica Acta 56(12) (2011) 4462-4466.

[173] T.K. Das, S. Prusty, Graphene-based polymer composites and their applications, Polymer-Plastics Technology and Engineering 52(4) (2013) 319-331.

[174] Q. Wu, Y. Xu, Z. Yao, A. Liu, G. Shi, Supercapacitors based on flexible graphene/polyaniline nanofiber composite films, ACS nano 4(4) (2010) 1963-1970.

[175] W.-L. Song, M.-S. Cao, M.-M. Lu, S. Bi, C.-Y. Wang, J. Liu, J. Yuan, L.-Z. Fan, Flexible graphene/polymer composite films in sandwich structures for effective electromagnetic interference shielding, Carbon 66 (2014) 67-76.

[176] Y. Sun, G. Shi, Graphene/polymer composites for energy applications, Journal of Polymer Science Part B: Polymer Physics 51(4) (2013) 231-253.

[177] R. Ruoff, Graphene: Calling all chemists, Nature Nanotechnology 3(1) (2008) 10.

[178] S. Sahoo, S. Dhibar, G. Hatui, P. Bhattacharya, C.K. Das, Graphene/polypyrrole nanofiber nanocomposite as electrode material for electrochemical supercapacitor, Polymer 54(3) (2013) 1033-1042.

[179] P.A. Basnayaka, M.K. Ram, E.K. Stefanakos, A. Kumar, Supercapacitors based on graphene–polyaniline derivative nanocomposite electrode materials, Electrochimica Acta 92 (2013) 376-382.

[180] F. Alvi, M.K. Ram, P.A. Basnayaka, E. Stefanakos, Y. Goswami, A. Kumar, Graphene–polyethylenedioxythiophene conducting polymer nanocomposite based supercapacitor, Electrochimica Acta 56(25) (2011) 9406-9412.

[181] P.A. Basnayaka, M.K. Ram, L. Stefanakos, A. Kumar, Graphene/polypyrrole nanocomposite as electrochemical supercapacitor electrode: electrochemical impedance studies, Graphene 2(02) (2013) 81.

[182] F. Alvi, P.A. Basnayaka, M.K. Ram, H. Gomez, E. Stefanako, Y. Goswami, A. Kumar, Graphene-polythiophene nanocomposite as novel supercapacitor electrode material, Journal of New Materials for Electrochemical Systems (2012) 89-95.

[183] J. Yan, T. Wei, B. Shao, Z. Fan, W. Qian, M. Zhang, F. Wei, Preparation of a graphene nanosheet/polyaniline composite with high specific capacitance, Carbon 48(2) (2010) 487-493.

[184] P. Damlin, B. Gadgil, C. Kvarnstrom, Ionic Liquid-Assisted Fabrication of Graphene-Based Electroactive Composite Materials, Electrochemical Nanofabrication: Principles and Applications (2017) 251.

[185] J. Xu, K. Wang, S.-Z. Zu, B.-H. Han, Z. Wei, Hierarchical nanocomposites of polyaniline nanowire arrays on graphene oxide sheets with synergistic effect for energy storage, ACS nano 4(9) (2010) 5019-5026.

[186] W. Liu, C. Zhao, R. Zhou, D. Zhou, Z. Liu, X. Lu, Lignin-assisted exfoliation of molybdenum disulfide in aqueous media and its application in lithium ion batteries, Nanoscale 7(21) (2015) 9919-9926.

[187] Z. Antar, J.F. Feller, G. Vignaud, Eco-friendly conductive polymer nanocomposites (CPC) for solar absorbers design, Polymers for Advanced Technologies 24(7) (2013) 638-645.

[188] K. Wang, L. Li, Y. Liu, C. Zhang, T. Liu, Constructing a “Pizza-Like” MoS2/Polypyrrole/Polyaniline Ternary Architecture with High Energy Density and Superior Cycling Stability for Supercapacitors, Advanced Materials Interfaces 3(19) (2016) 1600665.

[189] G. Ma, H. Peng, J. Mu, H. Huang, X. Zhou, Z. Lei, In situ intercalative polymerization of pyrrole in graphene analogue of MoS2 as advanced electrode material in supercapacitor, Journal of Power Sources 229 (2013) 72-78.

[190] T. Brousse, D. Bélanger, K. Chiba, M. Egashira, F. Favier, J. Long, J.R. Miller, M. Morita, K. Naoi, P. Simon, Materials for electrochemical Capacitors, Springer Handbook of Electrochemical Energy, Springer2017, pp. 495-561.

[191] M. Galiński, A. Lewandowski, I. Stępniak, Ionic liquids as electrolytes, Electrochimica acta 51(26) (2006) 5567-5580.

[192] J. Song, Y. Wang, C.C. Wan, Review of gel-type polymer electrolytes for lithium-ion batteries, Journal of Power Sources 77(2) (1999) 183-197.

[193] X. Lu, M. Yu, G. Wang, Y. Tong, Y. Li, Flexible solid-state supercapacitors: design, fabrication and applications, Energy & Environmental Science 7(7) (2014) 2160-2181.

[194] P. Sharma, T. Bhatti, A review on electrochemical double-layer capacitors, Energy conversion and management 51(12) (2010) 2901-2912.

[195] A. Schneuwly, R. Gallay, Properties and applications of supercapacitors: From the state-of-the-art to future trends, Rossens, Switzerland (2000).

[196] B. Szubzda, A. Szmaja, M. Ozimek, S. Mazurkiewicz, Polymer membranes as separators for supercapacitors, Applied Physics A 117(4) (2014) 1801-1809.

[197] maxwell, K2 ULTRACAPACITORS - 3.0V/3000F. <http://www.maxwell.com/images/documents/K2_3V_DS_3001423_EN_1.pdf>).

[198] AVX, SCC Series Supercapacitors. <http://datasheets.avx.com/AVX-SCC.pdf>).

[199] Nichicon-US, <http://nichicon-us.com/english/products/pdfs/e-jjd.pdf>).

[200] Eaton, XL60 Supercapacitors Cylindrical cells. <http://www.cooperindustries.com/content/dam/public/bussmann/Electronics/Resources/product-datasheets/bus-elx-ds-10339-xl.pdf>).

[201] Kemet, <https://media.digikey.com/pdf/Data%20Sheets/Kemet%20PDFs/S301Rx_Mar2014.pdf>).

[202] NESSCAP, NESSCAP® Ultracapacitor Products. <http://www.nesscap.com/common/download.jsp?dir=product&sfn=MSCWSMXHBBOMXOZ.pdf>).

[203] I. Capacitor, DGH low ESR Supercapacitor

[204] S. Wire, Reference electrodes, (1961).

[205] H. Tachikawa, L. Faulkner, P. Kissinger, W. Heineman, Laboratory Techniques in Electroanalytical Chemistry, Kissinger, PT, Heineman, WR, Eds, 1984.

[206] R.A. Aziz, I.I. Misnon, K.F. Chong, M.M. Yusoff, R. Jose, Layered sodium titanate nanostructures as a new electrode for high energy density supercapacitors, Electrochimica Acta 113 (2013) 141-148.

[207] H. Yang, Y. Zhang, Self-discharge analysis and characterization of supercapacitors for environmentally powered wireless sensor network applications, Journal of Power Sources 196(20) (2011) 8866-8873.

[208] R.J. Mortimer, Electrochromic materials, Chemical Society Reviews 26(3) (1997) 147-156.

[209] N.M. Rowley, R.J. Mortimer, New electrochromic materials, Science progress 85(3) (2002) 243-262.

[210] R. Mertens, The OLED Handbook, 2015.

[211] X. Huang, C. Tan, Z. Yin, H. Zhang, 25th Anniversary Article: Hybrid Nanostructures Based on Two-Dimensional Nanomaterials, Advanced Materials 26(14) (2014) 2185-2204.

[212] H. Wang, L. Yu, Y.-H. Lee, Y. Shi, A. Hsu, M.L. Chin, L.-J. Li, M. Dubey, J. Kong, T. Palacios, Integrated circuits based on bilayer MoS2 transistors, Nano letters 12(9) (2012) 4674-4680.

[213] A.M. White, R.C. Slade, Electrochemically and vapour grown electrode coatings of poly (3, 4-ethylenedioxythiophene) doped with heteropolyacids, Electrochimica acta 49(6) (2004) 861-865.

[214] M. Nakamura, M. Nakanishi, K. Yamamoto, Influence of physical properties of activated carbons on characteristics of electric double-layer capacitors, Journal of power sources 60(2) (1996) 225-231.

[215] J.M. Schnorr, T.M. Swager, Emerging applications of carbon nanotubes, Chemistry of Materials 23(3) (2010) 646-657.

[216] Y. Xu, J. Wang, W. Sun, S. Wang, Capacitance properties of poly (3, 4-ethylenedioxythiophene)/polypyrrole composites, Journal of Power Sources 159(1) (2006) 370-373.

[217] J.D. Stenger-Smith, C.K. Webber, N. Anderson, A.P. Chafin, K. Zong, J.R. Reynolds, Poly (3, 4-alkylenedioxythiophene)-based supercapacitors using ionic liquids as supporting electrolytes, Journal of the Electrochemical Society 149(8) (2002) A973-A977.

[218] D.K. Bhat, M.S. Kumar, N and p doped poly (3, 4-ethylenedioxythiophene) electrode materials for symmetric redox supercapacitors, Journal of materials science 42(19) (2007) 8158-8162.

[219] M. Khawaja, Synthesis and Fabrication of Graphene/Conducting Polymer/Metal Oxide Nanocomposite Materials for Supercapacitor Applications, (2015).

[220] A.V. Murugan, M. Quintin, M.-H. Delville, G. Campet, C.S. Gopinath, K. Vijayamohanan, Exfoliation-induced nanoribbon formation of poly (3, 4-ethylene dioxythiophene) PEDOT between MoS2 layers as cathode material for lithium batteries, Journal of power sources 156(2) (2006) 615-619.

[221] M.-W. Lin, L. Liu, Q. Lan, X. Tan, K.S. Dhindsa, P. Zeng, V.M. Naik, M.M.-C. Cheng, Z. Zhou, Mobility enhancement and highly efficient gating of monolayer MoS2 transistors with polymer electrolyte, Journal of Physics D: Applied Physics 45(34) (2012) 345102.

[222] F. Jiang, J. Xiong, W. Zhou, C. Liu, L. Wang, F. Zhao, H. Liu, J. Xu, Use of organic solvent-assisted exfoliated MoS 2 for optimizing the thermoelectric performance of flexible PEDOT: PSS thin films, Journal of Materials Chemistry A 4(14) (2016) 5265-5273.

[223] Y. Zhang, K.S. Suslick, Synthesis of poly (3, 4-ethylenedioxythiophene) microspheres by ultrasonic spray polymerization (USPo), Chemistry of Materials 27(22) (2015) 7559-7563.

[224] R. Pang, X. Hu, S. Zhou, C. Sun, J. Yan, X. Sun, S. Xiao, P. Chen, Preparation of multi-shelled conductive polymer hollow microspheres by using Fe 3 O 4 hollow spheres as sacrificial templates, Chemical Communications 50(83) (2014) 12493-12496.

[225] A.V. Murugan, M. Quintin, M.-H. Delville, G. Campet, A.K. Viswanath, C.S. Gopinath, K. Vijayamohanan, Synthesis and characterization of organic–inorganic poly (3, 4-ethylenedioxythiophene)/MoS 2 nanocomposite via in situ oxidative polymerization, Journal of materials research 21(1) (2006) 112-118.

[226] A. Monshi, M.R. Foroughi, M.R. Monshi, Modified Scherrer equation to estimate more accurately nano-crystallite size using XRD, World Journal of Nano Science and Engineering 2(3) (2012) 154-160.

[227] Y. Kim, J.-G. Song, Y.J. Park, G.H. Ryu, S.J. Lee, J.S. Kim, P.J. Jeon, C.W. Lee, W.J. Woo, T. Choi, Self-limiting layer synthesis of transition metal dichalcogenides, Scientific reports 6 (2016) 18754.

[228] S. Zhang, J. Yang, R. Xu, F. Wang, W. Li, M. Ghufran, Y.-W. Zhang, Z. Yu, G. Zhang, Q. Qin, Extraordinary photoluminescence and strong temperature/angle-dependent Raman responses in few-layer phosphorene, ACS nano 8(9) (2014) 9590-9596.

[229] A. Schaarschmidt, A.A. Farah, A. Aby, A.S. Helmy, Influence of nonadiabatic annealing on the morphology and molecular structure of PEDOT− PSS films, The Journal of Physical Chemistry B 113(28) (2009) 9352-9355.

[230] J. Ouyang, Q. Xu, C.-W. Chu, Y. Yang, G. Li, J. Shinar, On the mechanism of conductivity enhancement in poly (3, 4-ethylenedioxythiophene): poly (styrene sulfonate) film through solvent treatment, Polymer 45(25) (2004) 8443-8450.

[231] T. Park, C. Park, B. Kim, H. Shin, E. Kim, Flexible PEDOT electrodes with large thermoelectric power factors to generate electricity by the touch of fingertips, Energy & Environmental Science 6(3) (2013) 788-792.

[232] T. Nguyen, S. De Vos, An investigation into the effect of chemical and thermal treatments on the structural changes of poly (3, 4-ethylenedioxythiophene)/polystyrenesulfonate and consequences on its use on indium tin oxide substrates, Applied Surface Science 221(1-4) (2004) 330-339.

[233] X. Wang, K. Wong, Effects of a base coating used for electropolymerization of poly (3, 4-ethylenedioxythiophene) on indium tin oxide electrode, Thin Solid Films 515(4) (2006) 1573-1578.

[234] L. Gao, X. Li, X. Li, J. Cheng, B. Wang, Z. Wang, C. Li, A coaxial yarn electrode based on hierarchical MoS 2 nanosheets/carbon fiber tows for flexible solid-state supercapacitors, RSC Advances 6(62) (2016) 57190-57198.

[235] K.-J. Huang, L. Wang, J.-Z. Zhang, K. Xing, Synthesis of molybdenum disulfide/carbon aerogel composites for supercapacitors electrode material application, Journal of Electroanalytical Chemistry 752 (2015) 33-40.

[236] Q. Wang, J. Li, Facilitated lithium storage in MoS2 overlayers supported on coaxial carbon nanotubes, The Journal of Physical Chemistry C 111(4) (2007) 1675-1682.

[237] W. Yang, L. He, X. Tian, M. Yan, H. Yuan, X. Liao, J. Meng, Z. Hao, L. Mai, Carbon-MEMS-Based Alternating Stacked MoS2@ rGO-CNT Micro-Supercapacitor with High Capacitance and Energy Density, small 13(26) (2017) 1700639.

[238] A. Liu, H. Lv, H. Liu, Q. Li, H. Zhao, Two dimensional MoS 2/CNT hybrid ink for paper-based capacitive energy storage, Journal of Materials Science: Materials in Electronics 28(12) (2017) 8452-8459.

[239] K.-J. Huang, L. Wang, J.-Z. Zhang, L.-L. Wang, Y.-P. Mo, One-step preparation of layered molybdenum disulfide/multi-walled carbon nanotube composites for enhanced performance supercapacitor, Energy 67 (2014) 234-240.

[240] M.A. Bissett, I.A. Kinloch, R.A. Dryfe, Characterization of MoS2–graphene composites for high-performance coin cell supercapacitors, ACS applied materials & interfaces 7(31) (2015) 17388-17398.

[241] U.M. Patil, M.S. Nam, S. Kang, J.S. Sohn, H.B. Sim, S. Kang, S.C. Jun, Fabrication of ultra-high energy and power asymmetric supercapacitors based on hybrid 2D MoS 2/graphene oxide composite electrodes: a binder-free approach, RSC Advances 6(49) (2016) 43261-43271.

[242] N. Li, T. Lv, Y. Yao, H. Li, K. Liu, T. Chen, Compact graphene/MoS 2 composite films for highly flexible and stretchable all-solid-state supercapacitors, Journal of Materials Chemistry A 5(7) (2017) 3267-3273.

[243] J. Lei, Z. Jiang, X. Lu, G. Nie, C. Wang, Synthesis of few-layer MoS2 nanosheets-wrapped polyaniline hierarchical nanostructures for enhanced electrochemical capacitance performance, Electrochimica Acta 176 (2015) 149-155.

[244] G. Wang, L. Zhang, J. Zhang, A review of electrode materials for electrochemical supercapacitors, Chemical Society Reviews 41(2) (2012) 797-828.

[245] W. Chen, R. Rakhi, H.N. Alshareef, Capacitance enhancement of polyaniline coated curved-graphene supercapacitors in a redox-active electrolyte, Nanoscale 5(10) (2013) 4134-4138.

[246] K.R. Prasad, N. Munichandraiah, Fabrication and evaluation of 450 F electrochemical redox supercapacitors using inexpensive and high-performance, polyaniline coated, stainless-steel electrodes, Journal of Power Sources 112(2) (2002) 443-451.

[247] L. Li, E. Liu, J. Li, Y. Yang, H. Shen, Z. Huang, X. Xiang, W. Li, A doped activated carbon prepared from polyaniline for high performance supercapacitors, Journal of Power Sources 195(5) (2010) 1516-1521.

[248] L. Karasek, M. Sumita, Characterization of dispersion state of filler and polymer-filler interactions in rubber-carbon black composites, Journal of materials science 31(2) (1996) 281-289.

[249] Y. Cao, J. Qiu, P. Smith, Effect of solvents and co-solvents on the processibility of polyaniline: I. Solubility and conductivity studies, Synthetic Metals 69(1-3) (1995) 187-190.

[250] S. Bhadra, N.K. Singha, D. Khastgir, Polyaniline by new miniemulsion polymerization and the effect of reducing agent on conductivity, Synthetic Metals 156(16-17) (2006) 1148-1154.

[251] K. Gopalakrishnan, S. Sultan, A. Govindaraj, C. Rao, Supercapacitors based on composites of PANI with nanosheets of nitrogen-doped RGO, BC1. 5N, MoS2 and WS2, Nano Energy 12 (2015) 52-58.

[252] M. Kim, Y.K. Kim, J. Kim, S. Cho, G. Lee, J. Jang, Fabrication of a polyaniline/MoS 2 nanocomposite using self-stabilized dispersion polymerization for supercapacitors with high energy density, RSC Advances 6(33) (2016) 27460-27465.

[253] J.-C. Chiang, A.G. MacDiarmid, 'Polyaniline': Protonic acid doping of the emeraldine form to the metallic regime, Synthetic Metals 13(1-3) (1986) 193-205.

[254] R. Stockmann, H. Zandbergen, A. Van Langeveld, J. Moulijn, Investigation of MoS2 on γ-Al2O3 by HREM with atomic resolution, Journal of Molecular Catalysis A: Chemical 102(3) (1995) 147-161.

[255] Z. Ping, In situ FTIR–attenuated total reflection spectroscopic investigations on the base–acid transitions of polyaniline. Base–acid transition in the emeraldine form of polyaniline, Journal of the Chemical Society, Faraday Transactions 92(17) (1996) 3063-3067.

[256] M. Trchová, I. Šeděnková, E. Tobolková, J. Stejskal, FTIR spectroscopic and conductivity study of the thermal degradation of polyaniline films, Polymer Degradation and Stability 86(1) (2004) 179-185.

[257] R.R. Chianelli, M.B. Dines, Low-temperature solution preparation of Group 4B, 5B and 6B transition-metal dichalcogenides, Inorganic Chemistry 17(10) (1978) 2758-2762.

[258] H. Li, Q. Zhang, C.C.R. Yap, B.K. Tay, T.H.T. Edwin, A. Olivier, D. Baillargeat, From bulk to monolayer MoS2: evolution of Raman scattering, Advanced Functional Materials 22(7) (2012) 1385-1390.

[259] S.J. Sandoval, D. Yang, R. Frindt, J. Irwin, Raman study and lattice dynamics of single molecular layers of MoS 2, Physical Review B 44(8) (1991) 3955.

[260] J. Zhang, C. Liu, G. Shi, Raman spectroscopic study on the structural changes of polyaniline during heating and cooling processes, Journal of applied polymer science 96(3) (2005) 732-739.

[261] A. Shakoor, T.Z. Rizvi, A. Nawaz, Raman spectroscopy and AC conductivity of polyaniline montmorillonite (PANI–MMT) nanocomposites, Journal of Materials Science: Materials in Electronics 22(8) (2011) 1076-1080.

[262] K.R. Reddy, B.C. Sin, K.S. Ryu, J. Noh, Y. Lee, In situ self-organization of carbon black–polyaniline composites from nanospheres to nanorods: synthesis, morphology, structure and electrical conductivity, Synthetic Metals 159(19-20) (2009) 1934-1939.

[263] P.J. Hall, E.J. Bain, Energy-storage technologies and electricity generation, Energy policy 36(12) (2008) 4352-4355.

[264] A. Khaligh, Z. Li, Battery, ultracapacitor, fuel cell, and hybrid energy storage systems for electric, hybrid electric, fuel cell, and plug-in hybrid electric vehicles: State of the art, IEEE transactions on Vehicular Technology 59(6) (2010) 2806-2814.

[265] J.R. Miller, P. Simon, Electrochemical capacitors for energy management, Science Magazine 321(5889) (2008) 651-652.

[266] Y.J. Kang, S.-J. Chun, S.-S. Lee, B.-Y. Kim, J.H. Kim, H. Chung, S.-Y. Lee, W. Kim, All-solid-state flexible supercapacitors fabricated with bacterial nanocellulose papers, carbon nanotubes, and triblock-copolymer ion gels, ACS nano 6(7) (2012) 6400-6406.

[267] L.-F. Chen, X.-D. Zhang, H.-W. Liang, M. Kong, Q.-F. Guan, P. Chen, Z.-Y. Wu, S.-H. Yu, Synthesis of nitrogen-doped porous carbon nanofibers as an efficient electrode material for supercapacitors, ACS nano 6(8) (2012) 7092-7102.

[268] X. Xiao, T. Li, P. Yang, Y. Gao, H. Jin, W. Ni, W. Zhan, X. Zhang, Y. Cao, J. Zhong, Fiber-based all-solid-state flexible supercapacitors for self-powered systems, Acs Nano 6(10) (2012) 9200-9206.

[269] S.M. Jung, D.L. Mafra, C.-T. Lin, H.Y. Jung, J. Kong, Controlled porous structures of graphene aerogels and their effect on supercapacitor performance, Nanoscale 7(10) (2015) 4386-4393.

[270] Z. Xu, Z. Li, C.M. Holt, X. Tan, H. Wang, B.S. Amirkhiz, T. Stephenson, D. Mitlin, Electrochemical supercapacitor electrodes from sponge-like graphene nanoarchitectures with ultrahigh power density, The journal of physical chemistry letters 3(20) (2012) 2928-2933.

[271] W. Chen, R. Rakhi, L. Hu, X. Xie, Y. Cui, H.N. Alshareef, High-performance nanostructured supercapacitors on a sponge, Nano letters 11(12) (2011) 5165-5172.

[272] J. Xu, Z. Tan, W. Zeng, G. Chen, S. Wu, Y. Zhao, K. Ni, Z. Tao, M. Ikram, H. Ji, A Hierarchical Carbon Derived from Sponge-Templated Activation of Graphene Oxide for High-Performance Supercapacitor Electrodes, Advanced Materials 28(26) (2016) 5222-5228.

[273] M. Ram, M. Adami, P. Faraci, C. Nicolini, Physical insight in the in-situ self-assembled films of polypyrrole, Polymer 41(20) (2000) 7499-7509.

[274] M.K. Ram, M. Adami, S. Paddeu, C. Nicolini, Nano-assembly of glucose oxidase on the in situ self-assembled films of polypyrrole and its optical, surface and electrochemical characterizations, Nanotechnology 11(2) (2000) 112.

[275] M.K. Ram, O. Yavuz, M. Aldissi, NO 2 gas sensing based on ordered ultrathin films of conducting polymer and its nanocomposite, Synthetic Metals 151(1) (2005) 77-84.

[276] M.K. Ram, Ö. Yavuz, V. Lahsangah, M. Aldissi, CO gas sensing from ultrathin nano-composite conducting polymer film, Sensors and Actuators B: Chemical 106(2) (2005) 750-757.

[277] N. Sarkar, M.K. Ram, A. Sarkar, R. Narizzano, S. Paddeu, C. Nicolini, Nanoassemblies of sulfonated polyaniline multilayers, Nanotechnology 11(1) (2000) 30.

[278] M.K. Ram, M. Salerno, M. Adami, P. Faraci, C. Nicolini, Physical properties of polyaniline films: assembled by the layer-by-layer technique, Langmuir 15(4) (1999) 1252-1259.

[279] G. Nagaraju, C. Tharamani, G. Chandrappa, J. Livage, Hydrothermal synthesis of amorphous MoS_2 nanofiber bundles via acidification of ammonium heptamolybdate tetrahydrate, Nanoscale research letters 2(9) (2007) 461.

[280] A. Gambhir, M. Gerard, S.K. Jain, B. Malhotra, Characterization of DNA immobilized on electrochemically prepared conducting polypyrrole-polyvinyl sulfonate films, Applied biochemistry and biotechnology 96(1-3) (2001) 313-319.

[281] L. Zhang, Y. Long, Z. Chen, M. Wan, The Effect of Hydrogen Bonding on Self-Assembled Polyaniline Nanostructures, Advanced Functional Materials 14(7) (2004) 693-698.

[282] T. Weber, J. Muijsers, J. Van Wolput, C. Verhagen, J. Niemantsverdriet, Basic reaction steps in the sulfidation of crystalline MoO_3 to MoS_2, as studied by X-ray photoelectron and infrared emission spectroscopy, The Journal of Physical Chemistry 100(33) (1996) 14144-14150.

APPENDIX A: COPYRIGHT PERMISSIONS FOR MATERIAL USED IN CHAPTERS 4

Below is permission for the use of material in Chapter 4.

Copyright Clearance Center RightsLink®

Home | Account Info | Help

Title: Polyethylenedioxythiophene and molybdenum disulfide nanocomposite electrodes for supercapacitor applications

Author: Turki Alamro,Manoj K. Ram

Publication: Electrochimica Acta

Publisher: Elsevier

Date: 1 May 2017

Logged in as:
Turki Alarmo
University of South Florida
Account #:
3001191074

LOGOUT

Please note that, as the author of this Elsevier article, you retain the right to include it in a thesis or dissertation, provided it is not published commercially. Permission is not required, but please ensure that you reference the journal as the original source. For more information on this and on your other retained rights, please visit: https://www.elsevier.com/about/our-business/policies/copyright#Author-rights

BACK | CLOSE WINDOW

APPENDIX B: COPYRIGHT PERMISSIONS FOR FIGURES AND TABLES

Below is copyright permission for Figure 1.1.

Copyright Clearance Center RightsLink®

Home | Account Info | Help

SPRINGER NATURE

Title: Materials for electrochemical capacitors
Author: Patrice Simon, Yury Gogotsi
Publication: Nature Materials
Publisher: Springer Nature
Date: Nov 1, 2008
Copyright © 2008, Springer Nature

Logged in as:
Turki Alarmo
University of South Florida
Account #:
3001191074
LOGOUT

Order Completed

Thank you for your order.

This Agreement between University of South Florida -- Turki Alarmo ("You") and Springer Nature ("Springer Nature") consists of your license details and the terms and conditions provided by Springer Nature and Copyright Clearance Center.

Your confirmation email will contain your order number for future reference.

printable details

License Number	4412120496605
License date	Aug 18, 2018
Licensed Content Publisher	Springer Nature
Licensed Content Publication	Nature Materials
Licensed Content Title	Materials for electrochemical capacitors
Licensed Content Author	Patrice Simon, Yury Gogotsi
Licensed Content Date	Nov 1, 2008
Licensed Content Volume	7
Licensed Content Issue	11
Type of Use	Thesis/Dissertation
Requestor type	academic/university or research institute
Format	print and electronic
Portion	figures/tables/illustrations
Number of figures/tables/illustrations	1
High-res required	no
Will you be translating?	no
Circulation/distribution	<501
Author of this Springer Nature content	no
Title	Synthesis and Fabrication of Molybdenum Disulfide /Conducting Polymer Nanocomposite Materials for Supercapacitor Applications

Below is copyright permission for Figure 2.1.

Using AAAS material in a thesis or dissertation

NOTE: If you are the original author of the AAAS article being reproduced, please refer to your License to Publish for rules on reproducing your paper in a dissertation or thesis. AAAS permits the use of content published in its journals *Science, Science Immunology, Science Robotics, Science Signaling, and Science Translational Medicine*, but only provided the following criteria are met:

1. If you are using figure(s)/table(s), permission is granted for use in print and electronic versions of your dissertation or thesis.
2. A full-text article may be used only in print versions of a dissertation or thesis. AAAS does not permit the reproduction of full-text articles in electronic versions of theses or dissertations.
3. The following credit line must be printed along with the AAAS material: "From [Full Reference Citation]. Reprinted with permission from AAAS."
4. All required credit lines and notices must be visible any time a user accesses any part of the AAAS material and must appear on any printed copies that an authorized user might make.
5. The AAAS material may not be modified or altered except that figures and tables may be modified with permission from the author. Author permission for any such changes must be secured prior to your use.
6. AAAS must publish the full paper prior to your use of any of its text or figures.
7. If the AAAS material covered by this permission was published in *Science* during the years 1974–1994, you must also obtain permission from the author, who may grant or withhold permission, and who may or may not charge a fee if permission is granted. See original article for author's address. This condition does not apply to news articles.
8. If you are an original author of the AAAS article being reproduced, please refer to your License to Publish for rules on reproducing your paper in a dissertation or thesis.

Below is copyright permission for Figure 2.2.

Copyright Clearance Center RightsLink®

Home | Account Info | Help

ACS Publications
Most Trusted. Most Cited. Most Read.

Title: Graphene-Based Ultracapacitors
Author: Meryl D. Stoller, Sungjin Park, Yanwu Zhu, et al
Publication: Nano Letters
Publisher: American Chemical Society
Date: Oct 1, 2008
Copyright © 2008, American Chemical Society

Logged in as:
Turki Alarmo
University of South Florida
Account #:
3001191074
LOGOUT

PERMISSION/LICENSE IS GRANTED FOR YOUR ORDER AT NO CHARGE

This type of permission/license, instead of the standard Terms & Conditions, is sent to you because no fee is being charged for your order. Please note the following:

- Permission is granted for your request in both print and electronic formats, and translations.
- If figures and/or tables were requested, they may be adapted or used in part.
- Please print this page for your records and send a copy of it to your publisher/graduate school.
- Appropriate credit for the requested material should be given as follows: "Reprinted (adapted) with permission from (COMPLETE REFERENCE CITATION). Copyright (YEAR) American Chemical Society." Insert appropriate information in place of the capitalized words.
- One-time permission is granted only for the use specified in your request. No additional uses are granted (such as derivative works or other editions). For any other uses, please submit a new request.

If credit is given to another source for the material you requested, permission must be obtained from that source.

BACK | CLOSE WINDOW

Below is copyright permission for Figure 2.3(a & b)

Copyright Clearance Center RightsLink®

Home | Account Info | Help

ACS Publications
Most Trusted. Most Cited. Most Read.

Title: Effects of Pore Structure on Performance of An Activated-Carbon Supercapacitor Electrode Recycled from Scrap Waste Tires

Author: Mingjia Zhi, Feng Yang, Fanke Meng, et al

Publication: ACS Sustainable Chemistry & Engineering

Publisher: American Chemical Society

Date: Jul 1, 2014

Copyright © 2014, American Chemical Society

Logged in as:
Turki Alarmo
University of South Florida
Account #:
3001191074

LOGOUT

PERMISSION/LICENSE IS GRANTED FOR YOUR ORDER AT NO CHARGE

This type of permission/license, instead of the standard Terms & Conditions, is sent to you because no fee is being charged for your order. Please note the following:

- Permission is granted for your request in both print and electronic formats, and translations.
- If figures and/or tables were requested, they may be adapted or used in part.
- Please print this page for your records and send a copy of it to your publisher/graduate school.
- Appropriate credit for the requested material should be given as follows: "Reprinted (adapted) with permission from (COMPLETE REFERENCE CITATION). Copyright (YEAR) American Chemical Society." Insert appropriate information in place of the capitalized words.
- One-time permission is granted only for the use specified in your request. No additional uses are granted (such as derivative works or other editions). For any other uses, please submit a new request.

If credit is given to another source for the material you requested, permission must be obtained from that source.

BACK | CLOSE WINDOW

Below is copyright permission for Figure 2.3(c).

Copyright Clearance Center RightsLink®

Home | Account Info | Help

Title: Hydrothermal synthesis of microalgae-derived microporous carbons for electrochemical capacitors

Author: M. Sevilla,W. Gu,C. Falco,M.M. Titirici,A.B. Fuertes,G. Yushin

Publication: Journal of Power Sources

Publisher: Elsevier

Date: 1 December 2014

Logged in as:
Turki Alarmo
University of South Florida
Account #:
3001191074

LOGOUT

Order Completed

Thank you for your order.

This Agreement between University of South Florida -- Turki Alarmo ("You") and Elsevier ("Elsevier") consists of your license details and the terms and conditions provided by Elsevier and Copyright Clearance Center.

Your confirmation email will contain your order number for future reference.

printable details

License Number	4412171470709
License date	Aug 18, 2018
Licensed Content Publisher	Elsevier
Licensed Content Publication	Journal of Power Sources
Licensed Content Title	Hydrothermal synthesis of microalgae-derived microporous carbons for electrochemical capacitors
Licensed Content Author	M. Sevilla,W. Gu,C. Falco,M.M. Titirici,A.B. Fuertes,G. Yushin
Licensed Content Date	Dec 1, 2014
Licensed Content Volume	267
Licensed Content Issue	n/a
Licensed Content Pages	7
Type of Use	reuse in a thesis/dissertation
Portion	figures/tables/illustrations
Number of figures/tables/illustrations	1
Format	both print and electronic
Are you the author of this Elsevier article?	No
Will you be translating?	No
Original figure numbers	Scheme 1
Title of your thesis/dissertation	Synthesis and Fabrication of Molybdenum Disulfide /Conducting Polymer Nanocomposite Materials for Supercapacitor Applications
Publisher of new work	University of South Florida

Below is copyright permission for Figure 2.4.

Copyright Clearance Center RightsLink®

Home | Account Info | Help

ACS Publications
Most Trusted. Most Cited. Most Read.

Title: Printable Thin Film Supercapacitors Using Single-Walled Carbon Nanotubes
Author: Martti Kaempgen, Candace K. Chan, J. Ma, et al
Publication: Nano Letters
Publisher: American Chemical Society
Date: May 1, 2009
Copyright © 2009, American Chemical Society

Logged in as:
Turki Alarmo
University of South Florida
Account #:
3001191074
LOGOUT

PERMISSION/LICENSE IS GRANTED FOR YOUR ORDER AT NO CHARGE

This type of permission/license, instead of the standard Terms & Conditions, is sent to you because no fee is being charged for your order. Please note the following:

- Permission is granted for your request in both print and electronic formats, and translations.
- If figures and/or tables were requested, they may be adapted or used in part.
- Please print this page for your records and send a copy of it to your publisher/graduate school.
- Appropriate credit for the requested material should be given as follows: "Reprinted (adapted) with permission from (COMPLETE REFERENCE CITATION). Copyright (YEAR) American Chemical Society." Insert appropriate information in place of the capitalized words.
- One-time permission is granted only for the use specified in your request. No additional uses are granted (such as derivative works or other editions). For any other uses, please submit a new request.

If credit is given to another source for the material you requested, permission must be obtained from that source.

BACK | CLOSE WINDOW

Below is copyright permission for Figure 2.5.

Copyright Clearance Center RightsLink®

Home | Account Info | Help

Title: Enhanced capacitance in partially exfoliated multi-walled carbon nanotubes

Author: Gongming Wang,Yichuan Ling,Fang Qian,Xunyu Yang,Xiao-Xia Liu,Yat Li

Publication: Journal of Power Sources

Publisher: Elsevier

Date: 1 June 2011

Published by Elsevier B.V.

Logged in as:
Turki Alarmo
University of South Florida
Account #:
3001191074

LOGOUT

Order Completed

Thank you for your order.

This Agreement between University of South Florida -- Turki Alarmo ("You") and Elsevier ("Elsevier") consists of your license details and the terms and conditions provided by Elsevier and Copyright Clearance Center.

Your confirmation email will contain your order number for future reference.

printable details

License Number	4412180844813
License date	Aug 18, 2018
Licensed Content Publisher	Elsevier
Licensed Content Publication	Journal of Power Sources
Licensed Content Title	Enhanced capacitance in partially exfoliated multi-walled carbon nanotubes
Licensed Content Author	Gongming Wang,Yichuan Ling,Fang Qian,Xunyu Yang,Xiao-Xia Liu,Yat Li
Licensed Content Date	Jun 1, 2011
Licensed Content Volume	196
Licensed Content Issue	11
Licensed Content Pages	6
Type of Use	reuse in a thesis/dissertation
Portion	figures/tables/illustrations
Number of figures/tables/illustrations	1
Format	both print and electronic
Are you the author of this Elsevier article?	No
Will you be translating?	No
Original figure numbers	Figure 1
Title of your thesis/dissertation	Synthesis and Fabrication of Molybdenum Disulfide /Conducting Polymer Nanocomposite Materials for Supercapacitor Applications
Publisher of new work	University of South Florida

Below is copyright permission for Figure 2.6.

Copyright Clearance Center RightsLink®

Home | Account Info | Help

ACS Publications
Most Trusted. Most Cited. Most Read.

Title: Supercapacitor Devices Based on Graphene Materials
Author: Yan Wang, Zhiqiang Shi, Yi Huang, et al
Publication: The Journal of Physical Chemistry C
Publisher: American Chemical Society
Date: Jul 1, 2009
Copyright © 2009, American Chemical Society

Logged in as:
Turki Alarmo
University of South Florida
Account #:
3001191074
LOGOUT

PERMISSION/LICENSE IS GRANTED FOR YOUR ORDER AT NO CHARGE

This type of permission/license, instead of the standard Terms & Conditions, is sent to you because no fee is being charged for your order. Please note the following:

- Permission is granted for your request in both print and electronic formats, and translations.
- If figures and/or tables were requested, they may be adapted or used in part.
- Please print this page for your records and send a copy of it to your publisher/graduate school.
- Appropriate credit for the requested material should be given as follows: "Reprinted (adapted) with permission from (COMPLETE REFERENCE CITATION). Copyright (YEAR) American Chemical Society." Insert appropriate information in place of the capitalized words.
- One-time permission is granted only for the use specified in your request. No additional uses are granted (such as derivative works or other editions). For any other uses, please submit a new request.

If credit is given to another source for the material you requested, permission must be obtained from that source.

BACK | CLOSE WINDOW

Below is copyright permission for Figure 2.7.

Order detail ID:	71490435
ISSN:	1099-0062
Publication Type:	Journal
Volume:	
Issue:	
Start page:	
Publisher:	ELECTROCHEMICAL SOCIETY, INC.
Author/Editor:	Institute of Electrical and Electronics Engineers ; Electrochemical Society

Permission Status: Granted

Permission type: Republish or display content
Type of use: Republish in a thesis/dissertation
Order License Id: 4412200023639

Hide details

Requestor type	Academic institution
Format	Print, Electronic
Portion	chart/graph/table/figure
Number of charts/graphs/tables/figures	1
The requesting person/organization	Turki Alamro
Title or numeric reference of the portion(s)	Figure 4
Title of the article or chapter the portion is from	A Symmetric RuO2/RuO2 Supercapacitor Operating at 1.6 V by Using a Neutral Aqueous Electrolyte
Editor of portion(s)	N/A
Author of portion(s)	Xia el al
Volume of serial or monograph	N/A
Page range of portion	100
Publication date of portion	Dec 2018
Rights for	Main product
Duration of use	Life of current edition
Creation of copies for the disabled	no
With minor editing privileges	no
For distribution to	Worldwide
In the following language(s)	Original language of publication
With incidental promotional use	no
Lifetime unit quantity of new product	Up to 499
Title	Synthesis and Fabrication of Molybdenum Disulfide /Conducting Polymer Nanocomposite Materials for Supercapacitor Applications

Below is copyright permission for Figure 2.8.

1. Journal of materials chemistry. A, Materials for energy and sustainability

ISSN:	2050-7496
Publication Type:	e-Journal
Volume:	
Issue:	
Start page:	
Publisher:	Royal Society of Chemistry
Author/Editor:	Royal Society of Chemistry (Great Britain)

Permission type:	Republish or display content
Type of use:	Thesis/Dissertation

⊟ Hide details

Requestor type	Academic institution
Format	Print, Electronic
Portion	chart/graph/table/figure
Number of charts/graphs/tables/figures	1
The requesting person/organization	Turki Alamro
Title or numeric reference of the portion(s)	Fig. 2 (a and b)
Title of the article or chapter the portion is from	High supercapacitor and adsorption behaviors of flower-like MoS2 nanostructures
Editor of portion(s)	N/A
Author of portion(s)	Wang et al.
Volume of serial or monograph	N/A
Page range of portion	100
Publication date of portion	Dec 2018
Rights for	Main product
Duration of use	Life of current edition
Creation of copies for the disabled	no
With minor editing privileges	no
For distribution to	Worldwide
In the following language(s)	Original language of publication
With incidental promotional use	no
Lifetime unit quantity of new product	Up to 499
Title	Synthesis and Fabrication of Molybdenum Disulfide /Conducting Polymer Nanocomposite Materials for Supercapacitor Applications

Below is copyright permission for Figure 2.10.

Copyright Clearance Center RightsLink®

Home | Account Info | Help

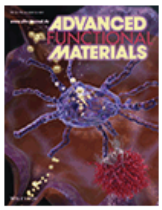

Title: High Electroactivity of Polyaniline in Supercapacitors by Using a Hierarchically Porous Carbon Monolith as a Support

Author: L.-Z. Fan, Y.-S. Hu, J. Maier, et al

Publication: Advanced Functional Materials

Publisher: John Wiley and Sons

Date: Aug 31, 2007

Logged in as:
Turki Alarmo
University of South Florida
Account #:
3001191074

LOGOUT

Order Completed

Thank you for your order.

This Agreement between University of South Florida -- Turki Alarmo ("You") and John Wiley and Sons ("John Wiley and Sons") consists of your license details and the terms and conditions provided by John Wiley and Sons and Copyright Clearance Center.

Your confirmation email will contain your order number for future reference.

printable details

License Number	4412570365576
License date	Aug 19, 2018
Licensed Content Publisher	John Wiley and Sons
Licensed Content Publication	Advanced Functional Materials
Licensed Content Title	High Electroactivity of Polyaniline in Supercapacitors by Using a Hierarchically Porous Carbon Monolith as a Support
Licensed Content Author	L.-Z. Fan, Y.-S. Hu, J. Maier, et al
Licensed Content Date	Aug 31, 2007
Licensed Content Volume	17
Licensed Content Issue	16
Licensed Content Pages	5
Type of use	Dissertation/Thesis
Requestor type	University/Academic
Format	Print and electronic
Portion	Figure/table
Number of figures/tables	1
Original Wiley figure/table number(s)	Figure 1
Will you be translating?	No
Title of your thesis / dissertation	Synthesis and Fabrication of Molybdenum Disulfide /Conducting Polymer Nanocomposite Materials for Supercapacitor Applications
Expected completion date	Dec 2018
Expected size (number of pages)	1
Requestor Location	University of South Florida 4202 E Fowler Ave

Below is copyright permission for Figure 2.11.

Journal of materials chemistry. A, Materials for energy and sustainability

Order detail ID:	71491094
Order License Id:	4412670026417
ISSN:	2050-7496
Publication Type:	e-Journal
Volume:	
Issue:	
Start page:	
Publisher:	Royal Society of Chemistry
Author/Editor:	Royal Society of Chemistry (Great Britain)

Permission Status: **Granted**

Permission type: Republish or display content
Type of use: Thesis/Dissertation

Hide details

Requestor type	Academic institution
Format	Print, Electronic
Portion	chart/graph/table/figure
Number of charts/graphs/tables/figures	1
The requesting person/organization	Turki Alamro
Title or numeric reference of the portion(s)	Figure 1
Title of the article or chapter the portion is from	Nanostructured conductive polypyrrole hydrogels as high-performance, flexible supercapacitor electrodes
Editor of portion(s)	N/A
Author of portion(s)	Shi el al
Volume of serial or monograph	N/A
Page range of portion	100
Publication date of portion	Dec 2018
Rights for	Main product
Duration of use	Life of current edition
Creation of copies for the disabled	no
With minor editing privileges	no
For distribution to	Worldwide
In the following language(s)	Original language of publication
With incidental promotional use	no
Lifetime unit quantity of new product	Up to 499
Title	Synthesis and Fabrication of Molybdenum Disulfide /Conducting Polymer Nanocomposite Materials for Supercapacitor Applications

Below is copyright permission for Figure 2.12.

Energy & environmental science

Order detail ID:	71491002
Order License Id:	4412580043112
ISSN:	1754-5706
Publication Type:	e-Journal
Volume:	
Issue:	
Start page:	
Publisher:	RSC Publishing
Author/Editor:	Royal Society of Chemistry (Great Britain)

Permission Status: **Granted**

Permission type: Republish or display content
Type of use: Thesis/Dissertation

Hide details

Requestor type	Academic institution
Format	Print, Electronic
Portion	chart/graph/table/figure
Number of charts/graphs/tables/figures	1
The requesting person/organization	Turki Alamro
Title or numeric reference of the portion(s)	Figure 1
Title of the article or chapter the portion is from	Polypyrrole-coated paper for flexible solid-state energy storage
Editor of portion(s)	N/A
Author of portion(s)	Yuan et al
Volume of serial or monograph	N/A
Page range of portion	100
Publication date of portion	Dec 2018
Rights for	Main product
Duration of use	Life of current edition
Creation of copies for the disabled	no
With minor editing privileges	no
For distribution to	Worldwide
In the following language(s)	Original language of publication
With incidental promotional use	no
Lifetime unit quantity of new product	Up to 499
Title	Synthesis and Fabrication of Molybdenum Disulfide /Conducting Polymer Nanocomposite Materials for Supercapacitor Applications

Below is copyright permission for Figure 2.13.

Copyright Clearance Center RightsLink®

Home | Account Info | Help

Title: Highly dispersed hydrous ruthenium oxide in poly(3,4-ethylenedioxythiophene)-poly(styrene sulfonic acid) for supercapacitor electrode

Author: Li-Ming Huang,Hong-Ze Lin,Ten-Chin Wen,A. Gopalan

Publication: Electrochimica Acta

Publisher: Elsevier

Date: 12 November 2006

Logged in as:
Turki Alarmo
University of South Florida
Account #:
3001191074

LOGOUT

Order Completed

Thank you for your order.

This Agreement between University of South Florida -- Turki Alarmo ("You") and Elsevier ("Elsevier") consists of your license details and the terms and conditions provided by Elsevier and Copyright Clearance Center.

Your confirmation email will contain your order number for future reference.

printable details

License Number	4412580648676
License date	Aug 19, 2018
Licensed Content Publisher	Elsevier
Licensed Content Publication	Electrochimica Acta
Licensed Content Title	Highly dispersed hydrous ruthenium oxide in poly(3,4-ethylenedioxythiophene)-poly(styrene sulfonic acid) for supercapacitor electrode
Licensed Content Author	Li-Ming Huang,Hong-Ze Lin,Ten-Chin Wen,A. Gopalan
Licensed Content Date	Nov 12, 2006
Licensed Content Volume	52
Licensed Content Issue	3
Licensed Content Pages	6
Type of Use	reuse in a thesis/dissertation
Portion	figures/tables/illustrations
Number of figures/tables/illustrations	2
Format	both print and electronic
Are you the author of this Elsevier article?	No
Will you be translating?	No
Original figure numbers	Figure 3, Figure 5
Title of your thesis/dissertation	Synthesis and Fabrication of Molybdenum Disulfide /Conducting Polymer Nanocomposite Materials for Supercapacitor Applications
Publisher of new work	University of South Florida

Below is copyright permission for Figure 2.14.

Copyright Clearance Center RightsLink®

Home | Account Info | Help

Title: Supercapacitive properties of polyaniline/Nafion/hydrous RuO2 composite electrodes

Author: Rak Young Song,Jun Ho Park,S.R. Sivakkumar,Sang Hern Kim,Jang Myoun Ko,Deok-Yong Park,Seong Mu Jo,Dong Young Kim

Publication: Journal of Power Sources

Publisher: Elsevier

Date: 30 March 2007

Logged in as:
Turki Alarmo
University of South Florida
Account #:
3001191074

LOGOUT

Order Completed

Thank you for your order.

This Agreement between University of South Florida -- Turki Alarmo ("You") and Elsevier ("Elsevier") consists of your license details and the terms and conditions provided by Elsevier and Copyright Clearance Center.

Your confirmation email will contain your order number for future reference.

printable details

License Number	4412590120914
License date	Aug 19, 2018
Licensed Content Publisher	Elsevier
Licensed Content Publication	Journal of Power Sources
Licensed Content Title	Supercapacitive properties of polyaniline/Nafion/hydrous RuO2 composite electrodes
Licensed Content Author	Rak Young Song,Jun Ho Park,S.R. Sivakkumar,Sang Hern Kim,Jang Myoun Ko,Deok-Yong Park,Seong Mu Jo,Dong Young Kim
Licensed Content Date	Mar 30, 2007
Licensed Content Volume	166
Licensed Content Issue	1
Licensed Content Pages	5
Type of Use	reuse in a thesis/dissertation
Portion	figures/tables/illustrations
Number of figures/tables/illustrations	2
Format	both print and electronic
Are you the author of this Elsevier article?	No
Will you be translating?	No
Original figure numbers	Figure 3, Figure 6
Title of your thesis/dissertation	Synthesis and Fabrication of Molybdenum Disulfide /Conducting Polymer Nanocomposite Materials for Supercapacitor Applications
Publisher of new work	University of South Florida

Below is copyright permission for Figure 2.15(a).

Copyright Clearance Center RightsLink®

Home | Account Info | Help

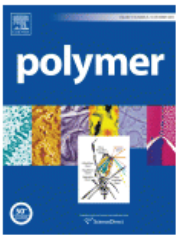

Title: Graphene/polypyrrole nanofiber nanocomposite as electrode material for electrochemical supercapacitor

Author: Sumanta Sahoo,Saptarshi Dhibar,Goutam Hatui,Pallab Bhattacharya,Chapal Kumar Das

Publication: Polymer

Publisher: Elsevier

Date: 5 February 2013

Logged in as:
Turki Alarmo
University of South Florida
Account #: 3001191074

LOGOUT

Order Completed

Thank you for your order.

This Agreement between University of South Florida -- Turki Alarmo ("You") and Elsevier ("Elsevier") consists of your license details and the terms and conditions provided by Elsevier and Copyright Clearance Center.

Your confirmation email will contain your order number for future reference.

printable details

License Number	4412590365461
License date	Aug 19, 2018
Licensed Content Publisher	Elsevier
Licensed Content Publication	Polymer
Licensed Content Title	Graphene/polypyrrole nanofiber nanocomposite as electrode material for electrochemical supercapacitor
Licensed Content Author	Sumanta Sahoo,Saptarshi Dhibar,Goutam Hatui,Pallab Bhattacharya,Chapal Kumar Das
Licensed Content Date	Feb 5, 2013
Licensed Content Volume	54
Licensed Content Issue	3
Licensed Content Pages	10
Type of Use	reuse in a thesis/dissertation
Portion	figures/tables/illustrations
Number of figures/tables/illustrations	1
Format	both print and electronic
Are you the author of this Elsevier article?	No
Will you be translating?	No
Original figure numbers	Figure 2
Title of your thesis/dissertation	Synthesis and Fabrication of Molybdenum Disulfide /Conducting Polymer Nanocomposite Materials for Supercapacitor Applications
Publisher of new work	University of South Florida

Below is copyright permission for Figure 2.15(b).

Copyright Clearance Center RightsLink®

Home | Account Info | Help

Title: Preparation of a graphene nanosheet/polyaniline composite with high specific capacitance

Author: Jun Yan,Tong Wei,Bo Shao,Zhuangjun Fan,Weizhong Qian,Milin Zhang,Fei Wei

Publication: Carbon

Publisher: Elsevier

Date: February 2010

Logged in as:
Turki Alarmo
University of South Florida
Account #: 3001191074

LOGOUT

Order Completed

Thank you for your order.

This Agreement between University of South Florida -- Turki Alarmo ("You") and Elsevier ("Elsevier") consists of your license details and the terms and conditions provided by Elsevier and Copyright Clearance Center.

Your confirmation email will contain your order number for future reference.

printable details

License Number	4412590494155
License date	Aug 19, 2018
Licensed Content Publisher	Elsevier
Licensed Content Publication	Carbon
Licensed Content Title	Preparation of a graphene nanosheet/polyaniline composite with high specific capacitance
Licensed Content Author	Jun Yan,Tong Wei,Bo Shao,Zhuangjun Fan,Weizhong Qian,Milin Zhang,Fei Wei
Licensed Content Date	Feb 1, 2010
Licensed Content Volume	48
Licensed Content Issue	2
Licensed Content Pages	7
Type of Use	reuse in a thesis/dissertation
Portion	figures/tables/illustrations
Number of figures/tables/illustrations	1
Format	both print and electronic
Are you the author of this Elsevier article?	No
Will you be translating?	No
Original figure numbers	Figure 5
Title of your thesis/dissertation	Synthesis and Fabrication of Molybdenum Disulfide /Conducting Polymer Nanocomposite Materials for Supercapacitor Applications
Publisher of new work	University of South Florida

Below is copyright permission for Figure 2.16.

Copyright Clearance Center RightsLink®

Home | Account Info | Help

ACS Publications
Most Trusted. Most Cited. Most Read.

Title: Supercapacitors Based on Flexible Graphene/Polyaniline Nanofiber Composite Films
Author: Qiong Wu, Yuxi Xu, Zhiyi Yao, et al
Publication: ACS Nano
Publisher: American Chemical Society
Date: Apr 1, 2010
Copyright © 2010, American Chemical Society

Logged in as:
Turki Alarmo
University of South Florida
Account #: 3001191074
LOGOUT

PERMISSION/LICENSE IS GRANTED FOR YOUR ORDER AT NO CHARGE

This type of permission/license, instead of the standard Terms & Conditions, is sent to you because no fee is being charged for your order. Please note the following:

- Permission is granted for your request in both print and electronic formats, and translations.
- If figures and/or tables were requested, they may be adapted or used in part.
- Please print this page for your records and send a copy of it to your publisher/graduate school.
- Appropriate credit for the requested material should be given as follows: "Reprinted (adapted) with permission from (COMPLETE REFERENCE CITATION). Copyright (YEAR) American Chemical Society." Insert appropriate information in place of the capitalized words.
- One-time permission is granted only for the use specified in your request. No additional uses are granted (such as derivative works or other editions). For any other uses, please submit a new request.

If credit is given to another source for the material you requested, permission must be obtained from that source.

BACK | CLOSE WINDOW

Below is copyright permission for Figure 2.17.

Copyright Clearance Center RightsLink®

Home | Account Info | Help

ACS Publications
Most Trusted. Most Cited. Most Read.

Title: Hierarchical Nanocomposites of Polyaniline Nanowire Arrays on Graphene Oxide Sheets with Synergistic Effect for Energy Storage

Author: Jingjing Xu, Kai Wang, Sheng-Zhen Zu, et al

Publication: ACS Nano

Publisher: American Chemical Society

Date: Sep 1, 2010

Logged in as:
Turki Alarmo
University of South Florida
Account #:
3001191074

LOGOUT

PERMISSION/LICENSE IS GRANTED FOR YOUR ORDER AT NO CHARGE

This type of permission/license, instead of the standard Terms & Conditions, is sent to you because no fee is being charged for your order. Please note the following:

- Permission is granted for your request in both print and electronic formats, and translations.
- If figures and/or tables were requested, they may be adapted or used in part.
- Please print this page for your records and send a copy of it to your publisher/graduate school.
- Appropriate credit for the requested material should be given as follows: "Reprinted (adapted) with permission from (COMPLETE REFERENCE CITATION). Copyright (YEAR) American Chemical Society." Insert appropriate information in place of the capitalized words.
- One-time permission is granted only for the use specified in your request. No additional uses are granted (such as derivative works or other editions). For any other uses, please submit a new request.

If credit is given to another source for the material you requested, permission must be obtained from that source.

BACK | CLOSE WINDOW

Below is copyright permission for Figure 2.18.

Copyright Clearance Center RightsLink®

Home | Account Info | Help

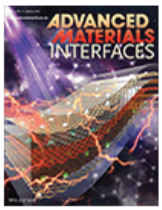

Title: Constructing a "Pizza-Like" MoS2/Polypyrrole/Polyaniline Ternary Architecture with High Energy Density and Superior Cycling Stability for Supercapacitors

Author: Kai Wang, Le Li, Ying Liu, et al

Publication: Advanced Materials Interfaces

Publisher: John Wiley and Sons

Date: Oct 6, 2016

Logged in as:
Turki Alarmo
University of South Florida
Account #:
3001191074

LOGOUT

Order Completed

Thank you for your order.

This Agreement between University of South Florida -- Turki Alarmo ("You") and John Wiley and Sons ("John Wiley and Sons") consists of your license details and the terms and conditions provided by John Wiley and Sons and Copyright Clearance Center.

Your confirmation email will contain your order number for future reference.

printable details

License Number	4412610135301
License date	Aug 19, 2018
Licensed Content Publisher	John Wiley and Sons
Licensed Content Publication	Advanced Materials Interfaces
Licensed Content Title	Constructing a "Pizza-Like" MoS2/Polypyrrole/Polyaniline Ternary Architecture with High Energy Density and Superior Cycling Stability for Supercapacitors
Licensed Content Author	Kai Wang, Le Li, Ying Liu, et al
Licensed Content Date	Oct 6, 2016
Licensed Content Volume	3
Licensed Content Issue	19
Licensed Content Pages	9
Type of use	Dissertation/Thesis
Requestor type	University/Academic
Format	Print and electronic
Portion	Figure/table
Number of figures/tables	3
Original Wiley figure/table number(s)	Figure 1, Figure 2, Figure 3
Will you be translating?	No
Title of your thesis / dissertation	Synthesis and Fabrication of Molybdenum Disulfide /Conducting Polymer Nanocomposite Materials for Supercapacitor Applications
Expected completion date	Dec 2018

Below is copyright permission for Figure 2.19.

Copyright Clearance Center RightsLink®

Home | Account Info | Help

Title: In situ intercalative polymerization of pyrrole in graphene analogue of MoS2 as advanced electrode material in supercapacitor

Author: Guofu Ma,Hui Peng,Jingjing Mu,Haohao Huang,Xiaozhong Zhou,Ziqiang Lei

Publication: Journal of Power Sources

Publisher: Elsevier

Date: 1 May 2013

Logged in as:
Turki Alarmo
University of South Florida
Account #:
3001191074

LOGOUT

Order Completed

Thank you for your order.

This Agreement between University of South Florida -- Turki Alarmo ("You") and Elsevier ("Elsevier") consists of your license details and the terms and conditions provided by Elsevier and Copyright Clearance Center.

Your confirmation email will contain your order number for future reference.

printable details

License Number	4412610379978
License date	Aug 19, 2018
Licensed Content Publisher	Elsevier
Licensed Content Publication	Journal of Power Sources
Licensed Content Title	In situ intercalative polymerization of pyrrole in graphene analogue of MoS2 as advanced electrode material in supercapacitor
Licensed Content Author	Guofu Ma,Hui Peng,Jingjing Mu,Haohao Huang,Xiaozhong Zhou,Ziqiang Lei
Licensed Content Date	1 May 2013
Licensed Content Volume	229
Licensed Content Issue	n/a
Licensed Content Pages	7
Type of Use	reuse in a thesis/dissertation
Portion	figures/tables/illustrations
Number of figures/tables/illustrations	2
Format	both print and electronic
Are you the author of this Elsevier article?	No
Will you be translating?	No
Original figure numbers	Figure 5, Figure 11
Title of your thesis/dissertation	Synthesis and Fabrication of Molybdenum Disulfide /Conducting Polymer Nanocomposite Materials for Supercapacitor Applications
Publisher of new work	University of South Florida